Alkene hydrogenation on reduced nickel A-zeolite catalysts.

WILLIAMS, S.G.

1983

ALKENE HYDROGENATION ON REDUCED NICKEL A-ZEOLITE CATALYSTS

By

Stephen George Williams BSc

A thesis submitted in partial fulfilment of the requirements of the Council for National Academic Awards for the Degree of Doctor of Philosophy (PhD).

School of Chemistry
Robert Gordon's Institute of Technology
Schoolhill
Aberdeen
AB9 1FR

DECLARATION

I hereby declare that this thesis is a record of work undertaken by myself, that it has not been the subject of any previous application for a degree, and that all sources of information have been duly acknowledged.

In the course of this research the following were included in an approved programme of advanced studies:

(i) Conference attendance:

(a) Discussion Meeting on Zeolite Catalysis Imperial College, 17/12/79

(b) Firbush Conference on Catalysis and Surface Chemistry, University of Edinburgh, 12/5/80 - 15/5/80

(c) Firbush Conference on Catalysis and Surface Chemistry, University of Edinburgh, 11/5/81 - 15/5/81

(ii) Lecture Course attendance:

Advanced Surface Chemistry (10 hrs) Robert Gordon's Institute of Technology, 1979

(iii) Guided reading:

Relevant textbooks, review articles and current literature on Catalysis and Surface Chemistry.

S G Williams
June 1983

C O N T E N T S

ABSTRACT

ALKENE HYDROGENATION ON REDUCED NICKEL A-ZEOLITE CATALYSTS

by

STEPHEN GEORGE WILLIAMS

The individual and competitive hydrogenation reactions of ethene propene and isobutene over various nickel metal loaded 4A zeolites have been investigated.

The reaction kinetics were found to be similar to those found by other workers for alkene hydrogenation over pure nickel metal. Reactions were first order in hydrogen and zero order in alkene at lower temperatures. However the order with respect to alkene increased towards unity as temperature increased and led to a decrease in apparent activation energy with increasing temperature. Activation energies generally became negative at temperatures greater than 170°C.

The catalytic reactions often exhibited pronounced induction periods. The catalytic activity during this induction period and the length of the period varied with the catalyst and reaction temperature used.

An explanation of some aspects of the results found in this work is proposed in terms of the presence of two different sets of catalytically active sites. One set of sites, residing in the zeolite pores, are more reactive towards the smaller alkene molecules and do not exhibit an induction effect. The other sites, which are responsible for the observed induction effect, are equally active towards all alkenes and are located either on the surface of the zeolite crystallites or on other amorphous material present in the zeolite samples used. The reaction sites are not always associated with the presence of nickel atoms as the parent zeolite, which contained no nickel, was also reasonably active for the hydrogenation reaction.

4A zeolite has been reported as being a good shape selective catalyst if the active centres are located within the pore structure. However, the results obtained from competitive hydrogenation in this work indicate that no selectivity for ethene hydrogenation in the presence of propene or isobutene can be obtained at temperatures below about 130°C as the larger alkenes block the zeolite pores.

ACKNOWLEDGEMENTS

The work presented in this thesis was carried out at the School of Chemistry, Robert Gordons Institute of Technology, Aberdeen under the supervision of Dr. R. McCosh and Dr. K.H. Tonge. I wish to say how grateful I am to Dr. McCosh and Dr. Tonge for their help and encouragement.

I would also like to thank all the people who have helped with this thesis, the following in particular:

The staff of the School of Physics, R.G.I.T., who carried out the electron microscopy and the X-ray diffraction work.

The staff of the MacAulay Institute for Soil Research, Aberdeen, who performed the trace element analyses.

Dr. G. Short and Dr. M. Spencer of I.C.I. Agricultural Division, Billingham, for helpful discussion of the work described here.

Dr. D.I. Bradshaw for proof-reading the entire manuscript.

Mrs. J.E. Rhodes for the typing, including the many alterations made to the typed script.

Chapter One

CATALYSTS AND CATALYSIS

1.1 Introduction

The word catalysis was first used by Berzelius in the 1830's to describe the effect that certain substances have on rates of chemical reaction. For example the enhancing effect of iron on the rate of decomposition of ammonia. A precise definition of a catalyst would be 'a substance which alters the rate at which a chemical system reaches equilibrium without itself appearing in the stoichiometric equation'. It does this by altering the mechanism of a reaction and thus affecting its kinetic parameters. An example of this is the oxidation of sulphur dioxide to form sulphur trioxide:-

$$2SO_2 + O_2 \rightleftharpoons 2SO_3$$

which is a slow process. In the presence of nitric oxide two reactions occur: -

$$2NO + O_2 \rightleftharpoons 2NO_2$$

$$NO_2 + SO_2 \rightleftharpoons NO + SO_3$$

both of which are fast reactions. Thus NO acts as a catalyst for the formation of SO_3.

There are three main categories of catalysis. These are:-

a) HOMOGENEOUS:- where the catalyst, reactant and products are all in the same phase.

b) HETEROGENEOUS:- in which the reaction occurs at an interface between phases. Catalysts are usually solid with the reactants being either liquid or gas.

c) ENZYME:- which is midway between homogeneous and

heterogeneous catalysis. Although enzyme reactions occur in solution (homogeneous) the enzymes are so large (10 to 100 nm.) that the reaction can be considered to occur at their surface (microheterogeneous).

1.2 Adsorption

Before catalysis of gas reactions by solids can be understood the gas/solid interaction must be considered. When a gas or vapour is brought into contact with a clean solid surface some of it will become attached in the form of an adsorbed layer. A single atom or molecule in the bulk of a solid is surrounded on all sides by other atoms and is connected to them via ionic or covalent bonding or by intermolecular forces. However, at the surface one side of the atom remains unbonded. Thus the forces acting upon it are fewer and there is a net resultant force acting in the direction of the bulk. This is reduced in the presence of gaseous molecules by the interaction between the surface atoms and the gas. The process is termed adsorption.

In thermodynamic terms the unsaturated nature of the surface is manifest as free energy (G). Adsorption causes a decrease in free energy (ΔG), and since adsorbed molecules lose a certain degree of freedom there is generally a decrease in entropy. Since:

$$\Delta G = \Delta H - T\Delta S$$

the heat adsorption (ΔH) is generally negative and the process exothermic. Endothermic adsorption is not unknown however and can occur when molecules are broken up during adsorption and an increase in entropy may occur.

There are two basic types of adsorption:-

1) PHYSICAL ADSORPTION: - where no chemical bonds are formed and

adsorbed molecules are held at the surface by van der Waals forces.

2) CHEMICAL ADSORPTION:- (chemisorption) where chemical bonds are formed between adsorbed molecules and the surface.

Chemical adsorption can be either 'associative' or 'dissociative'. In associative adsorption the bonds to the surface are formed via the breaking of a π bond between adjacent atoms of a molecule, thus leaving the molecule intact. Whereas in dissociative adsorption a σ bond is broken causing the molecule to be split.

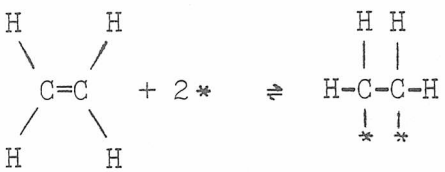

Associative Chemisorption.

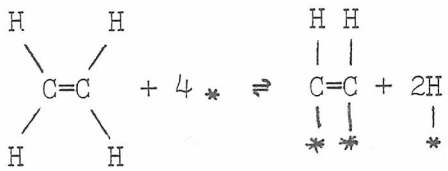

Dissociative Chemisorption.

where * represents a surface adorption site.

In all cases chemical adsorption occurs through a physically adsorbed precursor. The potential energy diagrams in Figure 1.1 show how the bond to the surface is formed as the interatomic distance is decreased. (a) and (b) represent exothermic adsorptions whilst (c) represents endothermic chemisorption. In the case of (a) chemisorption is not activated and will occur readily at all temperatures. In (b) and (c) however, chemisorption requires a certain amount of energy to surmount the energy barrier (E), and so below the temperature where the majority of adsorbate molecules possess energy equal to or greater than E only physical adsorption will occur. Two other points to note are that the heat of physical adsorption (ΔH_p) is always small and negative (exothermic), and endothermic chemisorption must always be activated.

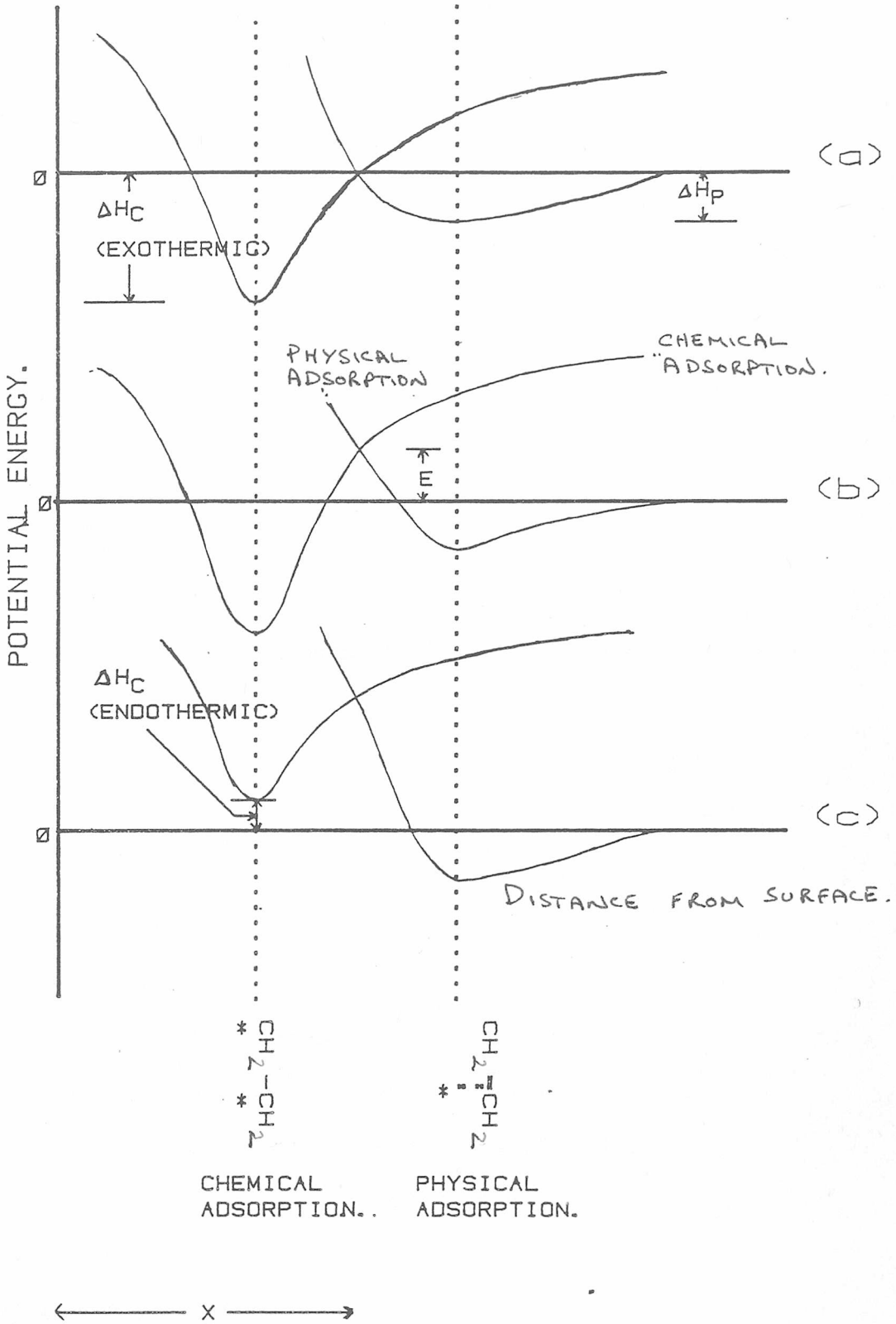

FIGURE 1.1

Potential Energy Curves for Adsorption.

In physical adsorption the forces which bond the adsorbate and the adsorbent are the same as those associated with liquification. Thus physical adsorption can result in multiple layers of adsorbate. In chemisorption however, since bonds are formed between the surface and the adsorbate, only monolayer adsorption can occur. This fact is the basis for the mathematical model for chemisorption of gaseous species proposed by Langmuir which he used to obtain the adsorption isotherm equation (1):-

$$\theta = \frac{bP}{1+bP}$$

where:-

θ = fraction of available surface covered by adsorbed gas at a given temperature.

b = constant related to the heat of adsorption. (adsorption equilibrium constant)

p = pressure of gas in equilibrium with the surface at coverage θ

This model for a single associatively adsorbed species uses several simplifying assumptions. These are:-

1) The adsorbate is immobile.
2) Each site accommodates only one molecule.
3) The heat of adsorption is the same on all sites.
4) The heat of adsorption is unaffected by adsorbed species on adjacent sites.
5) No dissociation occurs.

The model can be extended to predict dissociative and multispecies adsorption isotherms.

1.3 Heterogeneous Catalysis

For a bimolecular reaction there are two possible mechanisms for heterogeneous catalysis. These are:

1) LANGMUIR-HINSHELWOOD:- the two reactants are chemisorbed on adjacent sites before reaction.

2) ELEY-RIDEAL:- one of the reactants is chemisorbed on the surface and the second reactant is brought close enough for reaction by physical adsorption.

No reaction is known where catalysis occurs by physical adsorption of two species. The energy changes occurring during physical adsorption are too small to significantly alter the mechanism or energetics of reaction. The type of surface site available for adsorption will affect the suitability of a catalyst for a given reaction. Therefore, it is possible to classify heterogeneous catalysts according to their ability to provide specific types of adsorption site. One such classification is that of electrical and thermal conductivity. This is illustrated in Table 1.1 from which it can be seen that metals are most useful as hydrogenation and dehydrogenation catalysts.

1.4 Supported Metal Catalysts

Most industrial metal catalysts contain components other than the metal. These multicomponent catalysts can be divided into three groups:-

(a) PROMOTED METAL CATALYSTS:- which contain small quantities of additives that enhance the catalytic activity of the metal

(b) SUPPORTED METAL CATALYSTS:-where the metal is supported on an inert carrier which is not involved in the catalytic reaction.

TABLE 1.1.

A Classification of Heterogeneous Catalysts According to their Principal Functions (2).

Less important functions are placed in parenthesis.

CLASS	METALS	METAL OXIDES AND SULPHIDES		SALTS & ACIDS
CONDUCTIVITY TYPE	Conductors	Semiconductors	Insulators	
FUNCTIONS	hydrogenation dehydrogenation hydrogenolysis (oxidation) (reduction)	oxidation reduction cyclization dehydrogenation (hydrogenation)	dehydration isomerization (hydrogenation)	polymerization isomerization cracking alkylation hydrogen transfer

(c) BIFUNCTIONAL CATALYSTS: - where the metal is supported on a catalytically active carrier, and the combined metal and carrier functions affect the overall activity.

The main function of the support in supported metal catalysts is to create high dispersion of the metal. This gives a high specific surface area (surface area per gram of metal), thus achieving maximum specific activity (activity per gram of metal). Also, if the metal crystallites are sufficiently separated to prevent sintering an increased catalyst stability can be obtained due to retention of surface area and lowered susceptibility to poisons.

It is often hard to distinguish between supported and bifunctional catalysts. For example silica gel which is commonly used as catalyst support has a certain amount of intrinsic catalytic activity due to defects in its structure (3). Thus catalysis by metal on silica gel could occur by the same method as on the pure metal or by a bifunctional mechanism.

1.5 Catalyst Selectivity

Many catalysts only affect specific reactions and have little or no effect on those with similar or related kinetics. They can either be:-

(a) REACTANT SELECTIVE: - where they will only affect the rates of reaction of specific reactants without altering others of similar type.
e.g. The enzyme Urease will catalyse the hydrolysis of urea ($(NH_2)_2CO$), yet has no detectable effect on the rate of hydrolysis of substituted ureas such as methyl urea ($(NH_2)(CH_3NH)CO$).

(b) PRODUCT SELECTIVE: - where in a reaction that has multiple reaction pathways to produce alternative products the catalyst preferentially allows a specific route.

e.g.

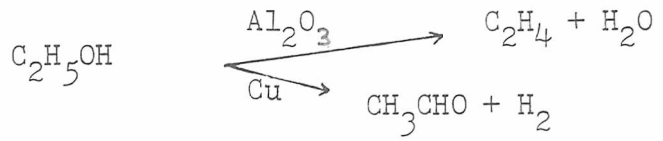

They do this by various mechanisms such as preferential adsorption of specific reactants, breaking of particular bonds, and breaking those bonds in a homolytic or heterolytic fashion.

1.6 Shape Selective Catalysts

Some supports can create or alter a catalyst's selectivity purely due to steric restrictions inherent in their structure.. Such supports are said to be shape selective. Porous supports can do this by one of four methods, all of which are due to the catalyst particles being held within intracrystalline cavities and pores. These are (4):-

a) REACTANT SELECTIVITY:-

Only molecules small enough to enter through the pores of the crystal can react with the catalyst sites.

b) PRODUCT SELECTIVITY:-

Only products small enough to diffuse out through the crystal structure will appear in the gas phase. This reaction type can slowly deactivate a catalyst as bulky product molecules block up the crystal pores.

c) RESTRICTED TRANSITION STATE SELECTIVITY:-

Only products with transition states small enough to fit inside the cavities within the support can be formed.

d) WINDOW EFFECT:-

Molecules whose length match that of the crystal cavities have reduced reactivity due to restricted diffusion (5).

Types a), b) and d) are all dependent on the diffusivity of either reactants or products, and in general a porous support will be shape selective if the diffusivity of the primary reactant/product is at least one or two orders of magnitude greater than its competitors (4).

REFERENCES

1) I.LANGMUIR, J. Amer.Chem.Soc., 40,1361,(1918)

2) G.C. BOND, "CATALYSIS BY METALS", Academic Press,London and New York, (1962)

3) A.J. VAN ROOSMALEN, M.C.G.HARTMANN,J.C.MOL, J.Cat.,66,112,(1980)

4) G.M.CSICSERY, "ZEOLITE CHEMISTRY AND CATALYSIS",ed.J.A.Rabo A.C.S. Monograph,171,680-713,(1976)

5) R.L.GORING,J.Cat.,31,13,(1973)

Chapter Two

ZEOLITES.

2.1 Introduction

Zeolites are hydrated crystalline aluminosilicates with well defined pore structures. Their frameworks are composed of three dimensionally linked SiO_4 and AlO_4 tetrahedra and have a net negative charge due to the isomorphic replacement of Si by Al. This charge is compensated by Group 1 or Group 2 cations held within the intra-crystalline cavaties and co-ordinated to the framework and/or adsorbed molecules. Zeolites can be represented by the general formula:-

$$M^{n+}_{a/n} \; ((AlO_2^-)_a \; (SiO_2)_b)cH_2O$$

where M is the compensating cation and n is its valency. In all cases 'a' is less than or equal to 'b' since it was shown by Loewenstein (1) that two aluminium atoms cannot share an oxygen atom and remain tetrahedrally co-ordinated.

2.2. Structures

There are many different structural types of zeolite most of which have been reviewed by Breck (2). Meier (3) showed that all zeolites can be constructed from at least one of eight framework groupings or secondary building units (SBU's) shown in Figure 2.1 - the primary units being the SiO_4 and AlO_4 tetrahedra. From these SBU's the polyhedra which comprise the unit cell of a given structure can be constructed. Some of these are shown in Figure 2.2 For example D6R units are used to form the structure shown in Figure 2.3, six of which make up the unit cell of zeolite 13X.

There are 34 known mineral zeolites and about 100 synthetic

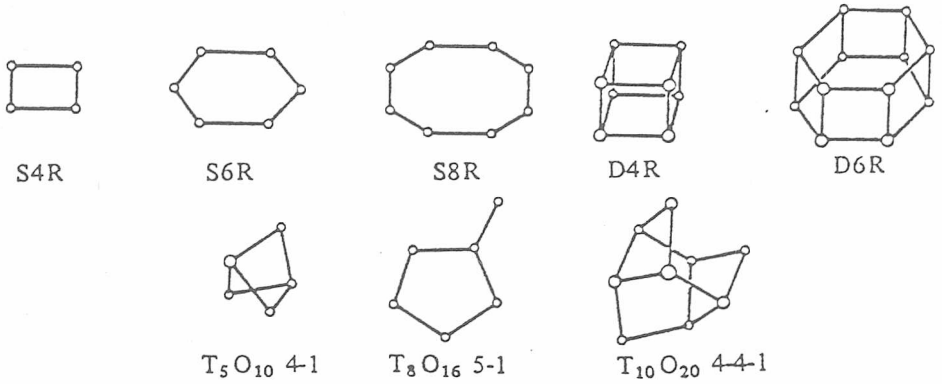

FIGURE 2.1

SECONDARY BUILDING UNITS (SBU) in zeolite structures according to Meier(2): vertices and corners represent Silicon or Aluminium atoms, lines represent oxygen.

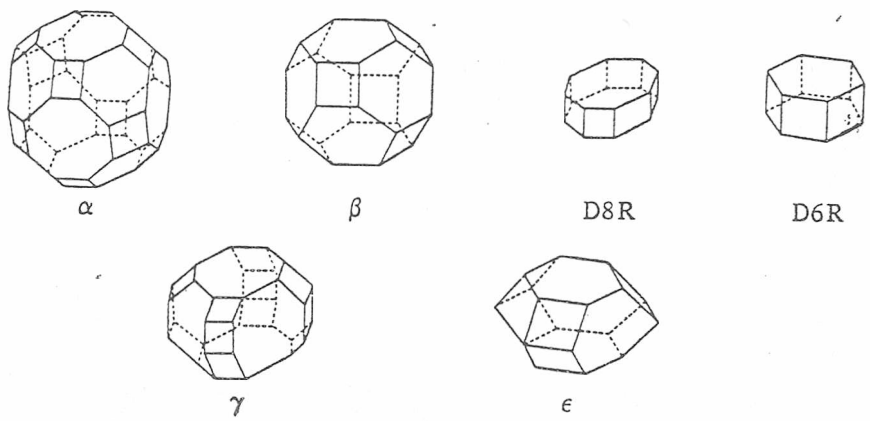

FIGURE 2.2

Some POLYHEDRA found in zeolite frameworks.

α cage - composed of S4R, S6R or S8R SBU's.
β cage - also known as a sodalite unit since it is the basic unit of the cubic felspathoids such as sodalite. It is composed of S4R or S6R SBU's.
D8R - composed of S4R or S8R SBU's.
D6R - hexagonal prism and is infact an SBU.
γ cage - composed of S4R SBU's.
ε cage - composed of S6R SBU's.

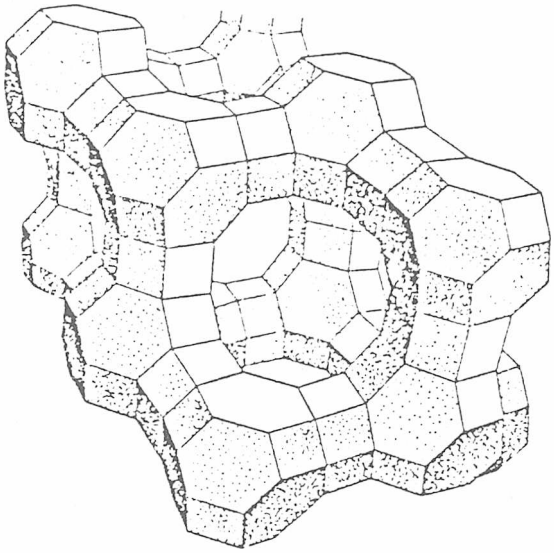

FIGURE 2.3

LINDE 13X ZEOLITE

$Na_{86}(AlO_2)_{86}(SiO_2)_{106} \cdot 264H_2O$

Composed of S4R, S6R, S8R or D6R SBU's made up into β cage or D6R polyhedra

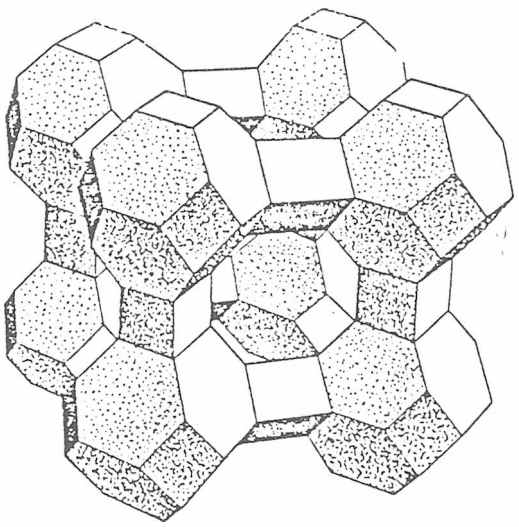

FIGURE 2.4

LINDE 4A ZEOLITE

$Na_{12}(AlO_2)_{12}(SiO_2)_{12} \cdot 27H_2O$

Composed of S4R, S6R, S8R or D4R SBU's made into α cage or β cage polyhedra.

zeolites. However, many show partial or total structural collapse, due to irreversible structural changes, upon dehydration. Therefore, since most applications require the zeolite to be in the dehydrated state, very few are of commercial value.

2.3 Uses of zeolites

Zeolites have four primary uses. These are as:-

(a) MOLECULAR SIEVES: -

If a porous adsorbant is contacted with two adsorbates, only one of which is smaller than its pore diameter, then the smaller molecule will be selectively adsorbed, thus separating the mixture. Zeolites are very effective in this area as they have precisely defined structures of molecular dimensions, and are very strong adsorbents when dehydrated.

(b) DRYING AGENTS: -

Since interstitial water is a major component of most zeolites, they have a very high affinity for water when in the dehydrated state, and are therefore often used to dry moist gases.

(c) ION EXCHANGERS: -

The interstitial cations within zeolites are exchangeable. Thus zeolites can be used as cation exchangers to alter the cation content of solutions. This ability is also useful when zeolites are used as catalysts, since catalytically interesting cations can be introduced by exchange.

(d) CATALYSTS: -

When dehydrated, zeolites have two types of potentially catalytically active site. These are:-

1) Interstitial cations - as mentioned above specific cations can be introduced by selective exchange. These may then be used as catalysts either in their ionic state or after reduction to their

uncharged state. This latter process results in what are known as metal loaded zeolites.

2) Acid sites - Bronsted acidity can occur due to hydroxyl groups:

i) terminating the crystal structure or at lattice defects.

ii) formed by hydrogen addition across Si-O-Al bonds. This can be caused by either cation deficiency, or reduction of the interstitial metal ions. i.e.

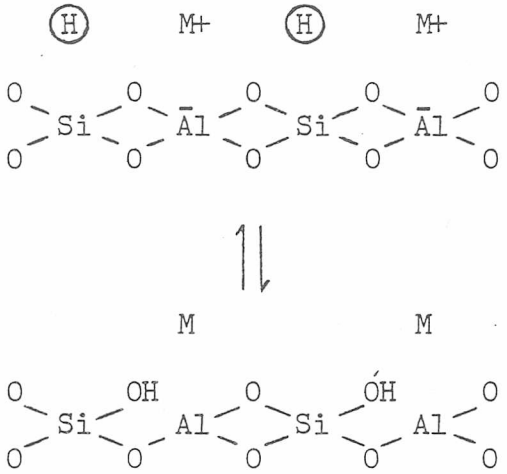

where M+ = metal ion and (H) = hydrogen source such as H_2 or NH_4^+

Lewis acid sites are found on structural silicon that is not tetrahedrally co-ordinated (i.e. one which has an unpaired electron in its outer shell). For example, Lewis acid sites are formed by dehydration of the Bronsted acid sites shown above, or at lattice defects in the crystal structure. i.e.

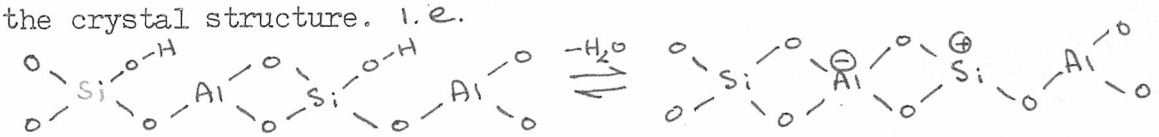

2.4 Shape Selective Zeolites

The possibility of using zeolites as shape selective catalysts was first demonstrated by Weisz and Frilette (4). Since then many illustrations of that potential have been shown. For example, the

selective hydrogenation of 1,3 butadiene from a mixture with isobutene on NiNaA(5), and the hydrogenation of n-butene in a mixture with isobutene over PtNaA(6).

This selectivity, due to active site retention within the zeolite cavities, is not absolute since a certain number of sites will be on the external surface. These are only a small percentage of the total active area. For example, Venuto and Landis (7) calculated that the external sites of rare earth, ammonium and hydrogen faujasites constitute only 0.5% to 1.3% of the total B.E.T. surface. However, internal sites are often less accessible than external and so their effective activity can be reduced. In the case of metal loaded zeolites, reduction of the cations results in the loss of their electrostatic bonding, thus lowering their site stability and allowing metal migration and agglomeration. This can cause a reduction in the internal specific surface of the metal and an increase in external metal as it migrates to the surface. Therefore, when reduction is utilised to activate a catalyst a compromise between activity and selectivity must be found.

2.5 Linde 4A Zeolite

The objective of this work was to study the characteristics and catalytic properties of nickel loaded 4A zeolite. Potentially this could create a good shape selective catalyst due to the catalytic properties of the nickel and the small diameter of the zeolite pores. The main problems with this system are the low thermal stability of the zeolite (8), and a strong tendency for nickel crystals to migrate to the zeolite exterior (9,10).

The structure and properties of Linde 4A zeolite were first reported by Breck et.al.(8). It has the formula $Na_{12}^{+}(AlO_2^{-}SiO_2)_{12}27H_2O$.

Its cell is made up of D4R secondary building units formed into eight sodalite units or β cages joined through their square faces to form a central ∝ cage (as defined in Chapter 2.2). The structure is shown in Figure 2.4. The β cages have an internal void diameter of 0.65 nm. accessible through their 0.22 nm. hexagonal faces. The large void of the ∝ cage has an internal diameter of 1.14 nm. and is accessible through the six eight membered rings of oxygen atoms which have a free aperture diameter of 0.42 nm.

In the hydrated zeolite eight of the sodium ions are located near the centre of the six sided rings inside the ∝ cage. Another three are located in three of the eight sided rings (11,12) whilst the twelfth one is thought by Yanagida et.al.(13), to be fully hydrated in the centre of the ∝ cage. The water molecules themselves are located as follows:-

1) Four in each β cage forming distorted tetrahedra.
2) One related to each sodium ion in the eight sided rings.
3) Twenty forming a pentagonal dodecahedron at the centre of the ∝ cage. This is shown in Figure 2.5 (14).

Complete dehydration of this zeolite is not possible without destroying the crystal structure. However, 99% dehydration can be achieved (9) and when this occurs the sodium ions are repositioned as follows. Eleven show only minor changes in position, marked NA1 and NA2 in Figure 2.6, whilst the previously hydrated ion from the centre of the ∝ cage takes up position NA3 near a four sided face of the unit cell (13).

2.6 Nickel Exchanged 4A Zeolite

Replacement of up to 55% of the interstitial sodium ions by

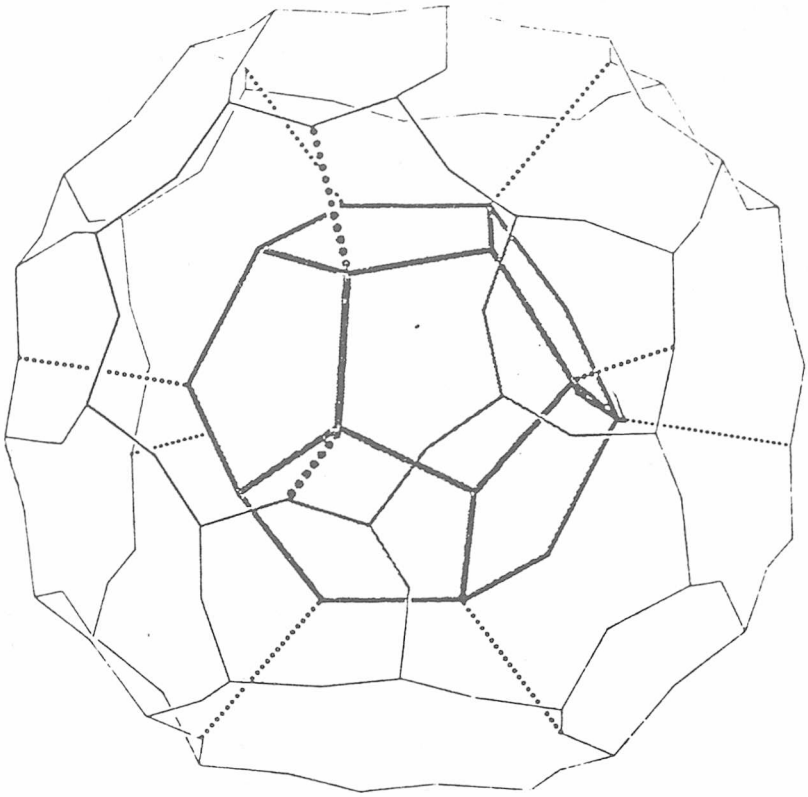

FIGURE 2.5

PENTAGONAL DODECAHEDRON of water molecules in the major cavity of LINDE 4A ZEOLITE.

Si. Al and O atoms of the α cage lie at the vertices of the thin lines. Water molecules lie at the vertices of the pentagonal dodecahedron. Whilst the dotted lines represent the shortest H_2O-Al/Si distances.

FIGURE 2.6

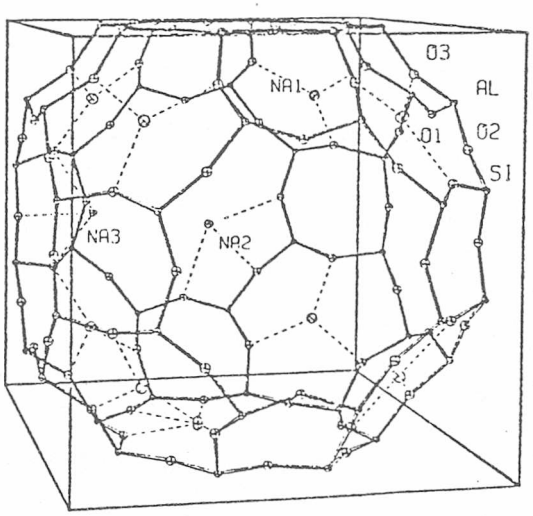

LINDE 4A ZEOLITE unit cell.

Al. Si and O atoms are represented by ⊛ . lines represent bonds.

The possible cation positions in the dehydrated stucture are marked as: -

NA1 - Eight Na ions are located at these threefold axis positions near the centre of the six oxygen windows.

NA2 - Three Na ions are distributed over the 12 fold equipoint near the centre of the eight oxygen windows.

NA3 - One Na ion is statistically distributed over the 12 fold equipoint located within the major cavity on a two fold axis normal to the four oxygen windows.

nickel have been reported by Penchev et.al.(9), although Amaro et.al. (15) reported their maximum obtainable degree of exchange to be 42%. This represents a placement of 3.3 and 2.5 nickel ions per unit cell respectively. Amaro et.al. also reported the nickel ion locations as follows. The first ion held the position within the water dodecahedron, the second took up a position within a β cage, and the third disrupted the first position within the dodecahedron. Upon dehydration the crystals became black and had a metallic lustre, indicating metallic nickel. This was considered to be due to disproportionation of the Ni(2+) to give Ni(0) and Ni(3+ or 4+). The latter being formed by the disproportionation of water to give H_2 and $Ni_2O(4+)$, $Ni_2O(6+)$ or $Ni_2OH_2(6+)$.

2.7 Nickel Loaded 4A Zeolite

Reduction of the interstitial nickel ions in a 4A zeolite results in some of the nickel migrating out of the cavities and on to the external surface (16). Here it forms large metal crystallites of up to 30nm in diameter (16,17). It has been found that concurrent dehydration of the zeolite and reduction of the nickel ions by hydrogen increases the amount of migration and agglomeration of the nickel (18). Therefore, separate dehydration and reduction procedures are recommended. However, Steinbach and Minchev (19) showed that pre-drying increased the difficulty of reduction of the nickel. This is probably due to migration of the nickel to sites wherein reduction is more difficult. They also showed that nickel migration was minimised by reduction of the nickel in liquid ammonia. However, with this technique hydrogen purging was required to remove the ammonia from the pore structure and this tended to cause the nickel to migrate unless the temperature was very carefully controlled.

2.8 Test Reaction

To measure the catalytic activity and shape selectivity of the nickel zeolite system a test reaction which is catalysed by nickel and will operate on a series of homologues of various shapes and sizes had to be found. As stated in Chapter 1.3, metals are most efficient as hydrogenation, dehydrogenation and hydrogenolysis catalysts. Therefore, it was decided to use alkene hydrogenation for the test.

Adsorption data for the low hydrocarbons is given in Table 2.1 along with the critical dimension for each molecule. The critical dimension is defined as the diameter of the circumscribed circle of the cross section of minimum area. This should give an indication whether the molecule can penetrate the 0.42 nm. pore openings of the zeolite. This diameter is only a qualitative measure because molecules can penetrate pores which are smaller than their critical dimension due both to structural vibrations in the adsorbate and the adsorbent and to structural defects in the adsorbent. The data indicates that both ethene and propene should adsorb throughout the zeolite structure whilst the butenes should not. This is in agreement with the work of Ushakova, et.al.(5) who showed that NiNaA could selectively hydrogenate divinyl in the presence of isobutene.

TABLE 2.1

Adsorption Capacity of 4A Zeolite (8)

ADSORBATE	Critical Dimension	Temp. (C)	Pressure (mm/Hg)	AMOUNT ADSORBED gram/gram	mole/mole
WATER	0.315nm	room	24	0.289	27.4
		100	24	0.193	
ETHANE	0.42 nm	room	700	0.074	4.2
ETHENE	0.425nm	room	700	0.084	5.1
PROPANE	0.489nm	room	600	0.017	0.7
PROPENE	0.50 nm	room	700	0.116	4.7
n-BUTANE	0.489nm	room	700	0.002	0.06
ISOBUTANE	0.558nm	room	400	0.006	0.2
BUT-1-ENE	0.51 nm	room	400	0.029	0.9

REFERENCES

1) W. LOEWENSTEIN,Am. Mineralogist,39,92,(1942)

2) D.W.BRECK, "ZEOLITE MOLECULAR SIEVES" Chapter 2, Wiley Interscience (1974)

3) W.M.MEIER, "MOLECULAR SIEVES" Soc.Chem.Ind.,London,(1968), Pg.10.

4) P.B.WEISZ, V.J.FRILETTE, J.Phys.Chem., 64,382,(1960)

5) V.A.USHAKOVA, D.P.DOBYCHIN, M.A.PIOTKOVSKAYA, I.E.NEIMARK, V.N.MAZIN L.E.FENELONOVA, Zh.PRIKLADNOI KHIMII,48,780,(1975)

6) P.B.WEISZ, V.J.FRILETTE, R.W.MAATMAN, E.B.MOWER,J.Cat.,1,307,(1962)

7) P.B.VENUTO, P.S.LANDIS, Adv.Cat.,18,259,(1968)

8) D.W.BRECK, W.G.EVERSOLE, R.M.MILTON, T.B.REED, T.L.THOMAS, J.Amer.Chem.Soc.,78,5963,(1956)

9) V.PENCHEV, H.MINCHEV, V.KANAZIREV,I.TSOLOVSKI, Adv.Chem.Ser., 102,434,(1971)

10) H.MINCHEV, F.STEINBACK, V.PENCHEV, Zeitschrift fur Phys.Chem., 99,223,(1976)

11) L.BROUSSARD, D.P.SHOEMAKER, J.Amer.Chem.Soc., 82,1041,(1960)

12) K.SEFF, D.P.SHOEMAKER, Acta Cryst., 22,162,(1967)

13) R.Y.YANAGIDA, A.A.AMARO, K.SEFF, J.Phys.Chem.,77,805(1973)

14) V.GRAMLICH, W.M.MEIER, Z.KRISTALLOGR.,133,134,(1971)

15) A.A.AMARO, C.L.KOVACINY, K.B.KUNZ, P.E.RILEY, T.B.VANCE,
R.Y.YANAGIDA, K.SEFF, Proc.3rd Int.Conf.Molecular Sieves, Zurich (1973)

16) D.J.C.YATES,J.Phys.Chem.,69,1676,(1965)

17) V.PENCHEV, Commun.Dept.Chem.Bulg.Akad.Sci., 4,573,(1971)

18) Kh.M.MINACHEV, V.I.GARANIN, V.V.KHARLAMOV.,L.I.PIGUZOVA
A.S.VITUKHINA, Neftekhimiya,9,808,(1969)

19) F.STEINBACH, H.MINCHEV, Zeitschrift fur Phys.Chem.,99,235,(1976)

Chapter Three

KINETICS AND MECHANISMS OF CHEMICAL REACTIONS

3.1 Introduction

The simplest approach to the investigation of a chemical reaction is the study of initial and final states. This yields information on the nature and yield of the products, and the thermodynamics of the reaction. However, chemical reactions do not occur instantaneously, but at a finite rate. Chemical thermodynamics yield no information about this aspect. The study of reaction rates, their relationship to reaction mechanisms and dependence on variables such as temperature, pressure, presence of catalyst, and the physical state of the reactants and products, is the province of chemical kinetics.

Kinetic studies generally involve measuring rates of chemical reactions in an attempt to discover the mechanisms by which reactant to product conversions occur.

The reaction rate for a reaction of the type:-

$$aA + bB \rightleftharpoons cC$$

can be represented by the equation:-

$$\text{RATE} = k[A]^x[B]^y[C]^z \qquad [X] = \text{concentration}$$

where k,k',x,y, and z are experimentally obtained constants. k is known as the rate constant and is dependent only on the temperature. They represent the rate of reaction at unit concentration. x, y and z represent the variation of rate as a function of reactant and product concentrations and are known as the partial reaction orders with respect to A, B and C. The overall forward reaction is said to be of the order $x+y+z$.

3.2 Rate and Order of Reaction

For an elementary reaction of the type:-

$$A + B \rightarrow C$$

where no reverse reaction or intermediate stages occur, it can be seen that for reaction to occur a molecule of A must collide with a molecule of B. Thus, since the probability of collision will be proportional to the reactant concentrations it can be shown that the isothermal rate equation would be:-

$$RATE = k[A][B]$$ - second order reaction, first order with respect to each reactant.

However, most reactions are not elementary but occur in stages. For these reactions the overall order of reaction can be fractional or even negative since it will depend on the nature of the steps involved. In a stepwise reaction the rate may sometimes be controlled by a rate determining step which could be, for example, decomposition or polarisation of one or both reactants to form intermediates, the further reaction of which leads to the observed products. In the specific case of heterogeneous catalysis, one of the intermediate stages is the adsorption of one or both reactants. Here at least one of the reactants reacts only when adsorbed and the reaction rate will depend on the degree of adsorption; the dependence of degree of adsorption on gas phase concentration is not linear as can be seen from the discussion of the Langmuir Isotherm discussed in Chapter 1.2. Experimentally reaction rate is normally measured with respect to a single reactant. If the rate equation takes the form:-

$$\frac{-d[A]}{dt} = k[A]^x$$

which can, when x = 1 be integrated to give the first order rate equation:-

$$\ln[A_o]-\ln[A] = kt \qquad A_o = A \text{ at } t=0$$

whilst if x=0 then:

$$\frac{-d[A]}{dt} = k$$

which becomes the zero order rate equation:-

$$[A_o]-[A] = kt$$

3.3 Temperature Dependence of k.

The dependence of k on temperature was first represented by the empirical Arrhenius equation which was based on experimental results:-

$$k = A \exp(-E/RT)$$

where R and T are the gas constant and the temperature (in Kelvin) respectively, and A is a constant known as the pre-exponential or frequency factor. E is the activation energy of the reaction and is defined as the energy barrier which must be surmounted by a molecule before it can react. Catalysts lower this barrier and thus increase the probability of reaction. This is shown in Figure 3.1.

This equation has since been shown to have some theoretical justification, through the collision theory, and more recently through the more general transition state theory. The collision theory states that for a bimolecular reaction:-

RATE = steric factor x collision frequency x fraction of reactants with required activation energy

where the collision frequency (Z), although proportional to $T^{\frac{1}{2}}$, is approximately constant over small temperature ranges. Whilst the fraction of reactants with the required energy is represented by the Boltzmann factor: $\exp(-E/RT)$. The steric factor (p) has an experimentally determined value and is based on the idea that

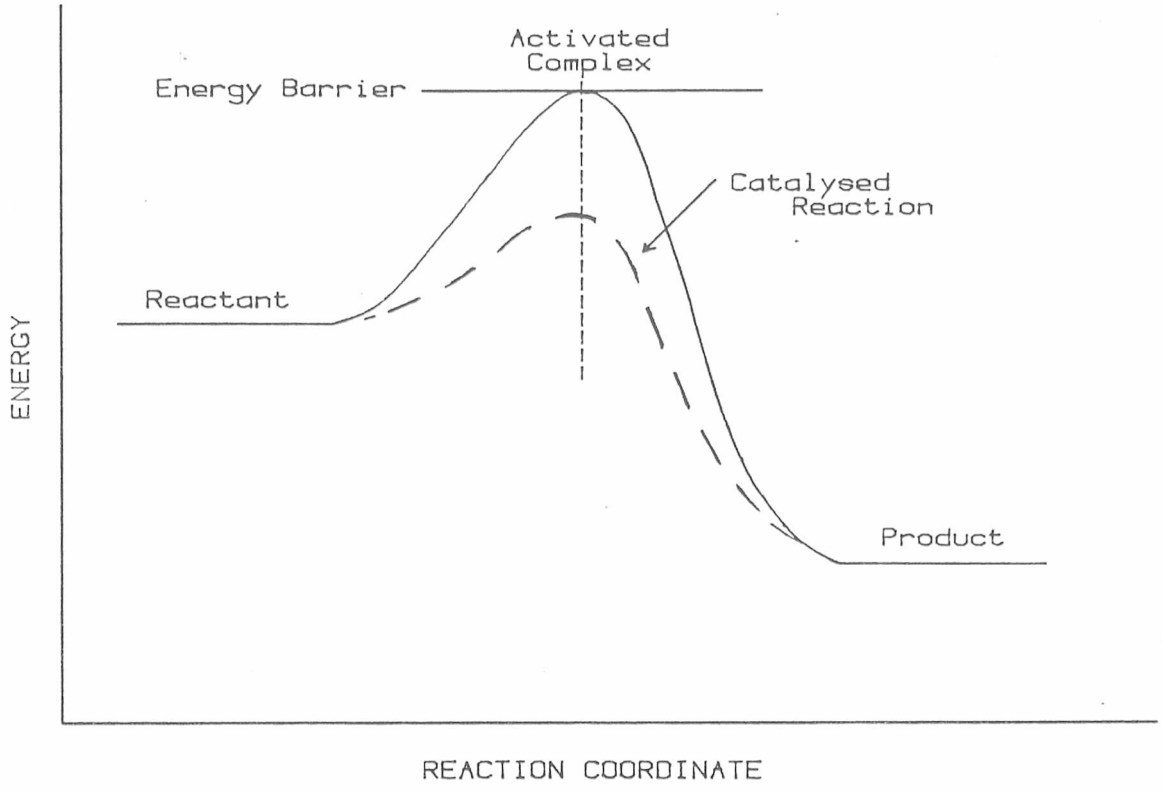

FIGURE 3.1

Potential Energy Curves for Reaction.

molecular co-ordination will affect the reaction probability. However, it is in fact included to correct the theory to fit the results obtained.

$$\text{i.e. RATE} = pZ \exp(-E/RT)$$

The transition state theory considers the reaction in terms of an activated complex existing at the peak of the energy barrier shown in Figure 3.1. The rate of reaction will be the number of complex molecules which pass over the energy barrier and form products per unit time. This depends on the concentration of the complex and the average frequency with which it moves over the energy barrier.

Thus:- $A + B \rightleftharpoons AB^{*} \rightarrow$ product

By considering the complex AB^{*} to be in equilibrium with the reactants, an equilibrium constant K can be defined:-

$$K = \frac{[AB^{*}]}{[A][B]}$$

Therefore:- $\text{RATE} = k[A][B] = [AB^{*}] \times$ (frequency of passage over the energy barrier (f))

$$\therefore \quad k = K f$$

The frequency of passage over the energy barrier is equal to the frequency with which a complex molecule flies apart. This can be considered as one of the degrees of vibrational freedom for the complex and can be expressed in terms of its vibrational partition function. This gives:

$$k = \frac{KkT}{h}$$

where k = Boltzmann's constant and h = Planck's constant

From thermodynamics it is known that:

$$\Delta G^{\circ} = -RT \ln(K)$$

and:

$$\Delta G^{\circ} = \Delta H^{\circ} - T \Delta S^{\circ}$$

Therefore:

$$k = \frac{kT}{h} \exp(\Delta S^\circ/R) \exp(-\Delta H^\circ/RT)$$

where ΔG°, ΔH°, and ΔS° are the free energy, the enthalpy and the entropy of activation respectively.

3.4 Controlling Factors in Heterogeneous Reactions

In static reaction systems where reactants are isolated in a sealed system the rate of reaction is often controlled by the rate determining step of the chemical reaction that is the step which exhibits the greatest resistance to change. In heterogeneous reaction, however, this is not always the case. Consider the mechanics of the entire process which produces the product in the gas phase.

1) Bulk diffusion of the reactants through the gas phase to the reaction surface.
2) Physical adsorption onto the reaction surface.
3) Possible diffusion along the surface or, if present, into micropores.
4) Chemisorption onto reaction sites.
5) Chemical reaction (consisting of one or more steps).
6) Desorption from the reaction sites.
7) Possible surface diffusion.
8) Desorption from the reaction surface.
9) Bulk diffusion of the products through the gas phase.

Any of these could potentially control the reaction rate and for meaningful results to be obtained control by steps 1) or 9) must be avoided since they are independent of the catalyst used. Also for a study of the reaction kinetics to yield information about the mechanism of reaction, 5) must control the rate.

3.5 Kinetics of Alkene Hydrogenation over Nickel

Most research into alkene hydrogenation over nickel has been carried out using ethene. However, the mechanism and kinetics have been shown to be applicable to the higher alkenes (1, 2, 3).

The kinetics of this reaction exhibits some interesting features. These are:-

i) At a temperature between 90°C and 170°C, depending on the experimental system used, the measured activation energy inverts and becomes negative.

ii) The reaction is first order with respect to hydrogen both above and below the temperature of the activation energy inversion.

iii) The reaction order with respect to alkene changes from fractional, or zero, at low temperatures to first above the inversion.

The most commonly accepted explanation of these facts is that they are due to alkene desorption (4), although Jenkins and Rideal explained it in terms of hydrogen desorption (5). However, all workers obtain the same theoretical and experimental rate equation. That is:

$$\text{Rate} = k \times \frac{b_a P_a P_h}{1 + b_a P_a} \qquad (1)$$

where k = rate constant

P_a = alkene pressure

P_h = hydrogen pressure

and b_a = adsorption coefficient for alkene

This is related to the Langmuir Adsorption Isotherm discussed in Chapter 1.2 as follows. In heterogeneous catalysis where a chemisorbed species is a reaction intermediate, the reaction rate

will be dependent on the surface concentration of that species rather than directly on its gas phase pressure. Alkene hydrogenation over nickel is generally considered to occur via an Eley-Rideal Mechanism between chemisorbed ethene and physically adsorbed or gas phase hydrogen, or via a Langmuir-Hinshelwood Mechanism between chemisorbed ethene and chemisorbed hydrogen. An Eley-Rideal Mechanism between gas phase ethene and chemisorbed hydrogen has also been proposed (5), but it is not generally considered since it cannot satisfactorily explain multiple exchange in the initial products of the ethene-deuterium reaction (6). Therefore, ignoring the latter case two possible rate equations can be formulated.

i) CHEMISORBED ETHENE AND GASEOUS HYDROGEN

$$\text{Rate} = k\,\theta_a\,P_h \qquad (2)$$

ii) CHEMISORBED ETHENE AND CHEMISORBED HYDROGEN

$$\text{Rate} = k\,\theta_a\,\theta_h \qquad (3)$$

where θ_a and θ_h are the fraction of available surface sites that are covered by ethene and hydrogen respectively.

If it is then assumed that ethene and hydrogen are both adsorbed on the same single sites then the Langmuir isotherm discussed in Chapter 1.2 gives:

$$\theta_a = \frac{b_a P_a}{1+b_a P_a+b_h P_h}$$

$$\text{and } \theta_h = \frac{b_h P_h}{1+b_a P_a+ b_h P_h}$$

where b_x = adsorption coefficient = $\dfrac{\text{adsorption rate constant}}{\text{desorption rate constant}}$

Substituting these values of θ into equations (2) and (3) then gives:

$$\text{Rate} = k\,\frac{b_a P_a P_h}{1+b_a P_a+ b_h P_h} \qquad (4)$$

and $$\text{Rate} = k \frac{b_a P_a b_h P_h}{(1+b_a P_a+b_h P_h)^2} \qquad (5)$$

Note that the adsorption of hydrogen is taken into account in equation (4) even though the hydrogen which participates in the hydrogenation reaction is in the gas phase. This is because chemisorbed hydrogen, even if inactive, will still affect the amount of ethene chemisorption.

Assuming that $b_a P_a + 1 \gg b_h P_h$, and for equation (5) that $b_a P_a < 1$, then the above equations can be simplified to:

$$\text{Rate} = k \frac{b_a P_a P_h}{1+b_a P_a}$$

and $$\text{Rate} = k \frac{b_a b_h P_a P_h}{1+2b_a P_a}$$

which are both the same form as equation (1). Now k and b have temperature dependencies such that:

$k = A \exp\left(\frac{-E_R}{RT}\right)$ where E_R = activation energy of the reaction

and $b = b_o \exp\left(\frac{-\Delta H}{RT}\right)$ and ΔH = enthalpy of adsorption

From this it can be seen that the value of k will increase with temperature. However, the enthalpy of adsorption of alkenes and hydrogen are negative (7) and therefore b will decrease with temperature. If above inversion $b_a P_a \ll 1$ then

$\text{Rate} = k\, b_a b_h P_a P_h$ for the Langmuir-Hinshelwood Mechanism

and $\text{Rate} = k\, b_a P_a P_h$ for the Eley-Rideal Mechanism

Substituting in the temperature dependencies into these then gives:

$$\text{Rate} = A \exp\left(\frac{-E_R}{RT}\right) b_{oa} \exp\left(\frac{-\Delta H_a}{RT}\right) b_{oh} \exp\left(\frac{-\Delta H_h}{RT}\right) P_a P_h$$

and $$\text{Rate} = A \exp\left(\frac{-E_R}{RT}\right) b_{oa} \exp\left(\frac{-\Delta H_a}{RT}\right) P_a P_h$$

Therefore, the apparent activation energy above inversion is:

$$E_{APP} = E_{REAL} + \Delta H_a + \Delta H_h$$

or $$E_{APP} = E_{REAL} + \Delta H_a$$

A similar treatment assuming $b_a P_a \gg 1$ for below the inversion temperature gives apparent activation energies of:-

$$E_{APP} = E_{REAL} - \Delta H_a + \Delta H_h$$

and $$E_{APP} = E_{REAL}$$

Therefore since all adsorption processes are exothermic the ΔH factors will be negative and the high temperature activation energy will be less than the low temperature one. A complete proof of these and other kinetic equations used in heterogeneous catalysis has been discussed by Satterfield (8).

Although widely used these equations must always be treated with caution as they do not allow for site loss due to coverage by inactive material such as acetylenic residues, or for multiple site adsorptions.

3.6 Mechanism of Alkene Hydrogenation over Nickel Catalysts

When increments of ethene are admitted to a clean nickel film, the first gas phase molecule found is ethane (4). This is shown in Figure 3.2 and is interpreted as follows: Ethene first chemisorbs dissociatively:-

$$CH_2CH_2 \rightleftharpoons CHCH_{(ads)} + 2H_{(ads)}$$

where (ads) indicates an adsorbed species.

As the surface coverage increases the dissociatively adsorbed hydrogen begins to react with either gaseous ethane:-

$$CH_2CH_2 + 2H_{(ads)} \rightleftharpoons CH_3CH_3$$

or adsorbed ethene:-

$$CHCH_{(ads)} + 4H_{(ads)} \rightleftharpoons CH_3CH_3$$

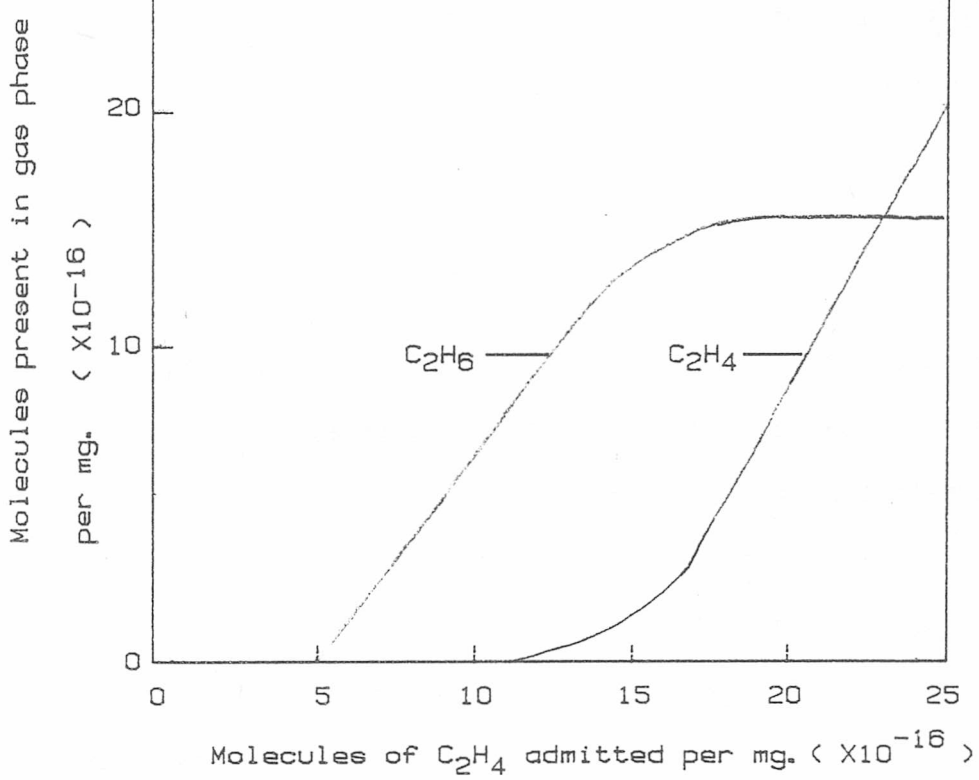

FIGURE 3.2

The chemisorption of ethene on evaporated nickel film (7).

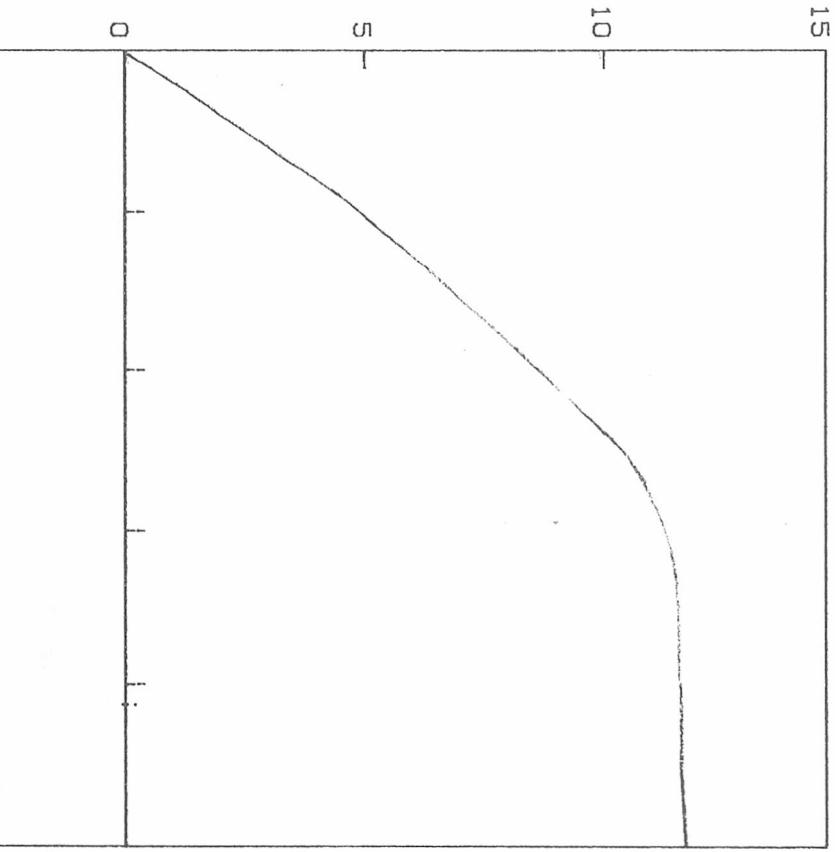
Molecules of C_2H_4 adsorbed per mg.
($X10^{-16}$)
0
5
10
15

This is known as a "self hydrogenation" reaction. The ethane produced and any ethane introduced to such an ethene covered surface is not measurably adsorbed. (9).

These results were supported by the work of Eischens and Pliskin (10) who showed, by infra red analysis of the C-H bond vibrations, that ethene adsorbed dissociatively onto nickel supported on non-porous silica at 35°C. Their work also revealed that the carbon-carbon bonds were saturated rather than unsaturated. Therefore, the adsorbed species is:-

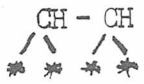

rather than

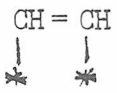

Selwood (9) concluded that this was not the case for ethene adsorbed onto co-precipitated nickel on silica at room temperature. He measured the change in magnetization of nickel with adsorption of measured amounts of ethene and concluded that it was mostly of an associative nature.

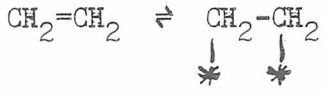

This was based on the assumption that nickel-carbon bonds affect nickel magnetization in the same way as nickel hydrogen bonds. At 100°C he found that dissociative adsorption predominates. He hypothesized that the variation between his and Eischens and Pliskin's results was due to the types of adsorption sites available. Some sites more readily form bonds with carbon than with hydrogen and vice versa. The relative amount of each allows associative or dissociative adsorption to various degrees.

Most recent discussion of the hydrogenation of ethene and other alkenes have discussed the participant alkene as being π bonded to the nickel (11, 12, 13, 14):-

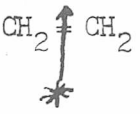

and in the higher alkenes the loss of a single hydrogen may produce a π - allyl-adsorbed species:-

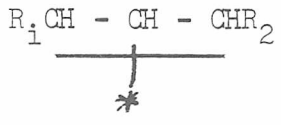

This argument does not refute the existence of the σ bonded alkene, but is an argument that such species are of less significance during hydrogenation.

The nature of the hydrogen is also uncertain. The reactive species may be molecular hydrogen from the gas phase or weakly adsorbed at the surface, or atomic hydrogen formed by the dissociative chemisorption of hydrogen molecules (15).

The hydrogenation is generally considered to proceed via the formation of an ethyl radical species first proposed by Horiuti and Polanyi (16):-

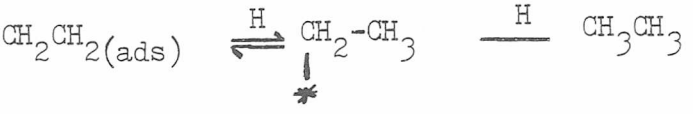

Hydrogen is known to add to alkene in a stepwise fashion for two reasons.

i) isomerization and double bond migration occur during the hydrogenation of the higher alkenes.

ii) when deuterium is used instead of hydrogen the dideuterated alkene is rarely the sole product. (6)

The first point indicates that intermediate species formed during reaction are reversible.

e.g. 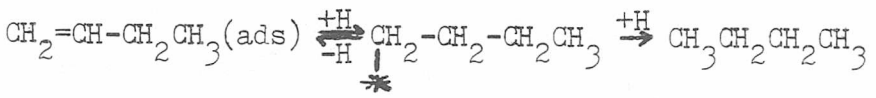

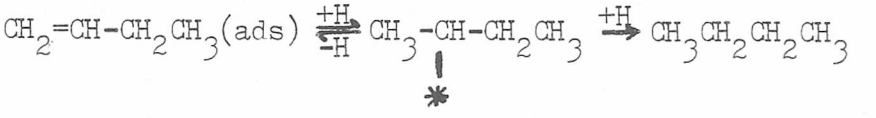

$$CH_2{=}CH{-}CH_2CH_3(ads) \overset{+H}{\underset{-H}{\rightleftharpoons}} CH_3{-}\underset{*}{CH}{-}CH_2CH_3 \overset{-H}{\underset{+H}{\rightleftharpoons}} CH_3{-}CH{=}CHCH_3$$

Whilst the latter can only be explained if a stepwise mechanism is considered:-

$$CH_2CH_2\,(ads) \overset{+D}{\underset{-D}{\rightleftharpoons}} \underset{*}{CH_2{-}CH_2D} \overset{-H}{\underset{+H}{\rightleftharpoons}} \underset{*}{CH_2}{-}\underset{*}{CHD} \overset{+D}{\underset{-D}{\rightleftharpoons}} \underset{*}{CH_2{-}CHD_2} \overset{-H}{\underset{+H}{\rightleftharpoons}} \text{etc.}$$

$$+H \uparrow\downarrow -H$$

$$CH_2CHD_{(ads)} \overset{+D}{\underset{-D}{\rightleftharpoons}} \underset{*}{CH_2D{-}CHD} \rightleftharpoons \text{etc.}$$

Thus with the release of free hydrogen into the system, and deuteration of the alkene all levels of alkane deuteration can then be obtained.

The ambiguity in the initial part of the above mechanism is probably due to the number of different catalysts used by the various researchers. That is, nickel film, nickel powder, nickel wire, supported nickel, etc. It is likely that more than one of the detailed approaches can occur and a different one predominates on different catalysts. Also in the case of supported metal catalysts there is evidence that the support can participate in the reaction (17).

REFERENCES

1. O.TOYAMA, Rev. Phys. Chem. of Japan, 14,86,(1940)
2. M.J.LEDOUX, F.G. GAULT, A.BOUGHY, G.ROUSSY, J.C.S.Faraday I, 76, 1547(1980)
3. P.CHUTOPANSKY, W.L.KPANICH, J.Cat., 21,1,(1971)
4. O.TOYAMA, Rev. Phys. Chem. of Japan, 12, 115(1938)
5. G.I. JENKINS, E.RIDEAL, J.Chem.Soc., 2490 & 2496 (1955)
6. C.KEMBALL, J.Chem.Soc., 735, (1956)
7. G.C.BOND, "Catalysis by Metals", Academic Press, London and New York, pg. (1962)
8. C.N. SATTERFIELD, "Heterogeneous Catalysis in Practice", McGraw-Hill Inc., Chapter 3, (1980)
9. P.W. SELWOOD, J.Am.Chem.Soc. 79,3346, (1957)

10. R.P. EISCHENS, W.A. PLISKIN, Adv.Cat., 10, 1, (1958)

11. J.J. ROONEY, J.Cat., 2, 53 (1963)

12. G.C. BOND, P.B.WELLS, Adv. Cat., 15,91, (1964)

13. J.L. GARNETT, W.A. SOLLICH-BAUMGARTNER, Adv. Cat., 16,95, (1966)

14. S. SIEGEL, Adv. Cat., 16, 123, (1966)

15. J.R. ANDERSON, B.G. BAKER, "Chemisorption and Reactions on Metallic Films Vol. 2", ed. J.R. Anderson, Academic Press, London and New York, pg. 63, (1971)

16. I. HORIUTI, M.POLANYI, Trans.Far.Soc., 163, 1164, (1934)

17. G.F. TAYLOR, S.J. THOMSON, G. WEBB, J.Cat. 12, 191, (1968)

Chapter Four

CATALYST PREPARATION AND CHARACTERIZATION

4.1 Introduction

A sample of 4A zeolite, reference number F.N.SD09560 was obtained from I.C.I. Agricultural Division and stored over saturated calcium nitrate solution to ensure complete hydration. Four catalyst samples of differing nickel cation content were prepared by ion exchange of NaA zeolite with nickel nitrate (Analar)/deionised water solution. The degree of exchange was determined by EDTA titration of the Ni(2+) in the filtrate and washings. X-ray diffraction, differential thermal analysis, thermogravimetric analysis, and electron microscopy were used to investigate the structural properties of the samples. Whilst semi-quantitative trace element analyses were performed by atomic emission spectroscopy, colorimetry, and energy dispersive X-ray fluorescence.

4.2 Ion Exchange

Introduction of nickel ions into the zeolite was performed by direct exchange using the following procedure in an attempt to obtain 0.1%, 1.0% 10% and 100% replacement of the interstitial sodium ions.

1) 15g of NaA was slurried with deionised water (100ml)
2) Standardised $Ni(NO_3)_2$ solution was added and the total volume made up to approximately 300ml with deionised water.
3) The slurry was evacuated by water pump to expel air.
4) Since acid conditions can cause the destruction of the zeolite lattice (1) and alkali conditions aid the formation of nickel hydroxide, an attempt was made to maintain the slurry at approximately pH 7 by addition of dilute hydrochloric acid. This is shown in Table 4.1.
5) The slurry was stirred magnetically for one hour at room temperature.

6) The zeolite was filtered and washed on a sintered glass crucible (porosity No. 3) with deionised water.

For sample d only:-

7) Steps 1) to 6) were repeated.

8) Steps 1) to 4) were repeated and the slurry stirred continually for 16 hours before the product was filtered and washed a final time.

TABLE 4.1

pH DURING EXCHANGE PROCEDURE:

pH of initial NaA slurry was 10.6-10.8

SAMPLE	pH on initial addition of $Ni(NO_3)_2$	pH on addition of HCl	pH after 1 hour
a	10.79	6.68	-
b	10.20	6.50	6.98
c	7.41	no addition	7.92
d	6.36	no addition	6.48

For comparative purposes a 'blank' was also prepared by following steps 1 to 6 using deionised water instead of nickel nitrate.

4.3 Titrimetric Analysis

The degree of exchange was measured as the amount of nickel lost from solution, assuming all losses were due to exchange into, and not deposition on, the zeolite. The validity of this assumption will be discussed later.

Measurements of nickel in solution were performed by titration with ethylenediaminetetra-acetic acid (EDTA) which forms a complex with all metal ions in a 1:1 ratio. The strength of the complex is

dependent on the specific ion and acidity of the solution, and can therefore be used in ion mixtures as long as the conditions are correctly chosen.

The EDTA was standardised by titration against a standard 9.656×10^{-3} molar solution of $MgSO_4 7H_2O$. 25ml aliquots of the magnesium sulphatesolution, buffered at pH 10, were used. Eriochrome Black T, which changes colour from red when complexed with Mg(2+) to blue when free, was used as indicator. The average concordant titre for the EDTA was 24.94ml. From this the EDTA concentration was calculated as:-

$$(\text{EDTA}) = 9.656 \times 10^{-3} \times \frac{25}{24.94} = 9.679 \times 10^{-3} \text{ moles/dm}^3$$

Aliquots of the original nickel nitrate solutions were titrated against the EDTA to obtain the initial nickel concentrations. Then the combined filtrates and washing for the exchanges were each made up, with deionised water, to one litre in volumetric flasks and also titrated. This was done by firstly neutralising aliquots of the nickel solutions by addition of 2M NaOH and then buffering these at pH10 by the addition of 6ml of NH_3/NH_4Cl. These were titrated with the EDTA using murexide, which changes from orange when complexed with nickel to violet when free, as indicator. The moles of nickel in each litre of solution were then calculated as:-

$$(\text{moles nickel}) = \frac{\text{moles EDTA}}{\text{litre}} \times \frac{\text{vol.EDTA}}{1000} \times \frac{\text{total vol.soln.}}{\text{vol.soln.for titre}}$$

From this the amount of nickel exchanged into the zeolite was obtained.

(moles nickel exchanged)=(moles nickel in exchange soln.)

- (moles nickel in filtrate and washings)

This then gave the number of nickel ions per unit cell of the zeolite,

which is equivalent to the number of moles of nickel per mole of zeolite, as:-

$$\text{(no.nickel ions/unit cell)} = \text{(moles nickel)/(moles zeolite)}$$
$$= \text{(moles nickel)/(15/XZ)}$$
$$= \text{(moles nickel)/}(6.846\times10^{-3})$$

where XZ = relative molar mass of the zeolite (hydrated

$$= 1914.8 + 22.99(12-2x) + 58.71x$$

where x = no. of nickel ions/unit cell of the zeolite.

Also, since one nickel ion replaces two sodium ions (if charge balance is to be maintained):-

$$\text{percentage sodium exchanged} = \frac{2\times100\times(\text{no.nickel ions/unit cell})}{12}$$

The results obtained from these analyses are shown in Table 4.2 along with the% exchange attempted.

4.4 Zeolite Crystallinity

To verify the crystallinity of the original zeolite and to ensure the structure retention of the exchanged samples a number of structural tests were employed.

1) X-RAY DIFFRACTION:-

X-ray diffraction patterns for the parent and the exchanged zeolites were obtained from the Department of Physics, RGIT, as chart recorder peaks. These are shown in Figure 4.1. The pattern of the parent zeolite is the same as that obtained by Broussard and Shoemaker (1). As the degree of exchange increases the only significant changes are in the peaks at approximately 10, 12, 16, 17 and 34 degrees and these changes are minor in the 0.1% and 1.0%. This would indicate that the parent-zeolite was structurally sound and no significant loss of crystallinity

TABLE 4.2

TITRIMETRIC ANALYSIS OF $Ni(NO_3)_2$ EXCHANGE SOLUTIONS

SAMPLE	EXCHANGE SOLUTION		Mole Ni^{2+} Available	Moles Ni^{2+} Exchanged	No. Ni^{2+} per unit cell of zeolite	% Na^+ Exchanged	% Na^+ Exchange attempted
	Molarity	Volume					
a	9.85×10^{-3}	4.11	4.050×10^{-5}	4.0×10^{-5}	5.915×10^{-3}	0.0986	0.1
b	0.0999	4.11	4.105×10^{-4}	4.105×10^{-4}	5.997×10^{-2}	0.9995	1.0
c	0.0999	50	4.995×10^{-3}	4.368×10^{-3}	0.638	10.63	10
d	1.00	450	0.450	0.024	3.506	58.4	100

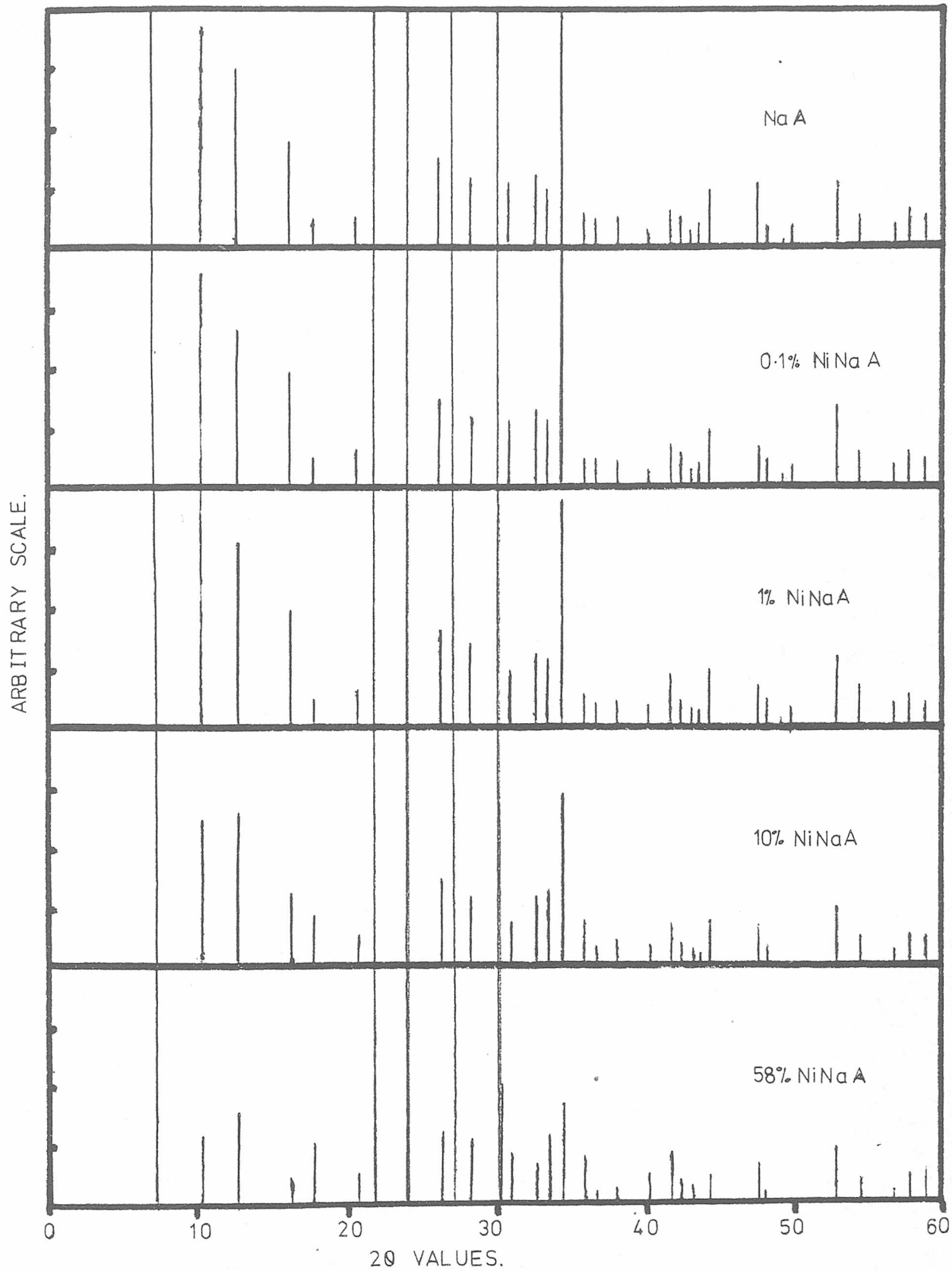

FIGURE 4.1

X-Ray Diffraction Patterns.

occurred with exchange of small amounts of nickel. However, higher exchange levels may have caused some degree of structural damage.

2) THERMAL ANALYSIS:

A good indication of crystallinity in zeolites is the water content since the crystal structure holds defined amounts of water. Thermogravimetric analysis (TGA) was therefore used on these samples to measure the weight loss on heating. NiNaA zeolites are stable to above 600C (2) and any weight loss below this temperature should be due to dehydration. Samples of approximately 0.3g were heated, in air, at a rate of 10C/min. up to a maximum of 700C. A calibration run with the TGA apparatus empty revealed that a buoyancy effect, due to air density variation with temperature, gave an apparent weight gain of 3mg which had to be allowed for during result analysis. The percentage of water in the zeolite was calculated as:-

$$(\%\text{wt.water}) = 100 \times \frac{(\text{corrected weight loss})}{(\text{original sample wt.})}$$

Differential thermal analysis (DTA) was performed on the samples to measure the temperatures of structural change as these have been shown to decrease with percentage nickel exchange (2). The endotherms for water desorption between 100C and 300C were not recorded as this section was uneven and irreproducible. The reason for this probably being due to a dependence of the intercrystalline diffusion and desorption of the water on packing and sample size. Samples of unmeasured size (the reaction crucible was simply filled) were heated from room temperature to about 1000C at 10C/min.-

The results from both sets of thermal analysis are shown in Table 4.3 along with those obtained by Penchev et.al.(2) for similar samples of NiNaA, and the DTA plots are shown in Figure 4.2

TABLE 4.3

SAMPLE	% EXCHANGE	T.G.A.(%wt.loss)	D.T.A.(Initial Temperature of destruction (°C) (start of first exotherm)
a	0.1%	21.0	824
b	1.0%	21.0	804
c	10.6%	21.3	770
d	58.4%	25.6	720
from reference (2)	0.0%	22.4	840
"	23.0%	24.0	780
"	34.0%	25.0	750
"	55.0%	26.3	640

As can be seen the weight losses during T.G.A. are slightly lower in this work than for Penchev et.al. This may be due to experimental error, or it may be an indication of the presence of a small amount of amorphous material. However, the general increase in the water content and decrease in the initial temperature of destruction is the same in both cases. Also the increase in the distance between the two high temperature exotherms with increase in nickel content shown in Figure 4.2 was also found by Penchev et.al. All indications from these results are therefore that the zeolite retained its structure when the nickel was exchanged into it.

3) ELECTRON MICROSCOPY

To ascertain if there were any major bulk effects due to exchange

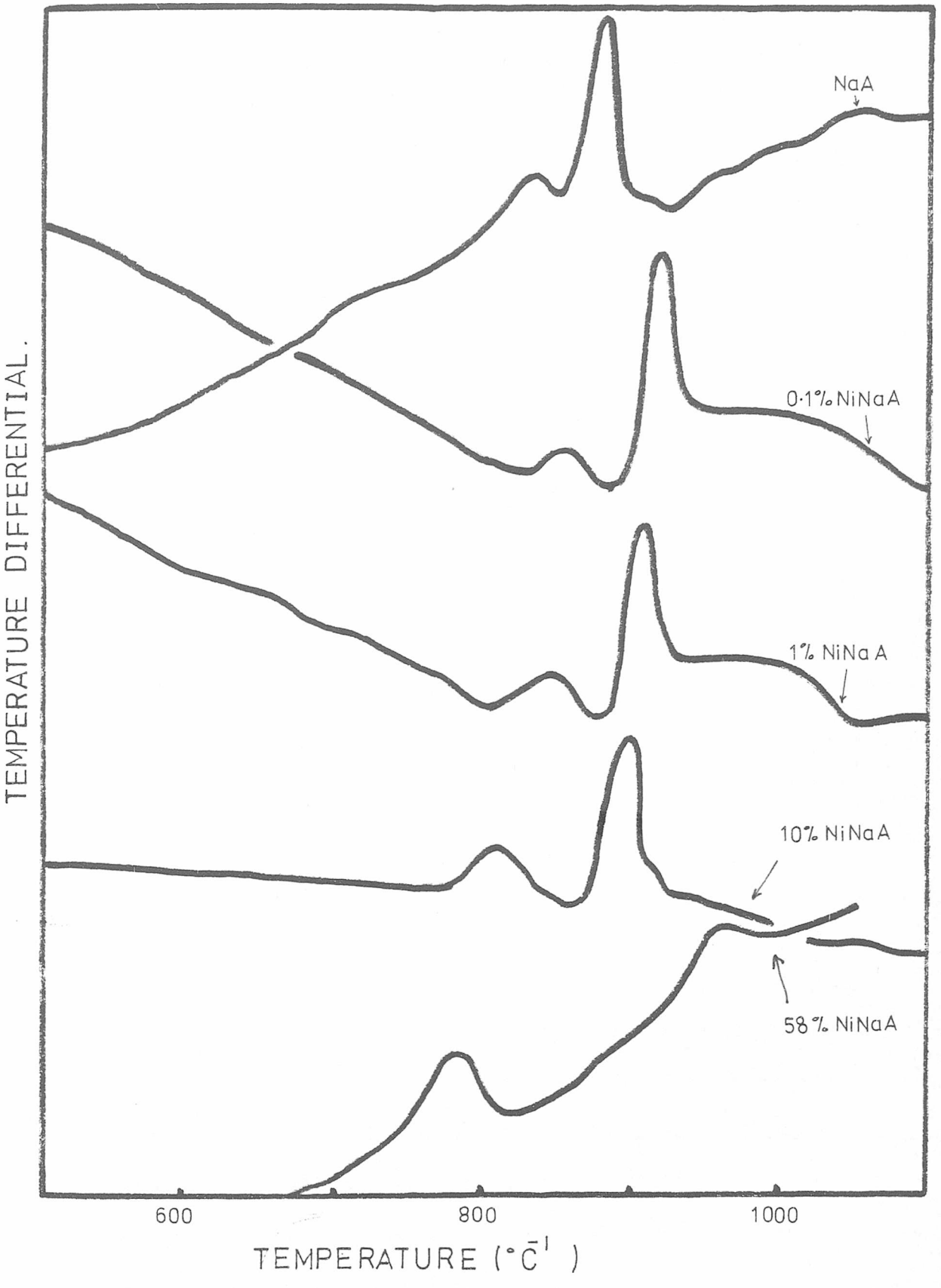

FIGURE 4.2

Differential Thermograms.

and use of the zeolite a number of scanning electron micrographs were obtained from the School of Physics, RGIT. A selection of the most informative photographs are shown in Figure 4.3, 4.4 and 4.5. They revealed that there was no significant change in the physical appearance of the samples with degree of exchange or reduction of the interstitial nickel. In all cases, however, there was a great heterogeneity in particle size which could well affect the reproducibility of the catalytic function. Also as is most clearly shown in Figure 4.5, some of the material present is not 4A zeolite. This material forms a small though potentially significant fraction of the total bulk. It is most probably either amorphous aluminosilicate or some other zeolite structure.

4.5 Semiquantitative Trace Element Anaysis

Because of the low concentrations of nickel used in these zeolites even traces of other metals could have a significant effect on their catalytic function. Therefore, a number of semiquantitative trace element analyses were performed.

1) SPARK EMISSION SPECTROSCOPY & COLORIMETRIC ANALYSIS

Spark Emission spectra for the unexchanged, the 0.1% and the 1.0% exchanged samples were obtained at the MacAulay Institute for Soil Research, Aberdeen. The level of metal impurities in the samples was then calculated by comparison of these results with calibration data.

The level of iron in the structures could not be quantitatively measured due to lack of calibration information, but the spectra showed significant amounts present in all the samples. Since iron impurities could affect the catalytic properties of the samples colorimetric analyses were performed to obtain an

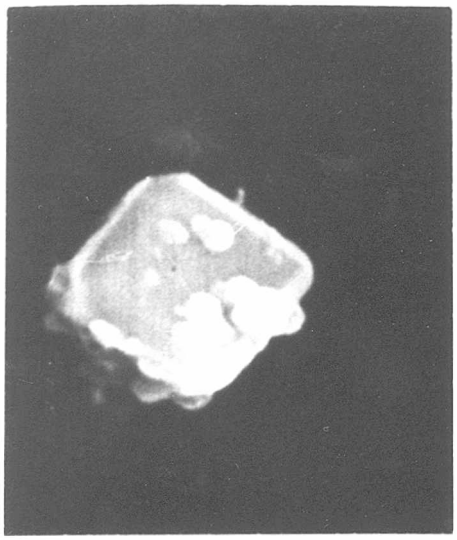

⟵10 μm⟶

NaA

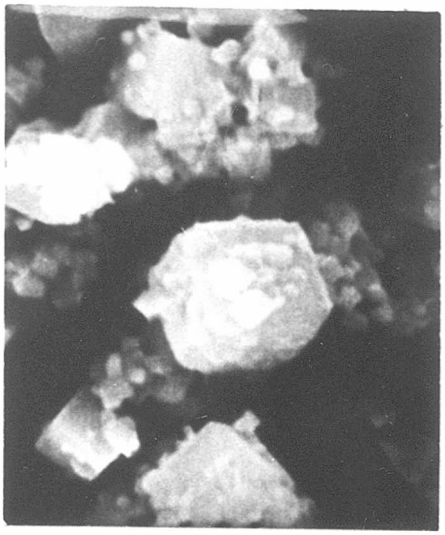

⟵10 μm⟶

0·1% NiNaA

⟵10μm⟶

10% NiNaA

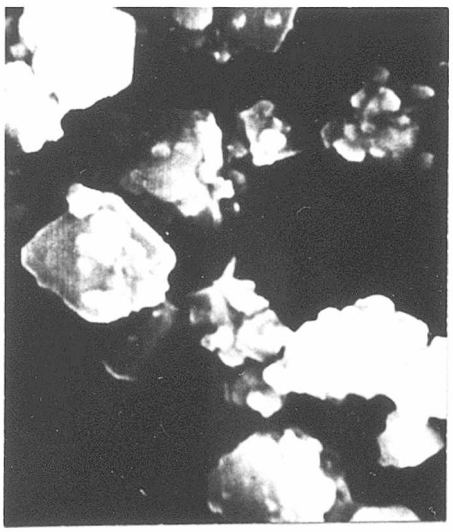

⟵10μm⟶

58%NiNaA

FIGURE 4.3

Electron micrographs of parent & nickel exchanged 4A Zeolite.

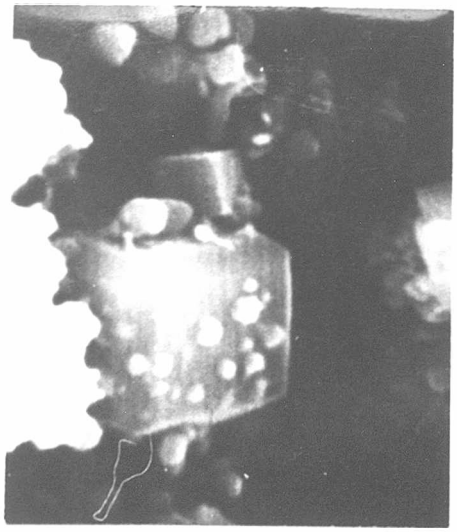

10 μm

UNREDUCED.

10 μm

200° C

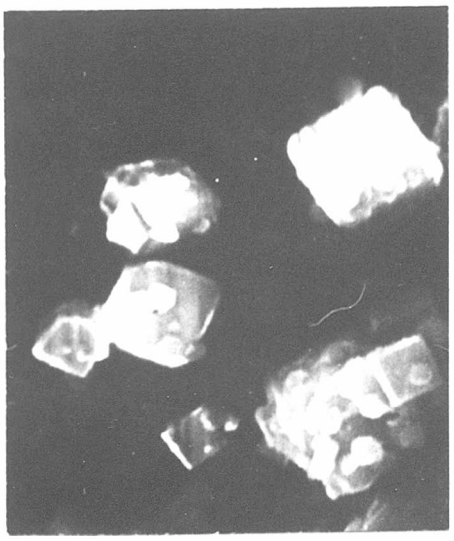

10 μm

250°C

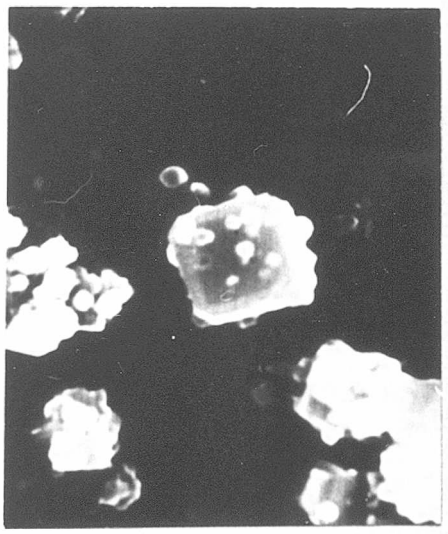

10 μm

300°C

FIGURE 4.4

Electron micrographs of 1·0%NiNaA after reduction in H_2

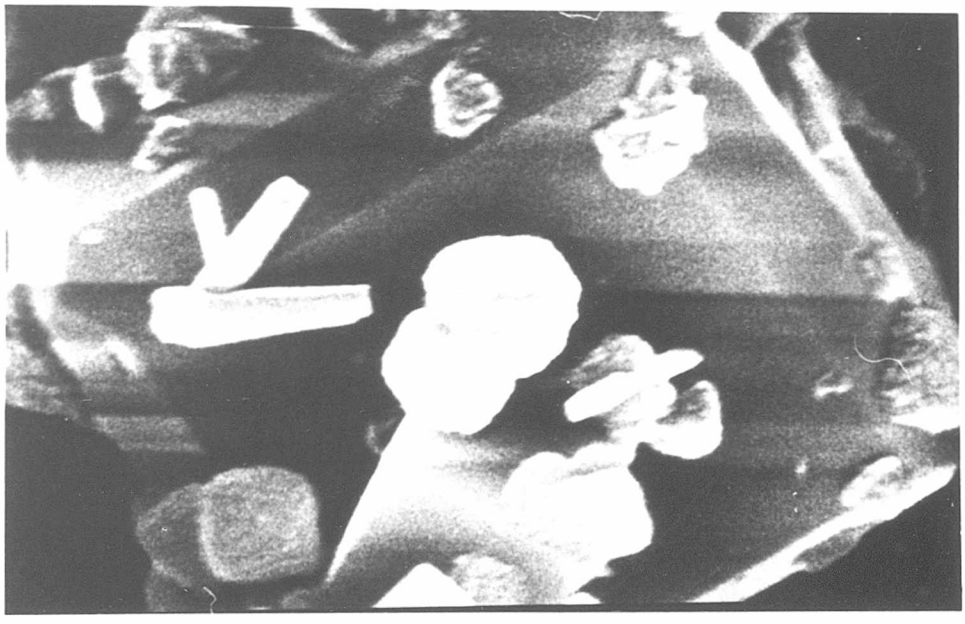

10 µm

FIGURE 4.5

Electron micrograph of "debris" surrounding 4A zeolite.

estimate of the concentration. The technique used for this was adapted from that of Wilson (3). 10mg. of the zeolite were dissolved overnight in nitric acid. The ferrous ions were then regenerated, as Fe O, by the addition of berylium sulphate and the ferric ions converted to ferrous by the addition of ascorbic acid. The pH was buffered at 5.5 using ammonium acetate and the solution made up to 100ml. with distilled water. This gave a red solution. The 525 nm. wavelength intensity was then measured and compared to that of a standard U.S. rock of known iron content.

The results of both these sets of analyses are shown in Table 4.4

As can be seen the levels of metal impurities in these samples are quite significant in comparison to the nickel content, this being particularly true for the zirconium and the iron content. These impurities could be present as either interstitial ions, impurities in the structure, or oxide impurities separate from the zeolite. However, there is no significant change in the level of impurity with percentage nickel content. Therefore, any catalytic effects should be of the same magnitude on all samples, although potentially more significant on the lower exchanged samples.

2) ENERGY DISPERSIVE X-RAY FLUORESCENCE

An energy dispersive X-ray fluorescence system (EDS) was also used for element analysis. This was carried out in the Radiochemistry section of the School of Chemistry, RGIT. The results are shown in Figures 4.6, 4.7 and 4.8. As can be seen the levels of metal impurity are similar in the three samples tested. However, there appears to be a significant quantity of iodine present in the parent zeolite which has been exchanged out of the other samples. The parent sample used had been treated as a 'blank' in the exchange process with the $Ni(NO_3)_2$ replaced by NaCl. Therefore, the iodine

TABLE 4.4

Semiquantitive Trace Element Analysis by Spark Emission Spectroscopy and Colorimetry

IMPURITY	Unexchanged/(ppm)	0.1%/(ppm)	1.0%/(ppm)
Silver	1	3	3
Barium	10	30	30
Beryllium	3	10	10
Bismuth	30	30	30
Chromium	3	3	3
Cobalt	3	3	3
Copper	3	4	10
Gallium	1	1	1
Lanthanum	10	30	30
Manganese	3	8	10
Molybdenum	1	3	3
Nickel	10	150	2000
Lead	3	3	3
Strontium	3	30	30
Tin	10	10	10
Vanadium	3	3	3
Yttrium	3	10	10
Zirconium	60	200	200
IRON (from colorimetry)	432	477	432

had not been simply washed off the crystals.

REFERENCES

1) L. BROUSSARD, D.P. SHOEMAKER, J.Amer.Chem.Soc.,82,1041,1960

2) V. PENCHEV, H. MINCHEV, V. KANAZIREV, I. TSOLOVSKI, Adv.Chem. Ser., 102,434,1971

3. A.D. WILSON, Analyst, 85,823,1960

FIGURE 4.6

ENERGY DISPERSIVE X-RAY FLUORESCENCE
ON UNEXCHANGED 4A ZEOLITE.

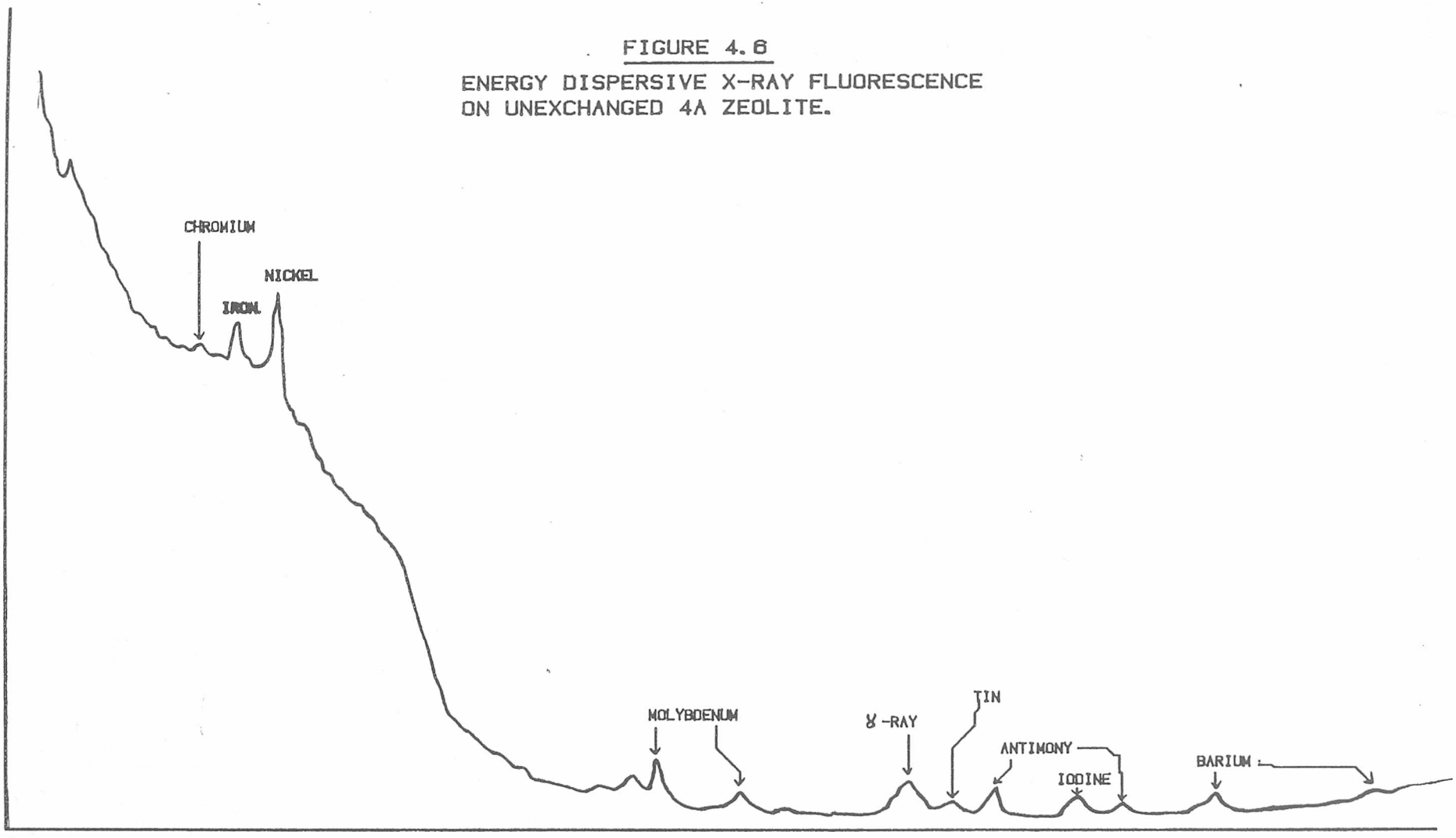

FIGURE 4.7

ENERGY DISPERSIVE X-RAY FLUORESCENCE
ON Ø.1% NICKEL EXCHANGED 4A ZEOLITE.

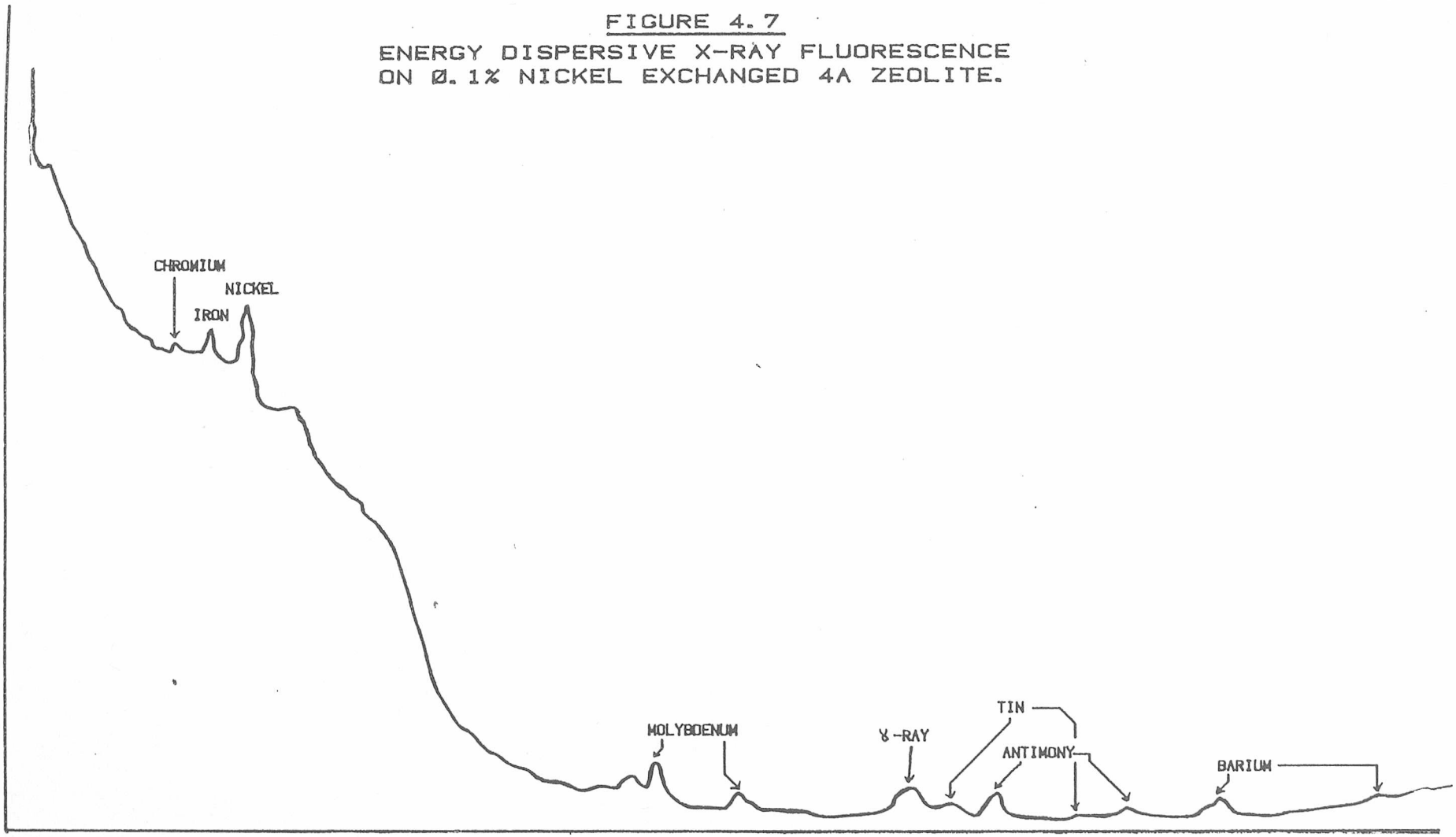

FIGURE 4.8

ENERGY DISPERSIVE X-RAY FLUORESCENCE
ON 1.0% NICKEL EXCHANGED 4A ZEOLITE.

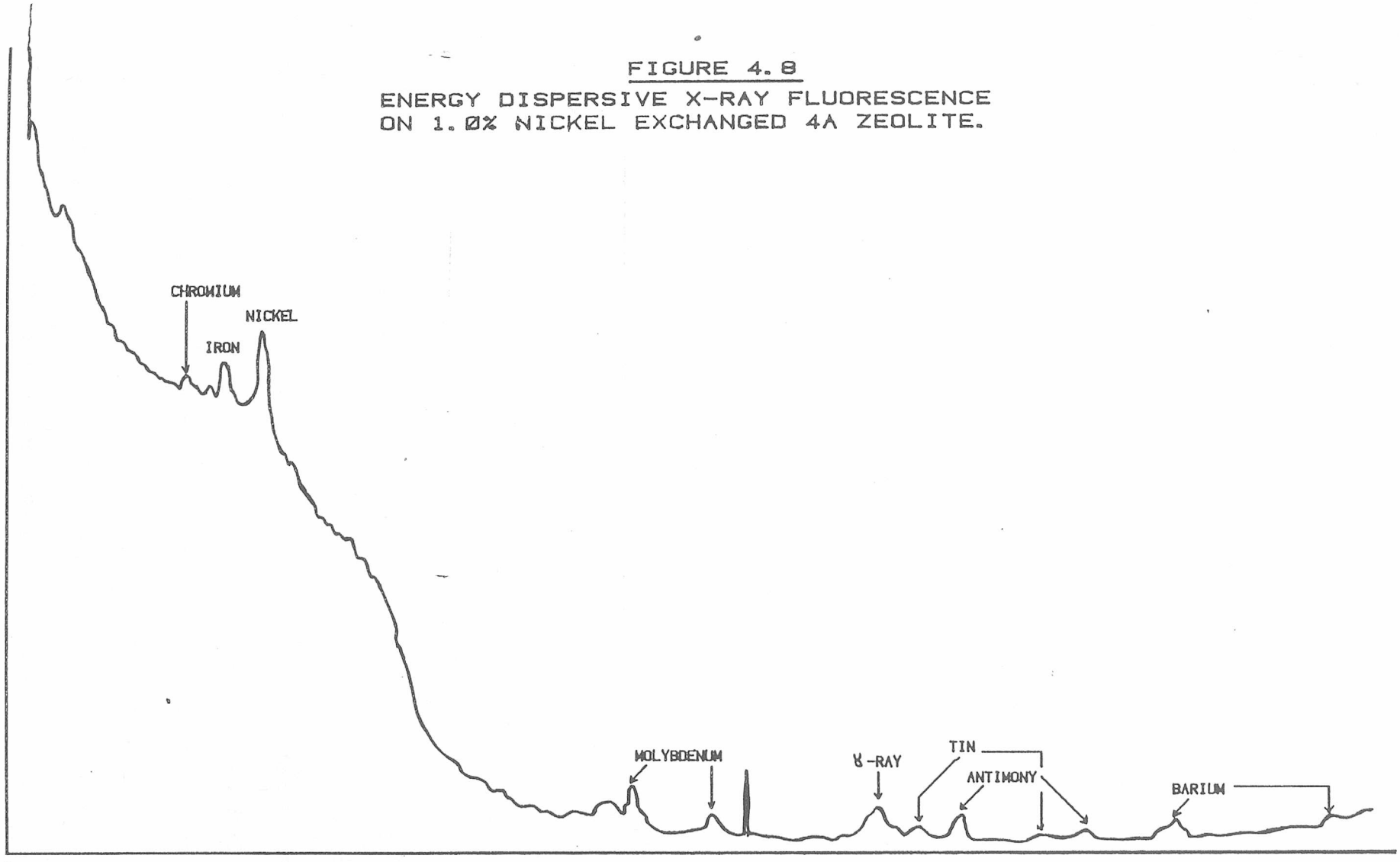

Chapter Five

APPARATUS FOR CATALYTIC STUDIES

5.1 Introduction

The kinetics of alkene hydrogenation over 4A zeolite catalysts were studied using an experimental system consisting essentially of three parts:-

a) A high vacuum gas handling system for preparation of gas mixtures of measured composition and pressure.

b) A reaction vessel with a heating system for isothermal or temperature programmed operation.

c) A sampling system to monitor the reaction vessel contents, consisting originally of a capillary leak to a mass spectrometer, but later converted to a discrete sampling system for a gas chromatograph.

5.2 Gas Handling System

Figure 5.1 is a diagrammatic representation of the gas handling system used in this work. It was constructed using pyrex glass, and all joints were lubricated with either Apiezon 'L' or 'T' vacuum grease. A vacuum of 10^{-6} Torr(10^{-4} N/m^2) was maintained by two METROVAC 022A oil diffusion pumps backed by a single EDWARDS ED50 rotary pump. The two diffusion pumps were used so that the gas handling and the reaction vessel sides of the system could be evacuated separately. However, since the two sides were connected via the rotary pump, care had to be taken not to pump contaminant materials across the backing lines during catalyst evacuation. The vacuum was monitored using the Pirani type vacuum gauge, the accuracy of which was periodically checked against a McLeod gauge. To prevent back diffusion of oil from the diffusion pumps into the system, liquid nitrogen traps (C) were inserted on their high vacuum sides. Protection against failure of the coolant water supply to

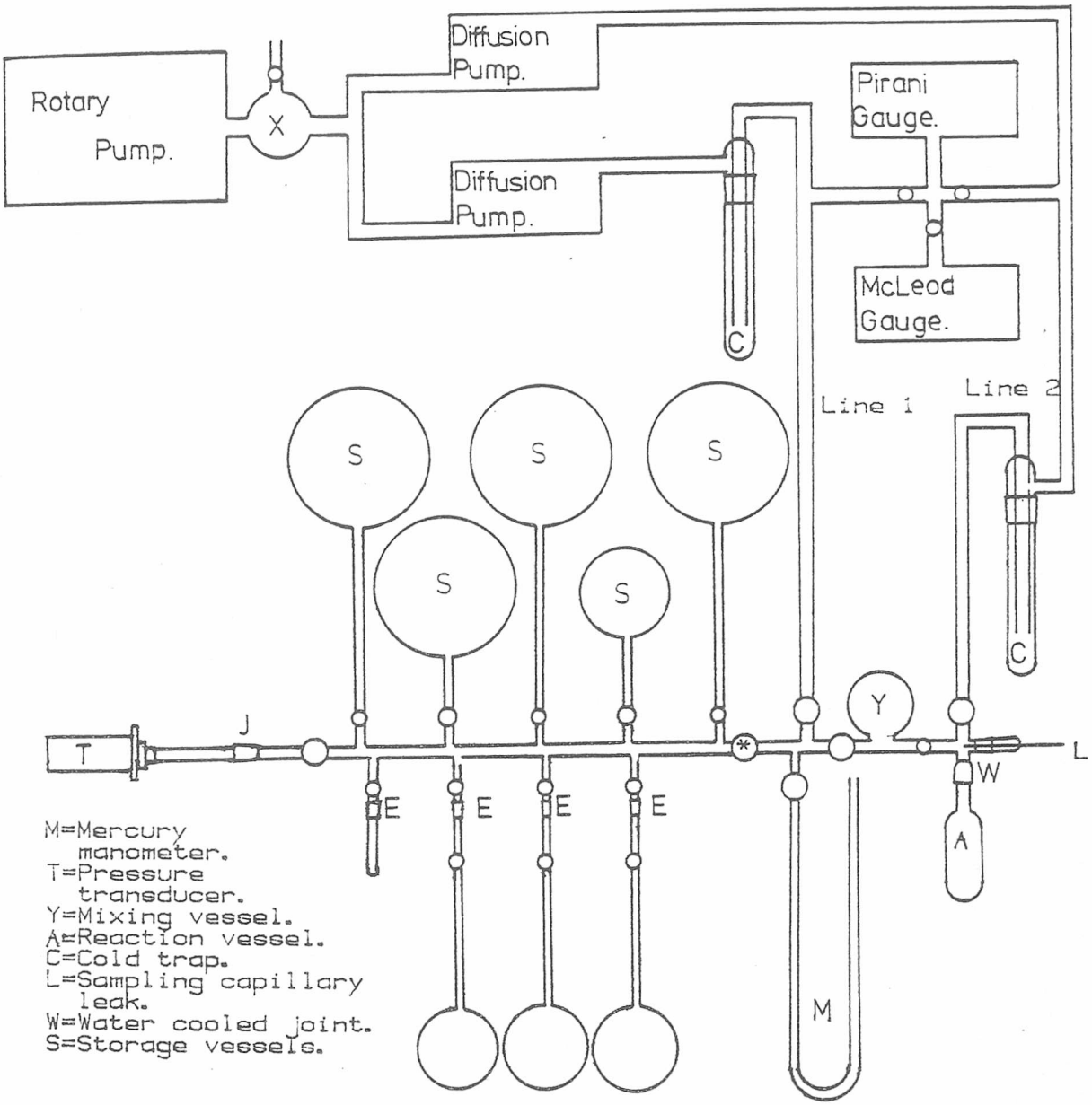

CALIBRATED VOLUMES.

WX' = Gas handling system up to tap marked * = 107 $cm.^3$

X = Gas handling system to right of tap marked * (excluding manometer) = 20 $cm.^3$

Mixing vessel = 295 $cm.^3$

Reaction vessel = 200 $cm.^3$

FIGURE 5.1

GAS HANDLING SYSTEM AND REACTION VESSEL.

the diffusion pumps and to the reaction vessel collar (W) was obtained by connecting it through the mass spectrometer protection system described in section 5.6. Failure of the electricity supply and the subsequent shutting off of the rotary pump can result in pump oil being sucked back along the pumping line. To prevent contamination of the system by such a failure a reservoir (X) of adequate volume was inserted to contain any oil so drawn back.

Hydrogen and n-butene were stored in the non-removable flasks (S). These were filled by disconnecting the pressure transducer (T) at point J and replacing it with a gas feed line. All other gases were supplied in sealed flasks which were connected into the system at points E. Reaction mixtures were made up in the mixing vessel (Y). Gas pressure being measured by either the mercury manometer (M) or the pressure transducer (T).

5.3 Gases

Hydrogen of stated purity 99.99% was supplied by B.O.C. Any residual water was removed from this by insertion of a liquid nitrogen trap into the feed line used to fill the storage flasks. N-butane was supplied by BDH Chemicals Ltd. whilst ethene, ethane, propene, propane, isobutene and isobutane were all obtained from the National Physical Laboratory. All the hydrocarbons had stated purities of 99.9%. No attempt was made to further purify them before use.

5.4 Reaction Vessel

The reaction vessel consisted of a removable pyrex cylinder, of 185 $cm.^3$ volume, connected to the system via a B14/23 ground glass joint. This was sealed with Apiezon 'T' grease and protected from heat by a water jacket around the socket. The vessel was evacuated through line 2 of the vacuum system and all gases were added by expansion from the mixing vessel (Y). The temperature was controlled by a close fitting

coil furnace connected to a EUROTHERM temperature controller with its controlling thermocouple set on the external surface of the heating coil. Reaction temperature was measured by a chromel-alumel thermocouple situated at the base of the vessel. This was connected to an L.E.D. digital voltmeter which gave a reading of approximately 0.04 mV/^{o}C. There was a significant vertical temperature gradient across the reaction vessel mainly due to the fact that:-

a) The top of the vessel was both water cooled and outside the temperature controlling furnace.

b) Neither the degree of heating along the furnace wall nor its thermal interface with the reactor were homogeneous.

This gradient was measured by placing a thermocouple at various points in the furnace. The results are shown in Table 5.1.

TABLE 5.1

Temperature Gradient of Reaction Vessel (inside furnace).

N.B. Top of vessel is always at room temperature

TEMPERATURE CONTROLLER/(K)	FURNACE POSITION BASE/(K)	MIDDLE/(K)	TOP/(K)
373	383	397	372
423	433	453	416
473	479	507	475

As can be seen the temperature gradient through the reactor is large. However, since this effect is consistent, it should not affect the comparative kinetic results. Also, since all reaction occurs on the catalyst, the temperature of greatest kinetic significance is that of the catalyst. Therefore, the more general kinetic results will be valid, within experimental limits, because the catalyst is

at the base of the reactor close to the measuring thermocouple.

This temperature gradient was to some extent useful because it aided mixing of the gas phase. This was especially true since the reaction was occurring at the base of the reactor, whilst samples were taken from point L at the top of the reactor.

5.5 Volume Calibration

The volumes of various sections of the gas handling system were measured by expansion of air into them from a bulb of known volume. The volume of the calibration bulb was found to be 560 cm^3 by measurement of its water capacity. Thus, by measuring the change in pressure as the air was released from the bulb into the evacuated sections of the system their volumes could be calculated from Boyles Law:-

$$P_1 \ V_1 = P_2 \ (V_1 + V_2)$$

The volumes thus calibrated are shown on Figure 5.1.

5.6 Analysis of Reaction Mixture

Originally progress of reaction was monitored using an AEI MS10 mass spectrometer. However, due to low stability and frequent malfunction of the instrument it was decided to replace this with a gas chromatograph. The gas chromatograph analysis had a slower sampling rate than the mass spectrometer, but gave more reliable results. Details of the two analysis systems are presented below.

5.7 Mass Spectrometer

Continuous sampling to the mass spectrometer was effected by a capillary leak, attached into the system as shown in Figure 5.1. Two types of leak were used, both of which are tapered to maintain a pressure of approximately 5×10^{-6} Torr in the mass spectrometer during

analysis (in the absence of sample the mass spectrometer pressure was normally 10^{-9} Torr). The first leak was a stainless steel capillary tubing flattened at one end to allow the correct flow rate. This was cemented with 'Araldite' into a B10/19 ground glass cone. The other was a drawn pyrex leak glass blown into a similar cone. The change was made when the original steel leak was blocked. The advantage of the glass leak was that although it was more fragile the flow rate was readily adjusted by chipping small fragments of its tip.

A block diagram of the MS10 mass spectrometer is shown in Figure 5.2. The vacuum was maintained by a METROVAC 033 GDR1 mechanical rotary pump. Back diffusion from this system into the spectrometer tube was prevented by a 2.5 litre liquid nitrogen trap. To prevent overheating of the diffusion pump in the event of failure of the coolant water supply, a water pressure sensitive relay was installed on the inlet side of the mass spectrometer water supply. This cut the electricity supply to all the diffusion pumps (including those of the gas handling system) if the water pressure dropped below a set minimum value. A second device was attached to the water outlet to cut off the water supply if the coolant system sprung a leak. This consisted of a reservoir into which the water from the system flowed. An adjustable tap in the base of the reservoir was set to maintain a constant water level so that inlet and outlet flow were identical. Under these conditions a ballcock valve was held open to maintain water flow. However, if the flow from the cooling system slowed or stopped the level in the reservoir fell and the supply was cut. The overall layout of this system is shown in Figure 5.3. The diffusion pump was protected from exposure to high pressure, and subsequent oxidation of the pump oil, by the insertion of a solenoid valve between it and the rotary pump. This valve closed automatically

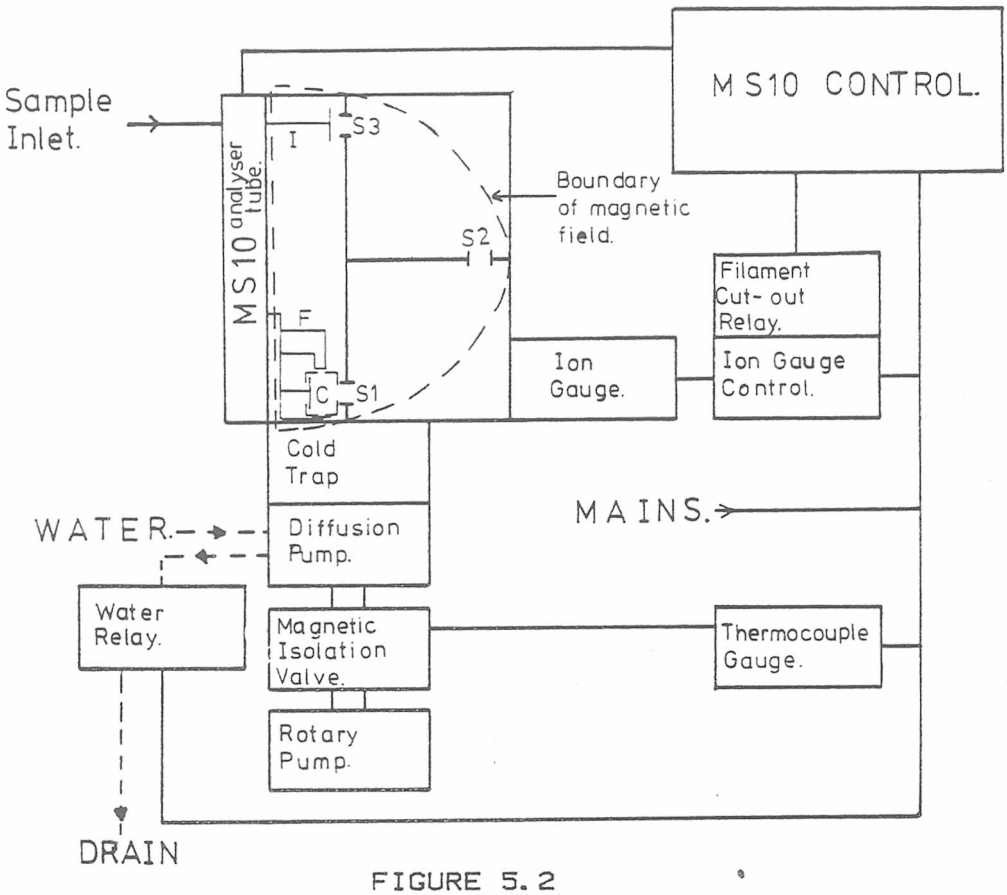

FIGURE 5.2

BLOCK DIAGRAM OF MS10 MASS SPECTROMETER.

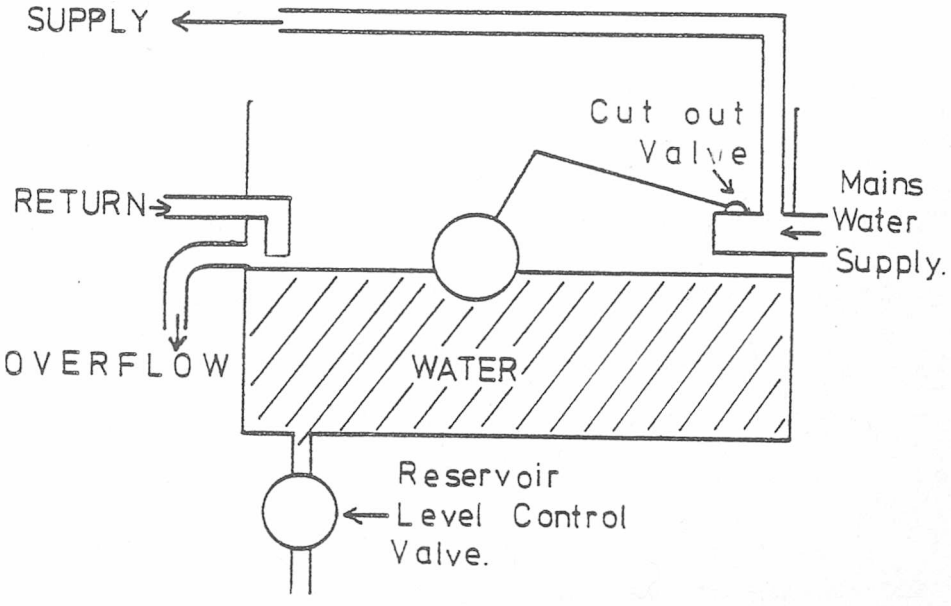

FIGURE 5.3

COOLANT SYSTEM SAFETY RESERVOIR.

if the rotary pump power supply was cut off.

The high vacuum section of the spectrometer could be baked to about 300°C using band heaters and a radiation shield. This reduced background interference in the spectra by desorbing residual molecules collected on the internal surfaces of the system.

Gas for analysis enters the spectrometer tube via the sample inlet shown in Figure 5.2. It is first ionised in the source cage 'C' by bombardment by an electron beam produced by the hot wire filament 'F'. The resulting positive ions are then accelerated, by a voltage applied between the cage and the exit slit 'S1', into a uniform magnetic field created by a large permanent magnet surrounding the analyser tube. The ions then describe a circular orbit in this field such that:

$$R^2 = \frac{M}{e} \quad \frac{2V}{H^2}$$

R = radius of orbit
M = mess) of ion
e = charge)
V = accelerating voltage
H = magnetic field of strength

Thus the ion beam is separated into beams of specific mass to charge ratios (m/e). By varying the voltage (V) the orbits can then be varied to bring different individual beams to focus on the collector plate 'I'. This registers the ion impacts on its surface as a current flow. The size of the current being proportional to the number of ions hitting the plate. The resolution and sensitivity of the mass spectrometer are controlled mainly by the size of the slits 'S1', 'S2', and 'S3', called respectively the resolving, defining and collector slits.

5.8 Gas Chromatograph

Initially a single gas chromatograph was used to measure the hydrocarbon concentrations in the reaction vessel. However, a column suitable for fast repetitive analysis of C_2 to C_4 hydrocarbons was not readily and economically available. Therefore, to allow complete

hydrocarbon analysis a twin system was devised. The units of this could be used individually during single alkene runs, or alternately during competitive reactions. One chromatograph was used to separate ethene and ethane, whilst the other separated the higher hydrocarbons. A discrete sampling system was used with an injection system designed to feed the sample to one or other of the chromatographs without interrupting the carrier gas flow to either. Figure 5.4 shows a diagram of the switching system along with the operating procedure. The maximum sampling rate for this system was one sample every 2.5 minutes, due to the speed of re-evacuation of the sample loop. Both GC's consisted of a packed column held in an oven, the temperature of which was controlled by an F&M mode 240 power proportioning temperature programmer operating isothermally. The carrier gas was nitrogen split from a single source by a stream splitter at point S (Figure 5.4). Detection was performed by flame ionisation detectors at the outlets of each column. The signals from these were amplified by a pair of E.I.L. Model 56A Vibron Flame Detector amplifiers, and recorded on a servoscribe 25 twin pen chart recorder.

GC1 contained PORAPAK Q and was maintained at a temperature of 50C. This separated ethene and ethane well, and also was initially used to separate propene and propane although this was unsatisfactory due to very long retention times. GC2 contained n-OCTANE on PORASIL C at temperatures of 23C and 30C. 30C was used when isobutene and isobutane only were being separated, whilst 23C was used if propene/propane and/or n-butene/n-butane were also required.

5.9 Effect of Discrete Sampling on Kinetic Analysis

The continuous sampling from the reaction vessel to the mass spectrometer maintained a pressure of less than 10^{-5} Torr in the spectrometer and therefore used only a very small amount of the reactant gases. Thus no major effect on reaction kinetics due to

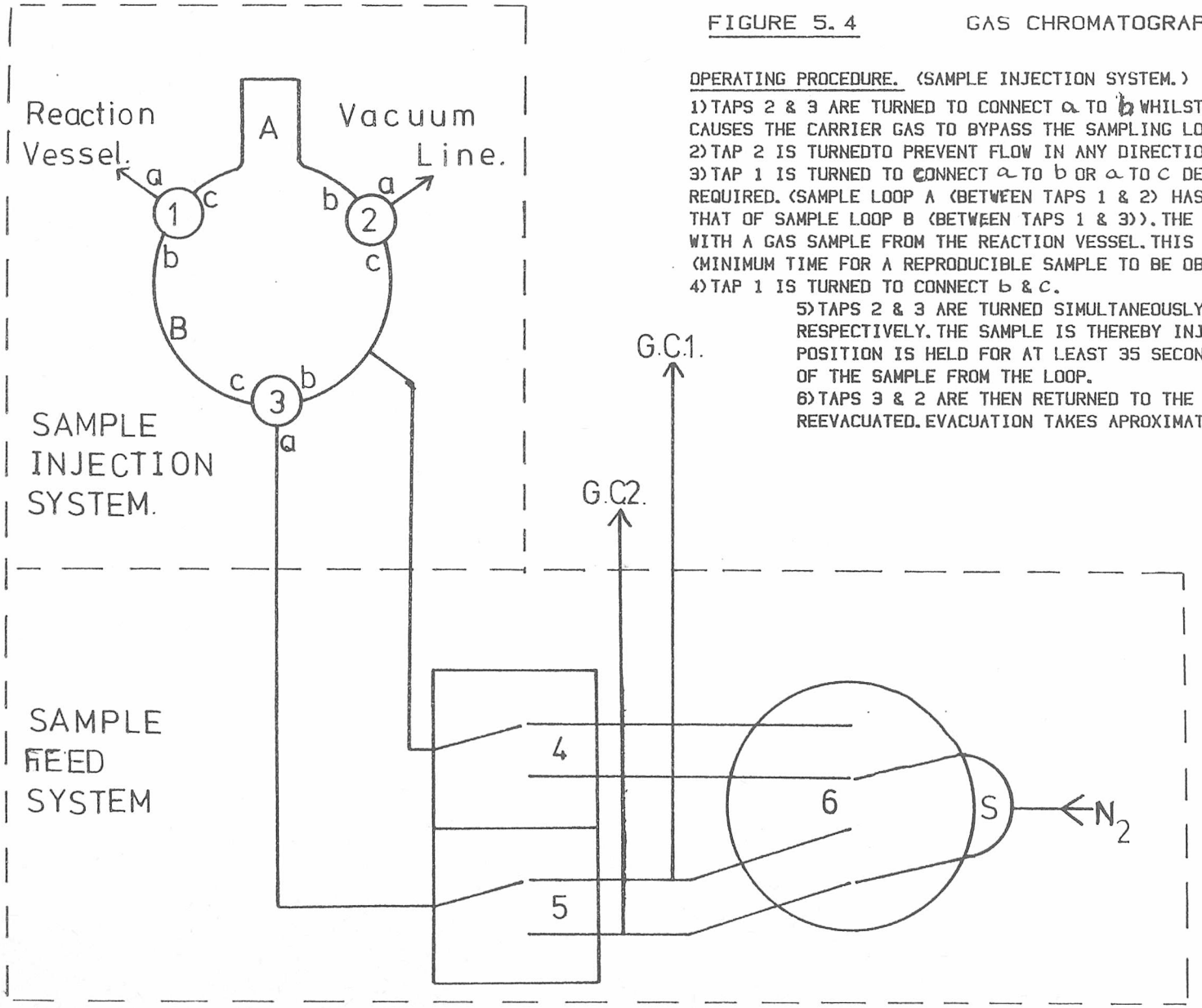

FIGURE 5.4 GAS CHROMATOGRAPH SAMPLING SYSTEM.

OPERATING PROCEDURE. (SAMPLE INJECTION SYSTEM.)

1) TAPS 2 & 3 ARE TURNED TO CONNECT a TO b WHILST TAP 1 CONNECTS b TO c. THIS CAUSES THE CARRIER GAS TO BYPASS THE SAMPLING LOOPS WHILST A & B ARE EVACUATED.
2) TAP 2 IS TURNEDTO PREVENT FLOW IN ANY DIRECTION.
3) TAP 1 IS TURNED TO CONNECT a TO b OR a TO c DEPENDING ON THE SAMPLE VOLUME REQUIRED. (SAMPLE LOOP A (BETWEEN TAPS 1 & 2) HAS A VOLUME OF APROXIMATELY 3X THAT OF SAMPLE LOOP B (BETWEEN TAPS 1 & 3)). THE CHOSEN SECTION IS THUS FILLED WITH A GAS SAMPLE FROM THE REACTION VESSEL. THIS POSITION IS HELD FOR SIX SECONDS (MINIMUM TIME FOR A REPRODUCIBLE SAMPLE TO BE OBTAINED).
4) TAP 1 IS TURNED TO CONNECT b & c.
5) TAPS 2 & 3 ARE TURNED SIMULTANEOUSLY TO CONNECT b & c, AND a & c RESPECTIVELY. THE SAMPLE IS THEREBY INJECTED INTO THE SYSTEM. THIS POSITION IS HELD FOR AT LEAST 35 SECONDS TO ENSURE COMPLETE REMOVAL OF THE SAMPLE FROM THE LOOP.
6) TAPS 3 & 2 ARE THEN RETURNED TO THE POSITIONS SHOWN AND THE SECTION REEVACUATED. EVACUATION TAKES APROXIMATELY 1 MINUTE 45 SECONDS.

OPERATING PROCEDURE. (SAMPLE FEED SYSTEM.)

WITH THE FEED SYSTEM SWITCHES (4, 5 & 6) IN THE POSITIONS SHOWN CARRIER GAS IS FED DIRECTLY TO GC2 WHILST GC1 IS FED VIA THE SAMPLE INJECTION SYSTEM. WHEN ALL THREE SWITCHES ARE SIMULTANEOUSLY REVERSED THE CARRIER GAS TO GC2 FLOWS THROUGH THE INJECTION SYSTEM WHILST GC1 IS FED DIRECTLY.

pressure changes would occur. The discrete sampling for the gas chromatograph, however, required significant amounts of reactant gas. Therefore, care had to be taken not to allow any large drop in reactor pressure with sampling since this could affect the rate of reaction.

Consider alkene hydrogenation. From the discussion in Section 3.6, it can be seen that the reaction is between first and second order. Pressure changes would affect the kinetics of a second order reaction more than those of a first. Therefore, for the most pressure sensitive case:-

$$R_i = k\,(C_2H_4)_i\,(H_2)_i \qquad \text{where } i = \text{value for initial sample}$$

$$R_f = k\,(C_2H_4)_f\,(H_2)_f \qquad \text{where } f = \text{value for last sample}$$

If the rate of reaction is not to drop by more than 10% due to pressure changes then, assuming consumption of gas due to reaction is negligible, the ratio of R_i and R_f must be such that: -

$$\frac{R_f}{R_i} = 0.9$$

if z is then defined as the fraction of the original gas remaining after the last sample, it can be seen that: -

$$(C_2H_4)_f\,(H_2)_f = (C_2H_4)_i\,z\,(H_2)_i\,z = (C_2H_4)_i(H_2)_i\,z^2$$

$$\frac{R_f}{R_i} = \frac{(C_2H_4)_i\,(H_2)_i\,z^2}{(C_2H_4)_i\,(H_2)_i} = 0.9$$

$$z^2 = 0.9$$

$$z = 0.949$$

Now the fractional pressure drop in the gas phase will be 1 - z. Therefore:

$$1 - z = 0.051$$

Therefore, the maximum pressure drop to allow a maximum rate variation of 10%, is 5%

In this work sample volume B as shown on Figure 5.4, was used. This has a capacity of 0.2 cm^3. Whilst the reaction vessel has a capacity of 200 cm^3. Therefore, from Boyles Law:-

$$P_1 = P_2 \quad \frac{200}{200.2}$$

Thus the fractional pressure drop/sample = y = 1 - 200/200.2

= 0.000999

and the % drop/sample = 0.099%

Since the pressure after one sample = P_1 x (1-y)

where P_1 = original pressure

it can be seen that:

Pressure after n samples = $P_n = P_1 \times (1-y)^n$

therefore:

$$N = \frac{\ln(P_n/P_1)}{\ln(1-y)}$$

thus the maximum permissible No. of samples for a 10% rate drop, n(max)

$$= \frac{\ln(0.95)}{\ln(1-0.000999)}$$

= 51.3 = 51 samples

By measurement of the change in peak height with no. of samples in a non-reactive mixture of alkene and hydrogen (i.e. no catalyst present) the experimental value of y was found to be 0.173%/sample. This is higher than the calculated value but still gives a safe n(max) of 30.

Chapter Six

EXPERIMENTAL PROCEDURES AND DATA ANALYSIS

6.1 Introduction

In this work a standardised experimental procedure was used so as to minimise variation from parameters other than those under study. All catalysts were pretreated in an identical manner and the gas mixtures were made up identically unless otherwise stated.

6.2 Pretreatment of Catalysts

Catalysts were stored over a saturated solution of calcium nitrate to ensure complete hydration. For reaction work, 0.1g (hydrated weight) samples were weighed in a weighing scoop on a three figure SARTORIUS top pan balance. The weights obtained were accurate to within .003g. Samples were transferred to the reaction vessel which was then connected to the gas handling system described in Chapter 5.2. Slow evacuation at room temperature was performed over a period of about 15 minutes. Care had to be taken over this evacuation because a rapid pressure drop resulted in 'jumping' of the catalyst due to desorption of gases from the zeolite. The furnace was then placed around the vessel, the temperature raised to $350(\pm 5)^{\circ}C$ over a period of approximately 30 minutes, and evacuation continued for 15 to 16 hours to dehydrate the catalyst.

The reaction system was isolated and the furnace control reset to the temperature chosen for catalyst reduction. This being either 200, 250, 300 or 400C. The system was then left to equilibrate. 100 mmHg pressure of hydrogen was measured into the mixing vessel and released into the reaction vessel. The reactor was isolated and reduction allowed to proceed for one hour. The system was then re-evacuated for three minutes.

To set the system at the initial reaction temperature the furnace was removed from the reaction vessel, cooled to below the desired temperature, replaced and allowed to reheat to the set temperature. This procedure was used, rather than simply allowing the furnace to cool, since it was found to be much faster.

6.3 Gas Mixtures

In the following section all the gas handling volumes are designated as in Figure 5.1 of Chapter Five.

All gas mixtures were first mixed in the mixing vessel (Y) before release into the reaction vessel (A). Normally an approximate 20:1 ratio of hydrogen to alkene was used. This was measured as follows:-

1) 41 mmHg of alkene were measured into WX'.
2) This was expanded into X+Y, resulting in a pressure of 10mmHg.
3) Y was isolated and the rest of the system evacuated with the liquid nitrogen removed from the cold traps. The removal of the nitrogen was found to be necessary because the alkenes partially condensed in the traps and tended to desorb slowly and diffuse back into the system.
4) 666 mmHg of hydrogen was measured into WX'X.
5) This was expanded into Y as quickly as possible to prevent backflow of alkene from Y. This resulted in an overall pressure in Y of 204 mmHg. 10 mmHg of alkene and 194 mmHg of hydrogen.

The mixture thus obtained could then be expanded into the reaction vessel (A) when desired.

6.4 Moles of Gas in Reaction Vessel

The number of moles of reactants in the reaction vessel was calculated using the ideal gas equation:-

$$PV = nRT$$

and Boyles's Law:-

$$P_1V_1 = P_2V_2 \quad \text{at constant temperature}$$

If Y and A were at the same temperature then since the volume of Y=295 cm^3 and the volume of A=200 cm^3 then:-

$$P_A = \frac{295\ P_Y}{295+200}$$

where P_A = pressure in A when gas from Y released into evacuated vessel

P_Y = initial pressure in Y.

and the number of moles of gas in A=n = $\frac{P_AV_A}{RT}$

which gives:-

No. moles hydrogen in A during reduction = 6.33×10^{-4}

No. moles alkene in A during reaction = 6.33×10^{-5}

No. moles hydrogen in A during reaction = 1.23×10^{-3}

But the reaction vessel is always hotter than the mixing vessel during reduction and frequently so during reaction. Therefore, the above calculations are not entirely correct. It can be argued that when they are released into the reaction vessel the gases are at the same temperature as Y and do not have time to absorb the heat of the reaction vessel before it is sealed. If this were true then the above calculations would be correct. However, to ensure that the error induced by this simplification is not too large a simple check was carried out. Assuming a reaction vessel temperature of 200°C; well above the maximum reaction temperature used in this work; then for the value of P_A obtained from the previous calculation, there would be 3.99×10^{-5} moles of alkene present in A. Thus, although it is an outside limit, this possible inaccuracy must be kept in mind when quantitative analysis of alkene concentrations are performed.

6.5 Kinetics and Order

Alkene hydrogenation over nickel catalysts exhibits an inversion of the apparent activation energy between 90°C and 170°C. The cause of this effect is discussed in Chapter 3.5 and 3.6, but for the kinetic analysis the important point to note is the reaction order. Although the reaction is always first order with respect to hydrogen, it gradually changes from zero or fractional order below inversion to first order above inversion with respect to alkene.

In this work a similar effect was found at around 170°C. However, most experimental work was performed at temperatures below that of inversion. Therefore, rate constants were generally calculated assuming zero order with respect to alkene and first order with respect to hydrogen:-

$$\text{RATE} = \frac{-d[C]}{dt} = k_1 [H_2]$$

where $[C]$ = alkene concentration
t = time
$[H_2]$ = hydrogen concentration
k_1 = first order rate constant

For a catalysed reaction the rate will also depend on the number of active sites available for reaction, which in turn will depend on the amount of catalyst present. Thus:-

$$\frac{-d[C]}{dt} = k_1' g [H_2] \quad \text{where } g = \text{amount of catalyst}$$

In all experiments $[H_2]$ was kept very much greater than $[C]$ and was therefore effectively constant:-

$$\frac{-d[C]}{dt} = k_o g \qquad \text{where } k_o = k_1' [H_2] = \text{apparent zero order rate constant.}$$

(It should be noted here that the rate is still dependent on $[H_2]$ and will vary if changes in the amount of hydrogen input to the system are made.)

This integrates to give:-

$$[C] = -k_o g t + [C_o] \qquad \text{where} \quad [C_o] = \text{initial concentration}$$

Multiplying by 100 and dividing by $[C_o]$ gives:-

$$\frac{100C}{[C_o]} = -k_o' g t + 100 \qquad \text{where } k_o' = 100k_o/[C_o] = 100k_1[H_2]/[C_o]$$

$100C/C_o$ is the percentage of the original alkene left after time t. Therefore, a graph of (% initial alkene concentration remaining) vs. time was used to obtain a straight line of slope = $-k_o' g$. Such that:-

$$k_o' = \frac{-\text{slope}}{g} \quad \% \text{ /min./gram.}$$

which represents the percentage of the original amount of reactant $[C_o]$ which is reacted each minute in the presence of one gram of catalyst. This is not the true rate constant since it is dependent on the initial concentrations of both reactants. However, since relative rather than absolute rate values were needed in this work the above constant was used. For the majority of experiments where:

$$[H_2] = 1.23\times10^{-3} / 200\times10^{-3} = 0.615 \text{ Moles M}^{-2}$$

and $$[C] = 6.33\times10^{-5} / 200\times10^{-3} = 3.165\times10^{-2} \text{ Moles M}^{-2}$$

the constant was used unaltered. However, for compatibility, values of k_o' obtained using other reactant concentrations had to be multiplied by:-

$$\frac{[C]}{0.615\times10^{-2}} \times \frac{[H_2]}{3.165}$$

Since the rate below inversion for hydrogenation over nickel is only approximated to zero order and in fact will be between zero and one (see Chapter 3.5) a number of results were treated using first order kinetics to determine what the effect of the approximation would be:-

$$\text{RATE} = \frac{-d[C]}{dt} = k_2 g [H_2][C] \qquad \text{where } k_2 = \text{second order rate constant.}$$

assuming $[H_2]$ to be constant:-

$$\frac{-d[C]}{dt} = k_1'g[C] \quad \text{where} \quad k_1' = [H_2]k_2$$

This gives:-

$$\ln[C] = -k_1'gt + \ln[C_o]$$

adding $\ln(100/[C_o])$ to both sides gives:-

$$\ln(100[C]/[C_o]) = -k_1'gt + \ln(100)$$

Thus a graph of ln(% of original alkene concentration) vs. time was used to obtain a straight line of slope $-k_1'g$, such that:-

$$k_1' = \frac{-\text{slope}}{g} \text{ /min./gram.}$$

This can be represented as a percentage:-

$$k_1' = \frac{-100\text{slope}}{g} \text{ \%/min./gram.}$$

which represents the percentage of the amount of alkene present at time t which will react in one minute.

Like k_o', k_1' is dependent on $[H_2]$ although not on alkene.

6.6. Kinetic Treatment During Extensive Adsorption of Alkene

The kinetic treatment described in the last section depends on the gas phase concentration (reactant + product) remaining approximately constant. In some instances it was found that adsorption of the alkene was so great, whilst that of the alkane remained low, that the overall gas phase hydrocarbon concentration was increased by four or five times as the reaction proceeded. When this occurred a second analysis technique, compatible with the normal one was used. Consider the zero order rate equation outlined in Chapter 6.5:-

$$\frac{100C}{[C_o]} = -k_o'gt + 100$$

assuming $[H_2]$ to be constant:-

$$\frac{-d[C]}{dt} = k_1'g[C] \quad \text{where} \quad k_1' = [H_2]k_2$$

This gives:-

$$\ln[C] = -k_1'gt + \ln[C_o]$$

adding $\ln(100/[C_o])$ to both sides gives:-

$$\ln(100[C]/[C_o]) = -k_1'gt + \ln(100)$$

Thus a graph of ln(% of original alkene concentration) vs. time was used to obtain a straight line of slope $-k_1'g$, such that:-

$$k_1' = \frac{-\text{slope}}{g} \text{ /min./gram.}$$

This can be represented as a percentage:-

$$k_1' = \frac{-100\text{slope}}{g} \text{ \%/min./gram.}$$

which represents the percentage of the amount of alkene present at time t which will react in one minute.

Like k_o', k_1' is dependent on $[H_2]$ although not on alkene.

6.6. Kinetic Treatment During Extensive Adsorption of Alkene

The kinetic treatment described in the last section depends on the gas phase concentration (reactant + product) remaining approximately constant. In some instances it was found that adsorption of the alkene was so great, whilst that of the alkane remained low, that the overall gas phase hydrocarbon concentration was increased by four or five times as the reaction proceeded. When this occurred a second analysis technique, compatible with the normal one was used. Consider the zero order rate equation outlined in Chapter 6.5:-

$$\frac{100C}{[C_o]} = -k_o'gt + 100$$

Assuming no side reactions occur:-

$$[C] = [C_o] - p \qquad \text{where } p = \text{alkane concentration}$$

Substitution gives:-

$$\frac{100([C_o]-p)}{[C_o]} = -k_o' gt + 100$$

and thus k_o' can be obtained. Note that this value is only compatible with the one obtained via the other method provided that no side reactions occur. And therefore it was only used provided that no side reactions were detected.

6.7 Induction Period

In many reactions carried out in this work a distinct induction period was found to be present at the beginning of the reaction. This was quantified by defining the induction period, I, to be the time axis value of the intercept of the slopes of the %alkene vs. time plot during and after induction. This is shown in Figure 6.1. The overall rate under these conditions was defined, as before, as the percentage of the initial alkene concentration reacted/second. But the slope was taken as the slope after the induction was over.

6.8 Isothermal and Temperature Programming Techniques

To obtain the rate constants outlined in Section 6.5, %alkene vs. time results were required. Two experimental techniques were utilized in this work. These were:-

1) ISOTHERMAL REACTION:-

   Where reactants were introduced to the catalyst at a preset temperature, and the temperature maintained throughout the reaction.

2) TEMPERATURE PROGRAMMED REACTION:-

   Where reactants were introduced to the catalyst at a preset temperature but when adsorption and reaction rate had reached a

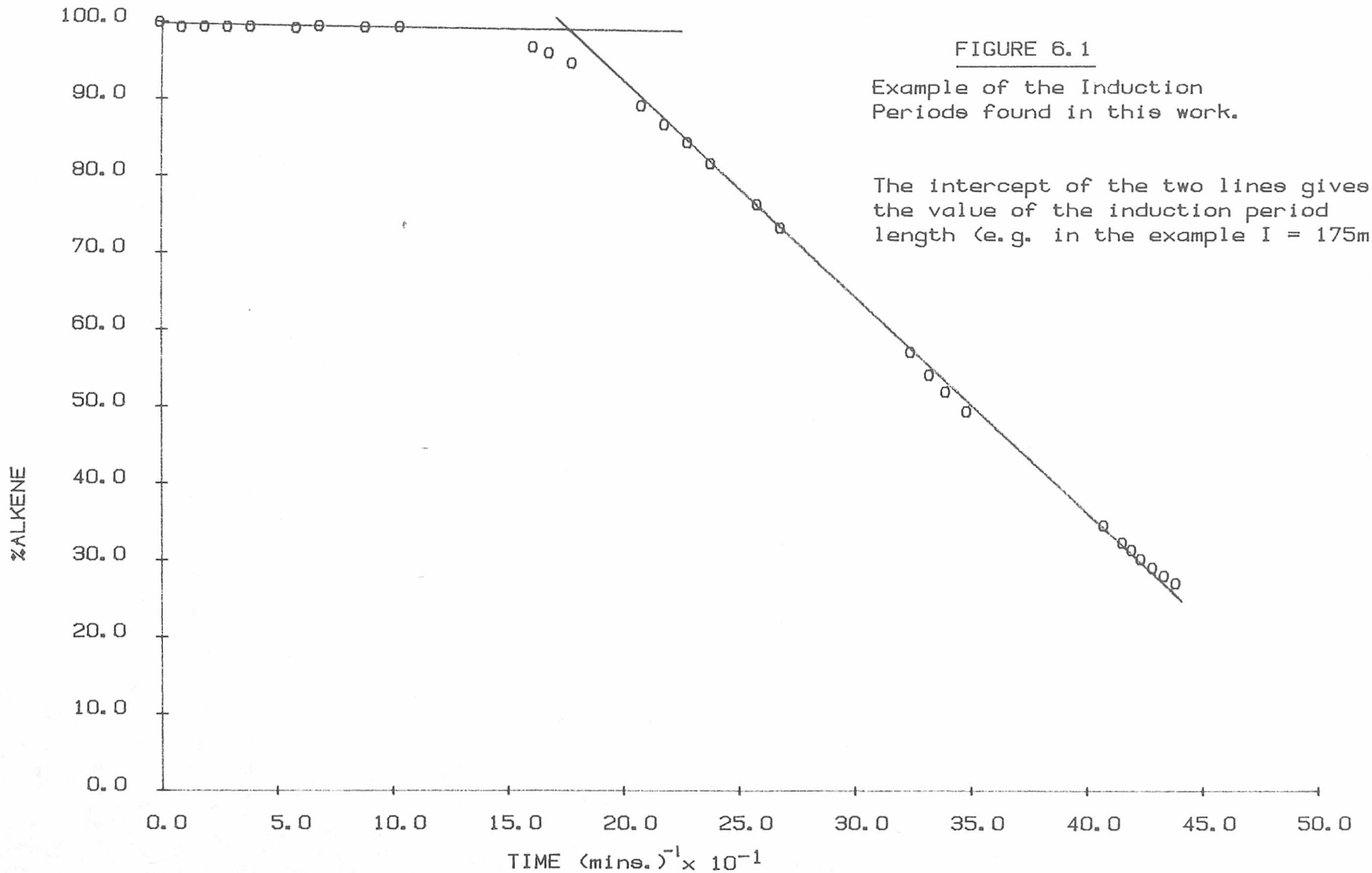

FIGURE 6.1

Example of the Induction Periods found in this work.

The intercept of the two lines gives the value of the induction period length (e.g. in the example I = 175mins)

steady state the temperature was increased at a steady rate.

During both these methods the alkene concentration was measured as 100(alkene in the gas phase)/(alkene + alkane in the gas phase). This can only be used to obtain the rate constants if there is no significant carbon loss by adsorption or side reactions such as cracking, polymerization, or surface carbide formation. A check that this did not occur was kept by:-

a) Checking the gas phase for the presence of higher and lower hydrocarbons.

b) Plotting graphs of raw alkene data vs. raw alkane data (the raw data being M.S. or G.C. peak heights in arbitrary units, see Section 7.8) and checking them for linearity. The slope should also give the relative sensitivities for the alkane and the alkene (see next section).

Isothermal rate constants were obtained by treatment of results as outlined in Section 6.5, whilst results from Temperature Programming were treated as follows. The plot of %alkene vs. time is curved due to the change in the rate constant with temperature. The rate constant for a given temperature was therefore obtained by taking the tangent of the curve at the time when the reactor was at the specified temperature. An example of this is shown in Figure 6.2. For first order results a plot of ln(%alkene) vs. time was used.

The advantage of temperature programming is that the rate constants for a reaction over a complete temperature range, and therefore the Arrhenius plot can be obtained from a single experiment. This is faster than a series of isothermal runs and also the activation energy is less likely to contain errors due to catalyst irreproducibility. However, caution must be exercised when using this technique because for valid results the programming rate must be low enough for all the

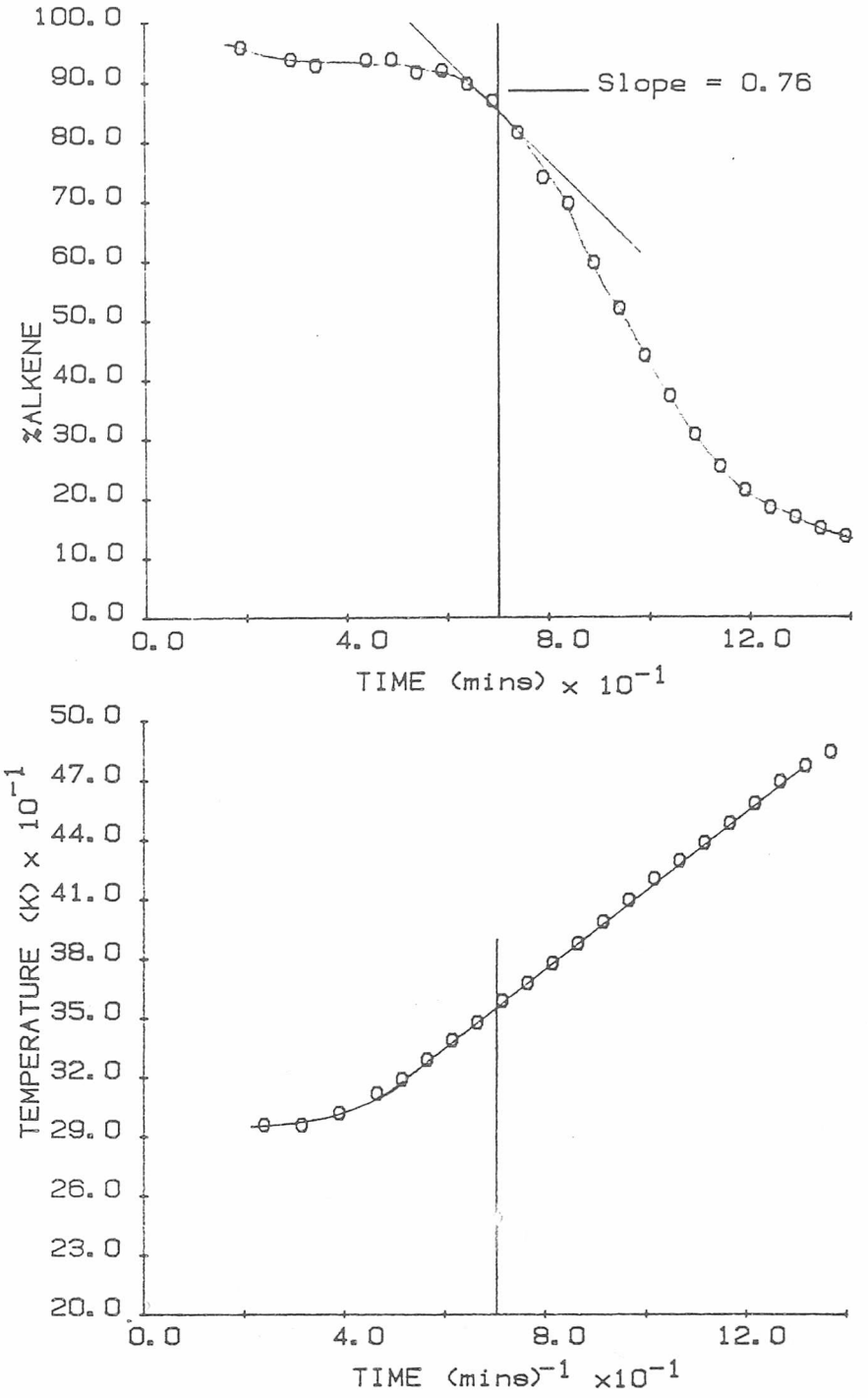

METHOD FOR CALCULATION OF RATES FROM NON-ISOTHERMAL DATA.
(e.g. rate at 352K = 0.76 %/min.)

FIGURE 6.2

surface conditions on the catalyst, such as adsorption, to be at equilibrium.

6.9 Calculation of %Alkene from Raw Data

%Alkene values were calculated from the raw data obtained from the mass spectroscopic and gas chromatographic analyses described in Chapter 5.7 and 5.8 as follows:

1) MASS SPECTROMETRY:

With no side reactions mass spectroscopic data gave percentage alkene via the equation:-

$$\%\text{ALKENE} = \frac{100(\text{alkene peak height} - \text{fragmentation})}{(\text{alkene pk.ht.} - \text{fragmentation}) + (\text{RS} \times \text{alkane pk.ht.})}$$

where RS is a sensitivity factor used to compensate for the difference in ionisation efficiencies of the alkane and alkene. The FRAGMENTATION subtraction comes about because during ionisation of molecules, fragmentation occurs creating characteristic 'fragmentation patterns' for various molecules. Alkanes are only two mass units heavier than their respective alkenes and so major alkane fragmentation peaks often lie on the alkene parent m/e value and therefore must be subtracted from that peak.

Both these factors are obtained from calibrations by measuring the peak heights and fragmentation patterns of measured amounts of alkane and alkene such that:-

$$\text{RS} = \frac{\text{alkene peak height}}{\text{alkane peak height}} \times \frac{\text{alkane concentration}}{\text{alkene concentration}}$$

and

$$\text{FRAGMENTATION} = \left[\frac{\text{fragment peak height}}{\text{parent peak height}}\right]_c \text{parent peak height}$$

where c = calibration data.

The magnitude of these corrections was minimised by reducing the energy of the ionising electron beam. However, as this is decreased, ionisation efficiency is reduced and both the sensitivity and reproducibility fall. It was found that the minimum ion beam energy that allowed reasonable sensitivity was a nominal 10eV for ethene/ethane and 5eV for propene/propane. This gave approximate values for fragmentation of alkane on alkene of 2.5 and 0.1 respectively. The exact values had to be recalibrated frequently due to instability of the system causing variations in the electron beam energy.

2) GAS CHROMATOGRAPHY:

For gas chromatography results the equation for %alkene is basically the same as for mass spectrometry except that there are no fragmentation corrections and peak area should be used:-

$$\%\text{ALKENE} = \frac{\text{alkene peak area}}{\text{alkene peak area} + (\text{RS} \times \text{alkane peak area})}$$

here the sensitivity factor is used to compensate for differences in the detector sensitivity to the different species. However, as will be shown in section 6.11, peak area can be replaced by the more easily measured peak height provided that a sensitivity factor which allows, not only for detector sensitivity, but also peak width, is used. This factor is obtained by the same technique as mass spectrometry, such that for a measured amount of alkane and alkene:-

$$\text{RS} = \frac{\text{alkene peak height}}{\text{alkane peak height}} \times \frac{\text{alkane concentration}}{\text{alkene concentration}}$$

6.10 Computer Programs

Since calculations of %alkene are repetitive and time consuming,

BASIC computer programmes were developed to process the raw data. A flow diagram showing the general nature of these programs is shown in Figure 6.3. Five separate programs were developed from this outline. These were:-

a) Calculation of %alkene and ln(%alkene) values from raw data from isothermal mass spectroscopy results.

b) As a) for gas chromatography results.

c) Calculation of %alkene, ln(%alkene), rate constants k_o', k_1', and $\ln k_o'$ and $\ln k_1'$ from raw data from temperature programme mass spectroscopy results.

d) As c) for gas chromatography results.

e) As c) for two alkenes in a competitive reaction. This was required for M.S. results, but not for G.C., because the M.S. fragmentation patterns for the higher hydrocarbon have to be subtracted from the lower hydrocarbon results, whereas in G.C. the two sets of results are independent.

Since all these programs are very similar only (e), which is the most complex is shown on page 84. All the components for the other programs are present in this one program since they are essentially subsets of this.

6.11 Adsorption

In parts of this work the extent of alkene adsorption was measured. The procedure in non-reactive systems was as follows. Adsorption was treated as a first order equilibrium reaction:-

$$\text{ALKENE(gas phase)} \rightleftharpoons \text{ALKENE(adsorbed)}$$

Thus $$\frac{d(C-C_e)}{dt} = -k(C-C_e)$$

where C = concentration of alkene in gas phase.

and C_e = equilibrium concentration of alkene in gas phase.

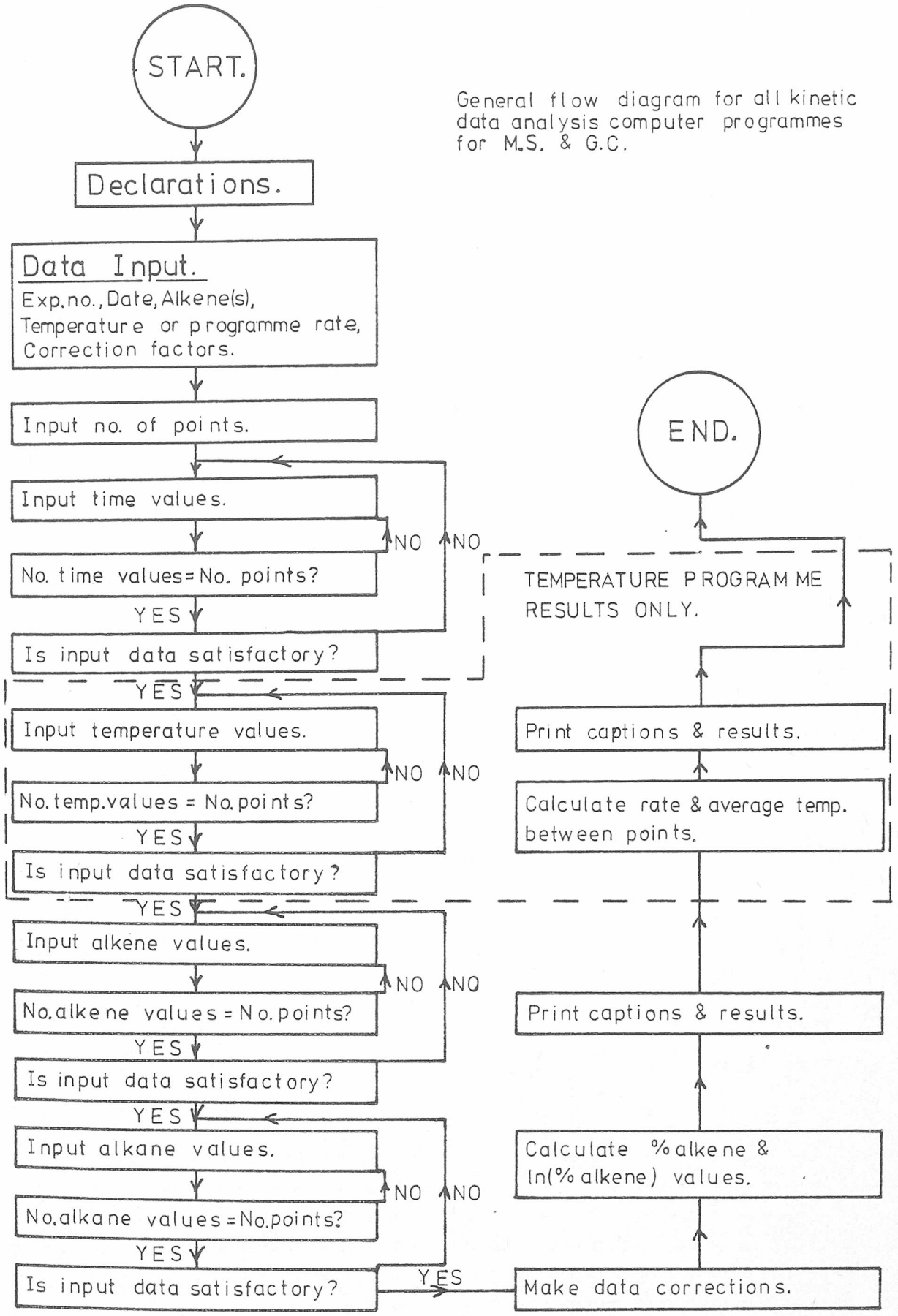

General flow diagram for all kinetic data analysis computer programmes for M.S. & G.C.

FIGURE 6.3

```
 10 PRINT"PROG.FOR CALC.LN(ALKENE) VALUES FOR A TWO ALKENE"
 20 PRINT"HYDROGENATION USING MASS SPEC.RAW DATA."
 30 PRINT
 40 PRINT"TYPE EXP.NO., DATE, AND ALKENE USED (HIGHER FIRST)"
 50 INPUT A,B$,C$,S$
 60 PRINT"FRG.OF HIGHER ALKANE(HIGHER ALKENE,LOWER ALKANE & ALKENE"
 70 PRINT"HIGHER ALKENE(2),LOWER ALKANE(1),R.S.(HIGHER & LOWER)"
 80 INPUT D1,D2,D3,E1,E2,F,R1,R2
 90 PRINT"TYPE NO.POINTS"
100 INPUT G
110 DIM T(30)
120 DIM K(30)
130 DIM L(30)
140 DIM N(30)
150 DIM M(30)
160 DIM H(30)
170 DIM J(30)
180 DIM P(30)
190 DIM Q(30)
200 PRINT"TYPE TIME VALUES"
210 MAT INPUT T'G'
220 LET T1=NUM
230 IF T1=G GOTO 405
240 MAT INPUT H'G'
250 LET T2=NUM
260 FOR I=1 TO T2
270 LET T(T1+I)=H(I)
280 NEXT I
290 IF T1+T2=G GOTO 405
300 MAT INPUT J'G'
310 LET T3=NUM
320 FOR I=1 TO T3
330 LET T(T1+T2+I)=J(I)
340 NEXT I
350 IF T1+T2+T3=G GOTO 405
360 MAT INPUT P'G'
```

```
370 LET T4=NUM
380 FOR I=1 TO T4
390 LET T(T1+T2+T3+I)=P(I)
400 NEXT I
405 PRINT
410 INPUT X
420 IF X=1 GOTO 200
430 PRINT"TYPE TEMPERATURE VALUES."
440 MAT INPUT K'G'
450 LET K1=NUM
460 IF K1=G GOTO 625
470 MAT INPUT H'G'
480 LET K2=NUM
490 FOR I=1 TO K2
500 LET K(K1+I)=H(I)
510 NEXT I
515 IF K1+K2=G GOTO 625
520 MAT INPUT J'G'
530 LET K3=NUM
540 FOR I=1 TO K3
550 LET K(K1+K2+I)=J(I)
560 NEXT I
570 IF K1+K2+K3=G GOTO 625
580 MAT INPUT P'G'
590 LET K4=NUM
600 FOR I=1 TO T4
610 LET K(K1+K2+K3+I)=P(I)
620 NEXT I
625 PRINT
630 INPUT Y
640 IF Y=1 GOTO 430
650 PRINT"TYPE HIGHER ALKENE VALUES"
660 MAT INPUT L'G'
670 LET L1=NUM
680 IF L1=G GOTO 855
```

```
 690 MAT INPUT H'G'
 700 LET L2=NUM
 710 FOR I=1 TO L2
 720 LET L(L1+I)=H(I)
 730 NEXT I
 740 IF L1+L2=G GOTO 855
 750 MAT INPUT J'G'
 760 LET L3=NUM
 770 FOR I=1 TO L3
 780 LET(L1+L2+I)=J(I)
 790 NEXT I
 800 IF L(L1+L2+L3)=G GOTO 855
 810 MAT INPUT P'G'
 820 LET L4=NUM
 830 FOR I=1 TO L4
 840 LET L(L1+L2+L3+I)=P(I)
 850 NEXT I
 855 PRINT
 860 INPUT V
 870 IF V=1 GOTO 650
 880 PRINT"PRINT HIGHER ALKANE VALUES"
 890 MAT INPUT N'G'
 900 LET N1=NUM
 910 IF N1=G GOTO 1085
 920 MAT INPUT H'G'
 930 LET N2=NUM
 940 FOR I=1 TO N2
 950 LET N(N1+I)=H(I)
 960 NEXT I
 970 IF N1+N2=G GOTO 1085
 980 MAT INPUT J'G'
 990 LET N3=NUM
1000 FOR I=1 TO N3
1010 LET N(N1+N2+I)=J(I)
1020 NEXT I
```

```
1030 IF N1+N2+N3=G GOTO 1085
1040 MAT INPUT P'G'
1050 LET N4=NUM
1060 LET M2=NUM
1070 FOR I=1 TO M2
1080 NEXT I
1085 PRINT
1090 INPUT W
1100 IF W=1 GOTO 880
1110 PRINT"TYPE LOWER ALKENE VALUES."
1120 MAT INPUT M'G'
1130 LET M1=NUM
1140 IF M1=G GOTO 1315
1150 MAT INPUT H'G'
1160 LET M2=NUM
1170 FOR I=1 TO M2
1180 LET M(M1+I)=H(I)
1190 NEXT I
1200 IF M1+M2=G GOTO 1315
1210 MAT INPUT J'G'
1220 LET M3=NUM
1230 FOR I=1 TO M3
1240 LET M(M1+M2+I)=J(I)
1250 NEXT I
1260 IF M1+M2+M3=G GOTO 1315
1270 MAT INPUT P'G'
1280 LET M4=NUM
1290 FOR I=1 TO M4
1300 LET M(M1+M2+M3+I)=P(I)
1310 NEXT I
1315 PRINT
1320 INPUT Z
1330 IF Z=1 GOTO 1110
1340 PRINT"TYPE LOWER ALKANE VALUES."
1350 MAT INPUT Q'G'
```

```
1360 LET Q1=NUM
1370 IF Q1=G GOTO 1500
1380 MAT INPUT H'G'
1390 LET Q2=NUM
1400 FOR I=1 TO Q2
1410 LET Q(Q1+I)=H(I)
1420 NEXT I
1430 IF Q1+Q2=G GOTO 1500
1440 MAT INPUT J'G'
1445 LET Q3=NUM
1447 FOR I=1 TO Q3
1450 LET Q(Q1+Q2+I)=J(I)
1455 NEXT I
1457 IF Q1+Q2+Q3=G GOTO 1500
1460 MAT INPUT P'G'
1465 LET Q4=NUM
1470 FOR I=1 TO Q4
1475 LET Q(Q1+Q2+Q3+I)=P(I)
1480 NEXT I
1500 PRINT
1510 INPUT V
1520 IF V=1 GOTO 1340
1530 FOR I=1 TO G
1540 LET L(I)=L(I)-D1*N(I)
1550 LET Q(I)=Q(I)-D2*N(I)-E2*L(I)
1560 LET M(I)=M(I)-D3*N(I)-E2*L(I)-
1570 LET N(I)=R1*N(I)
1580 LET Q(I)=R2*Q(I)
1590 LET J(I)=100*L(I)/(L(I)+N(I))
1600 LET P(I)=100*M(I)/(M(I)+Q(I))
1610 LET H(I)=LOG(J(I))
1620 LET Q(I)=LOG(P(I))
1630 NEXT I
1640 PRINT"EXP.NO.          DATE.
1650 PRINT"========          =====
```

F*Q(I)

ALKENES."
=========="

```
1660 PRINT A,B$,C$,"/"S$
1670 PRINT
1680 PRINT"TIME.          %" C$ "
1690 FOR I=1 TO G
1700 PRINT T(I),J(I),P(I),H(I),Q(I)
1710 NEXT I
1720 FOR I=1 TO G-1
1730 LET K(I)=(K(I)+K(I+1))/2
1740 LET H(I)=(H(I)-H(I+1))/(T(I+1)-
1750 LET Q(I)=(Q(I)-Q(I+1))/(T(I+1)-
1760 LET T(I)=(T(I)+T(I+1))/2
1770 LET M(I)=LOG(H(I))
1780 LET J(I)=LOG(Q(I))
1790 LET N(I)=1/K(I)
1800 NEXT I
1810 PRINT
1820 PRINT
1830 PRINT
1840 PRINT"TIME.          TEMP.
1850 PRINT"
1860 FOR I=1 TO G-1
1870 PRINT T(I),K(I),N(I),M(I),J(I)
1875 NEXT I
1880 PRINT
1890 PRINT C$," RATE."    S$" RATE."
1900 FOR I=1 TO G-1
1910 PRINT H(I),Q(I)
1920 NEXT I
2000 END
```

```
    %" S$ "        LN(%"C$")       LN(%"S$")"


-T(I))
-T(I))


    INV.TEMP.      LN("C$").       LN("S$")"
                     (RATE)          (RATE)"
```

This integrates to give:-

$$\ln(C-C_e) = -kt + \text{constant}$$

When t=0 then $C=C_o$:-

$$\ln(C_o-C_e) = \text{constant}$$

Therefore:

$$\ln(C-C_e) = -kt + \ln(C_o-C_e)$$

Now peak heights of M.S. and G.C. spectra are related to concentration such that:-

$$C = x\,H \qquad \text{where } x = \text{constant}, \; H = \text{Peak height}$$

Therefore:-

$$\ln(H-H_e) = -kt + \ln(H_o-H_e)$$

In a system where only adsorption occurred the amount of adsorption was then calculated as follows. The equilibrium peak height was obtained by extrapolation of the alkene peak height vs. time plot to the steady state. Then since initially the peak heights increased due to temperature equilibration effects, a graph of $\ln(H-H_e)$ vs. time was used to obtain the initial peak height by extrapolation to t=0. An example of these procedures is shown in Figure 6.4.

The amount of adsorption was then calculated as:

$$\text{MOLES ALKENE ADSORBED} = M_o - (M_o H_e/H_o)$$

where M_o = No. moles injected into reaction vessel

$$\text{Now the No. moles of zeolite} = \frac{g}{RMMz}$$

where g = weight of zeolite (hydrated) and RMMz = relative molar mass of the zeolite

Therefore:-

$$\frac{\text{MOLES ALKENE ADSORBED}}{\text{MOLE OF ZEOLITE}} = Z = \frac{RMMz(M_o-(M_o H_e/H_o)}{g}$$

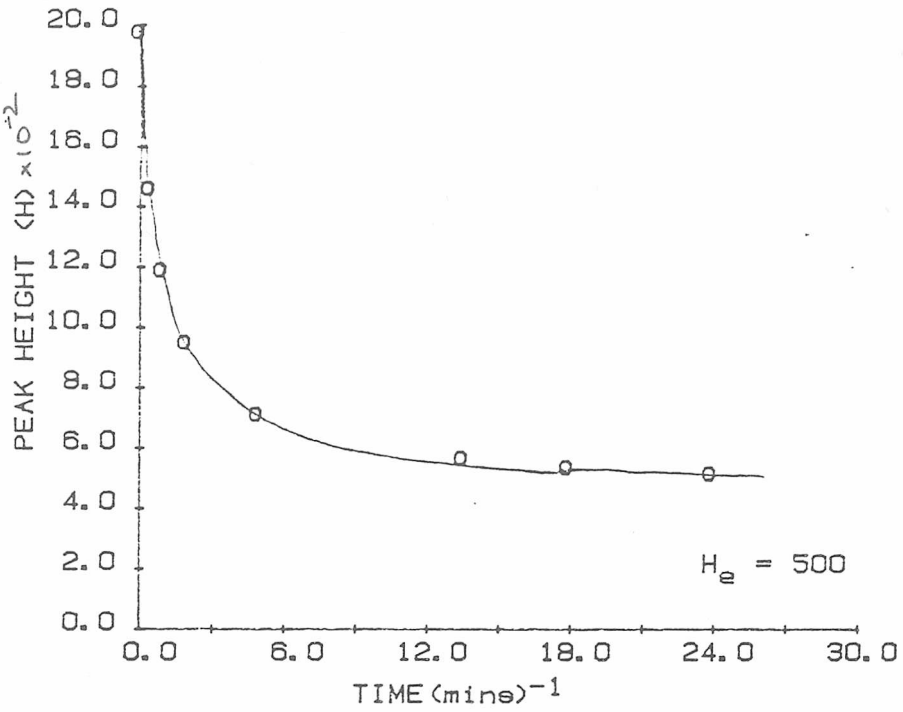

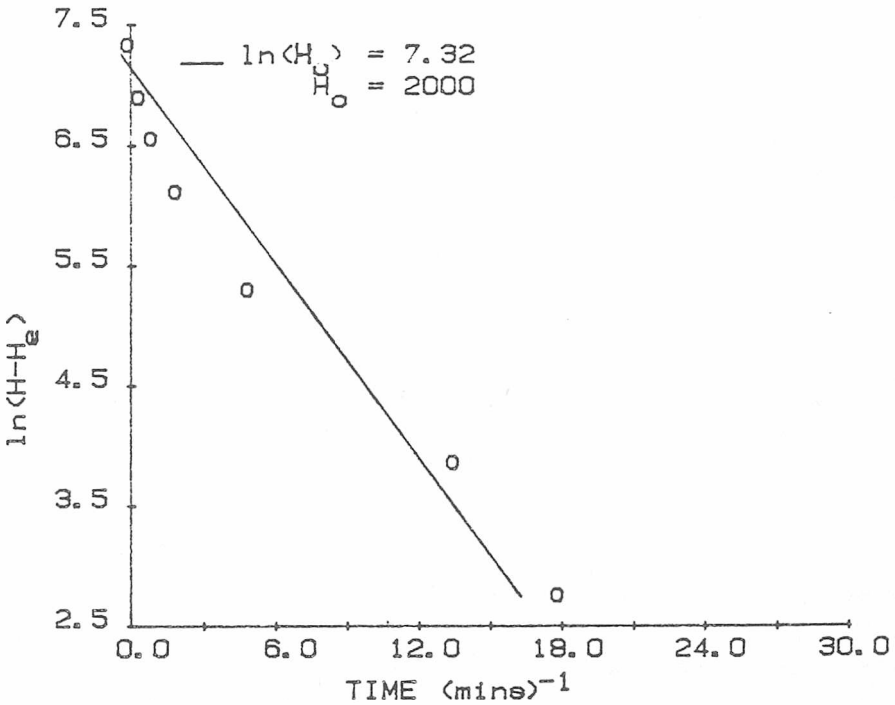

EXAMPLE OF ADSORPTION CALCULATION TECHNIQUE
(propene at 333K)

moles adsorbed = $(6.57-(6.57\times500/2000))\times10^{-5}$
$= 4.93\times10^{-5}$

moles adsorbed/mole of zeolite
$= (4.93/4.56)\times10^{-5} = 1.08$

FIGURE 6.4

and since the basic unit of A type zeolite contain a single ∝ cage:-

Z = No.alkene molecules/∝ cage.

This method was also applied to low hydrogenation activity systems. In these cases zero alkane adsorption was assumed and the total gas phase hydrocarbon used to calculate the amount of adsorption.

i.e. amount alkene not adsorbed = amount of alkene in the gas phase + amount of alkene converted into alkane (all in gas phase.)

This could only be used during initial stages of the reaction since a large change in the total amount of alkene would alter the amount adsorbed.

6.12 Errors and Reproducibility

With any experimental technique errors arise due to limits on the accuracy of parameter measurements and result processing. Also in heterogeneous catalysis results are often not very reproducible due to the fact that slight variations in pretreatment conditions for a catalyst can have major effects on the condition of its surface. Therefore, the margins for error and reproducibility of any result must be determined before comparisons of analyses can be considered valid.

a) TEMPERATURE MEASUREMENT

The measurement of the reaction temperature at the base of the reaction vessel was limited by the calibration graph (shown as Figure 6.5) used to convert thermocouple voltage readings into temperature values. This was accurate to within 2°C. The greatest variation in results due to temperature will have been due to the temperature gradient across the reactor as discussed in Chapter 5.4.

b) PRESSURE MEASUREMENT

The error in the measurement of the gas pressure in the gas

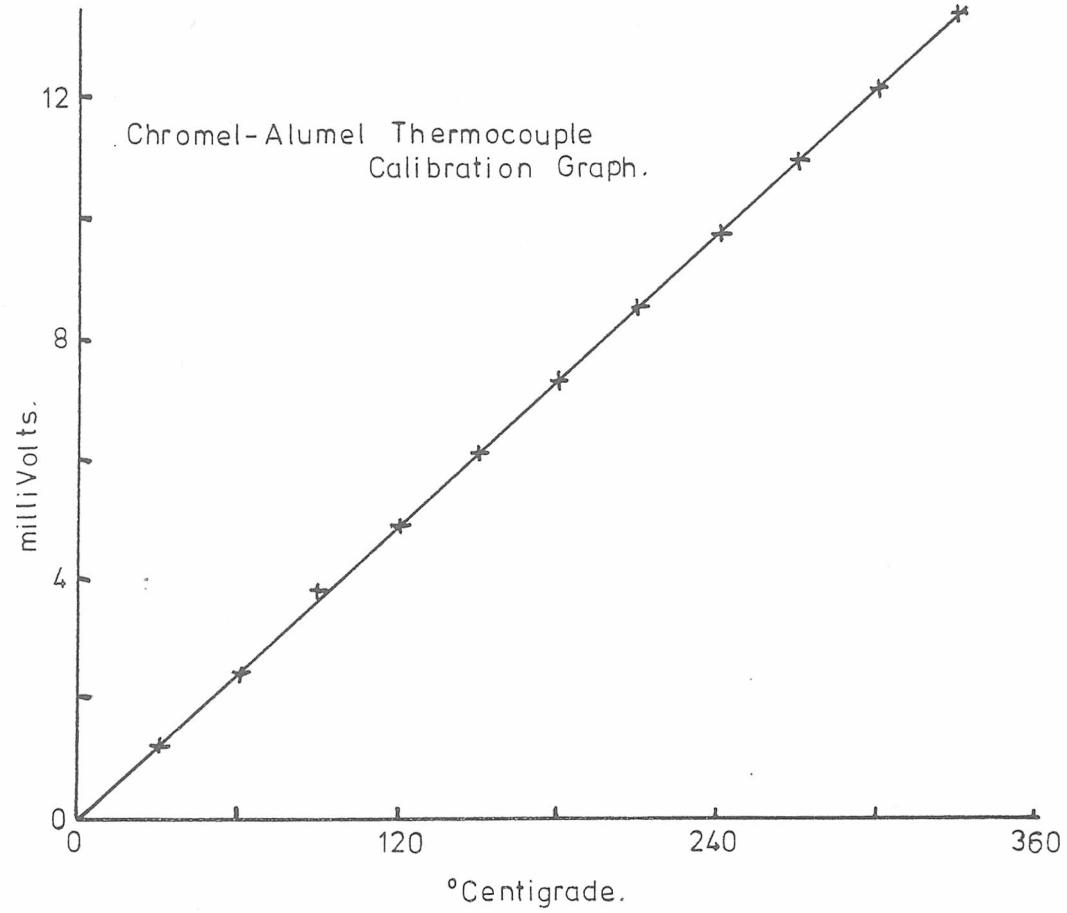

FIGURE 6.5

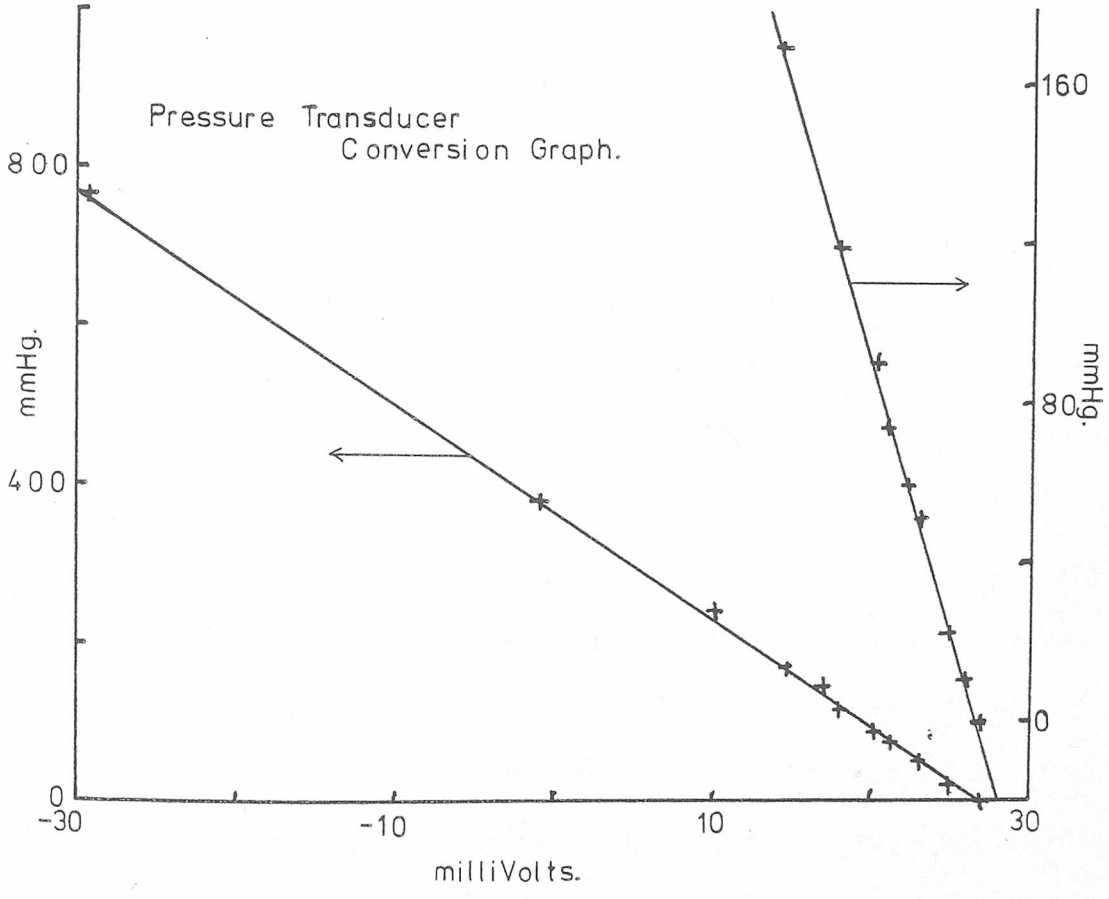

FIGURE 6.6

handling system was dependent on two factors.

(i) the accuracy of the pressure transducer, was quoted by the manufacturers as 1%. This figure embodies deviations due to nonlinearity and hysteresis, and is in any case inherent in the second factor below.

(ii) accuracy of the calibration graph (shown as Figure 6.6) for converting voltage readings into pressure values. This graph was obtained from calibration of the transducer with a mercury manometer. The accuracy achieved was o.5mmHg.

c) SENSITIVITY FACTORS

As discussed in Chapter 6.9 the alkene and alkane peaks were adjusted for equipment sensitivity by multiplication of the alkane peak heights by a sensitivity factor obtained from calibration. From the variation of the sensitivity factor between calibrations performed on different occasions, it can be safely assumed that they were accurate to within 10%.

d) KINETIC ANALYSIS

There were several sources of error in the kinetic analysis performed in this work, the effects of which would appear in the %alkene vs. time plot and/or the Arrhenius plot.

(i) %alkene vs. time: - The plot of %alkene vs. time is used in this work to obtain two pieces of kinetic data. The rate constant, k, obtained from the slope of the plot, and the induction period I, defined as the time intercept of the induction period slope and the overall rate slope. Any error in this will be due to error in plotting the points and the accuracy of the slope through those points.
The points may be inaccurate due to the use of incorrect alkane/alkene relative sensitivity factors, and, in the case

of G.C. results, the approximation made by the use of peak height rather than peak area (see Section 6.9). To ascertain the magnitude of the effect of these two factors the graphs shown in Figure 6.7 were plotted. Figure 6.7(a) shows the effect of using various sensitivity factors, whilst 6.7(b) shows the variation in a set of G.C. peaks from a single experiment analysed first by peak height and then by peak area measurement.

The curvature of this plot was affected both by the temperature of reaction and by the susceptibility of a given catalyst sample to deactivation. This meant that the accuracy with which the slope and the intercept could be measured varied from experiment to experiment. Therefore, errors in these values were calculated individually for different results. Figure 6.8 shows the method of calculating the error using a high temperature plot as an example of the most extreme errors normally found. As can be seen the maximum error expected is about $\pm$20%.

ii) lnk vs. 1/T: - The activation energies obtained from the Arrhenius plots of lnk vs. 1/T contain errors in the high temperature region because the high temperature results were treated as zero order, although they were probably first order, so that they would be compatible with the low temperature results.

To ascertain the effect of using the incorrect order of reaction a set of results were treated as zero order and then as first order. The result is shown in Figure 6.9. As can be seen the difference is less than the error in the rate values due to non-linearity of the %alkene vs. time slope.

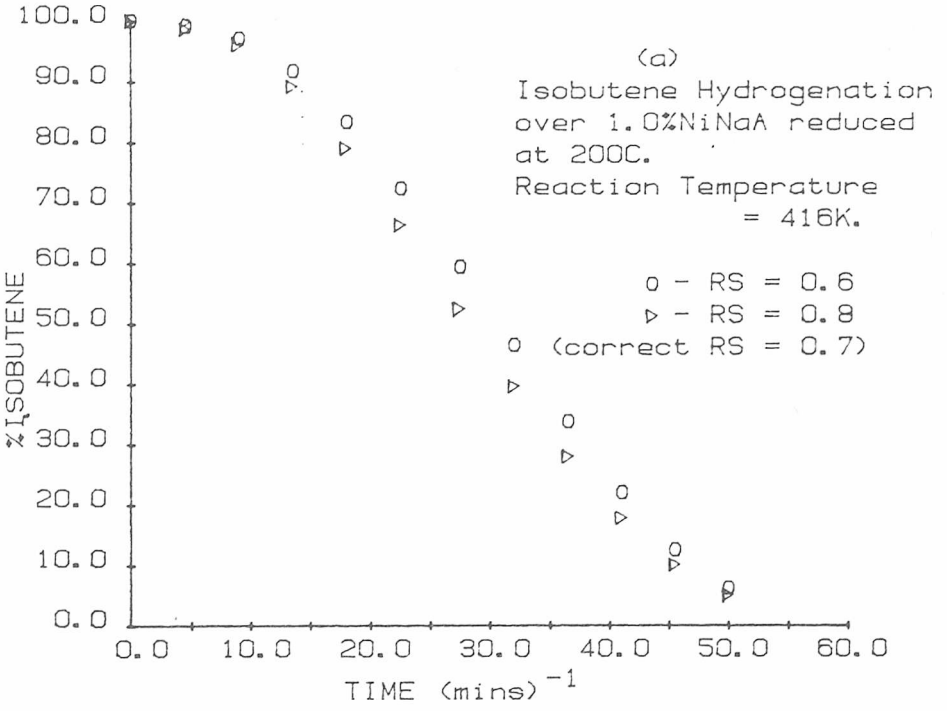

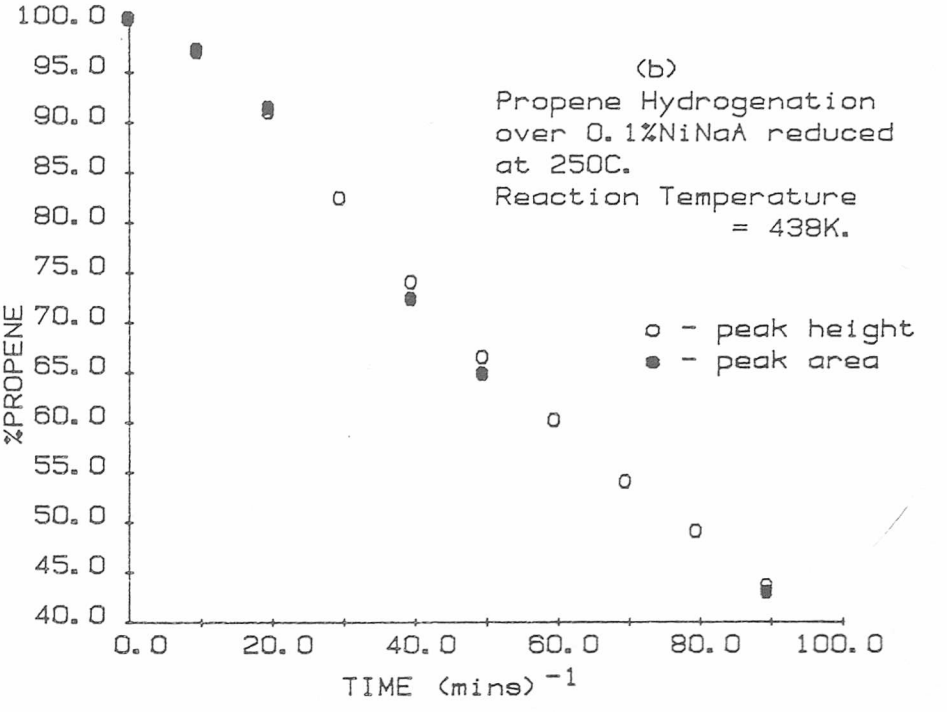

FIGURE 6.7

Effect of Errors in the Calibration of sensitivity factors.
a) incorrect sensitivity used
b) peak height rather than peak area used for G.C. results.

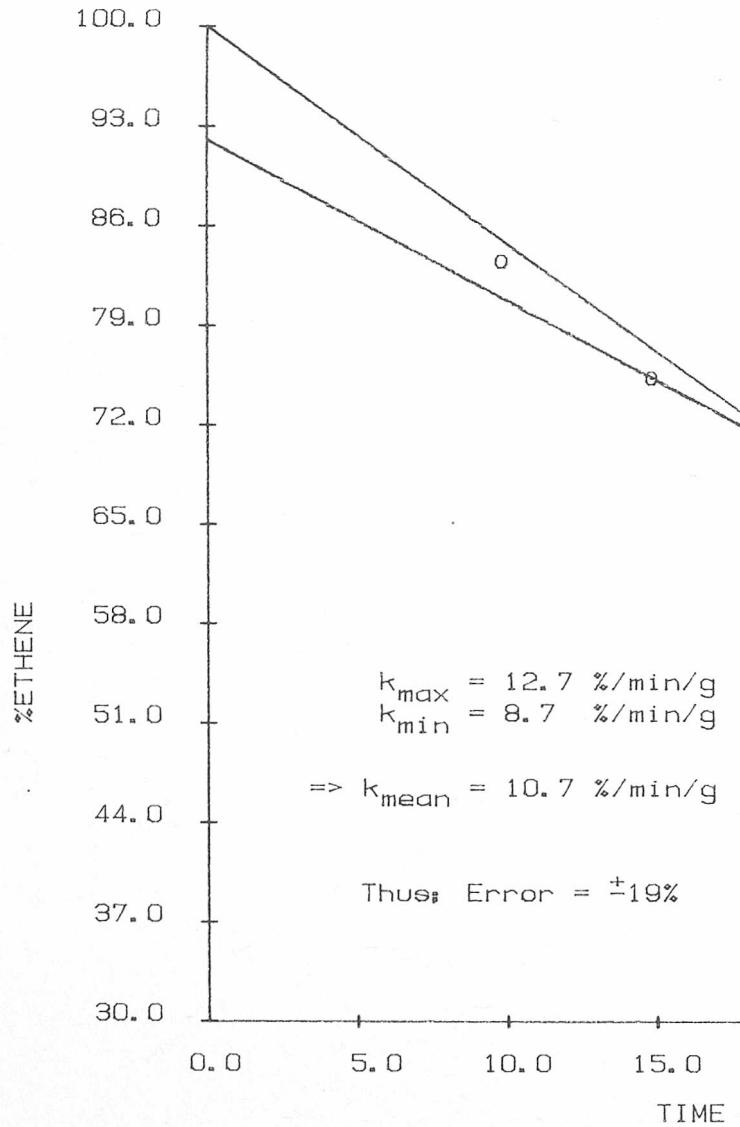
100.0
93.0
86.0
79.0
72.0
65.0
58.0
51.0
44.0
37.0
30.0
%ETHENE
0.0
5.0
10.0
15.0
TIME
k_{max} = 12.7 %/min/g
k_{min} = 8.7 %/min/g
=> k_{mean} = 10.7 %/min/g
Thus: Error = ±19%

FIGURE 6.8

Error in rate values obtained from Isothermal Rate Plots.
Ethene Hydrogenation over 0.1%NiNaA reduced at 250C.
Reaction Temperature = 439K.

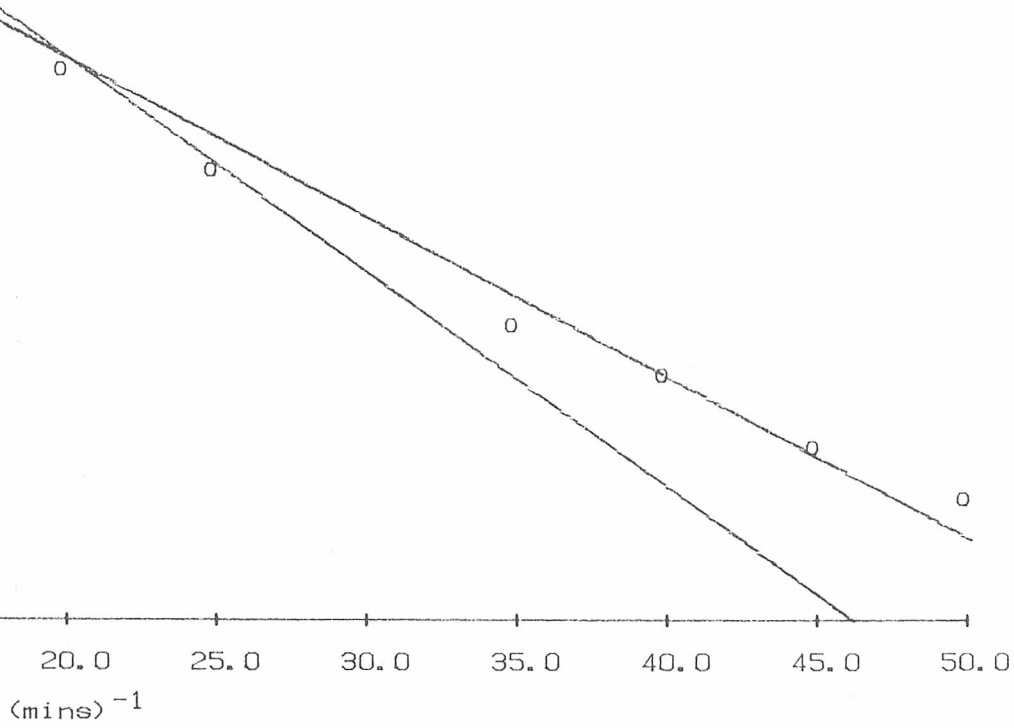

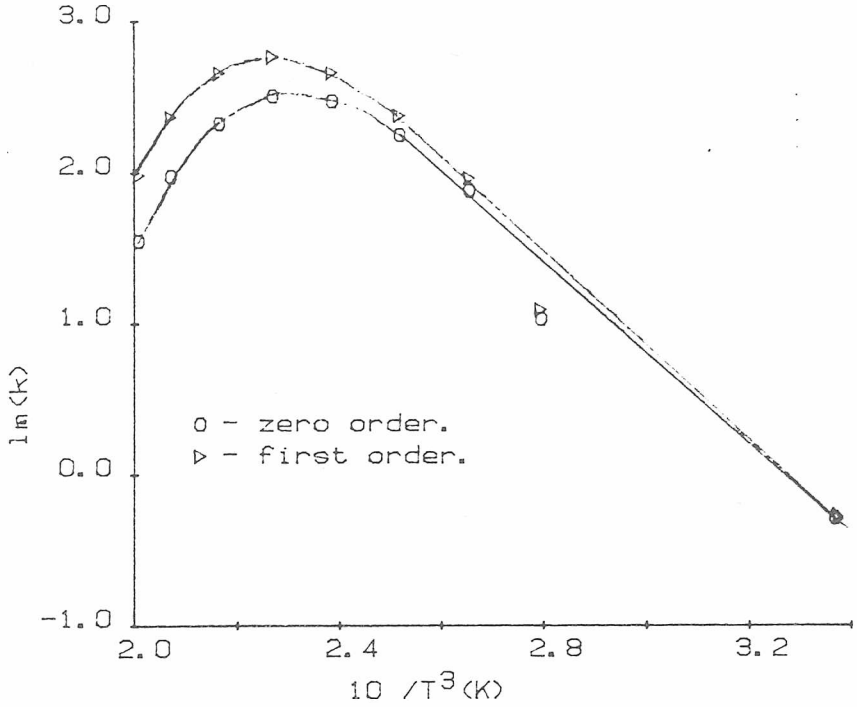

FIGURE 6.9

Arrhenius Plot for Ethene Hydrogenation over 0.1%NiNaA reduced at 250C.
Effect of assuming different reaction orders with respect to the alkene.

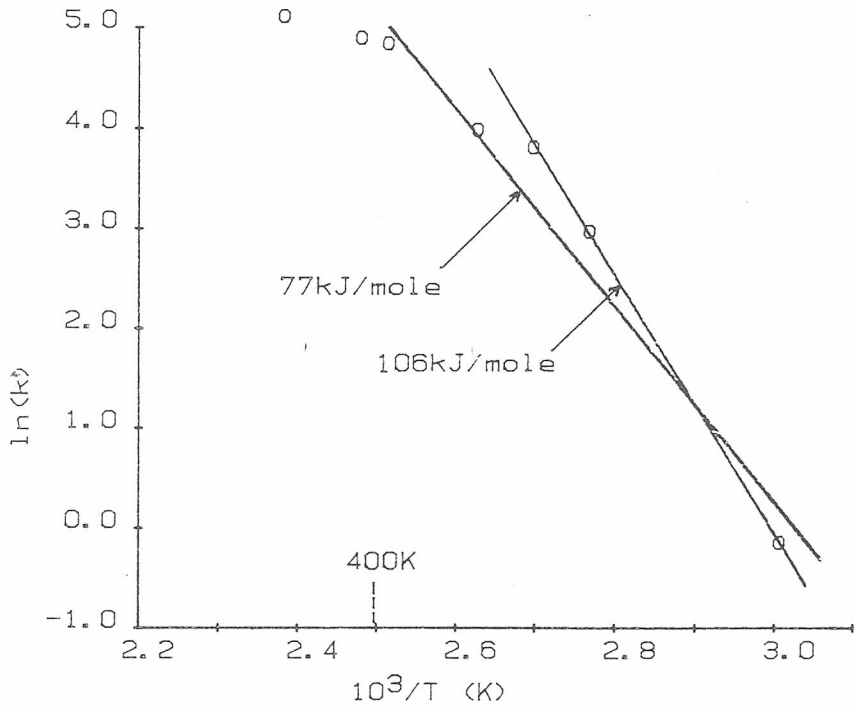

FIGURE 6.10

Error in Arrhenius Plots.
Isobutene Hydrogenation over 1.0%NiNaA reduced at 300C.
The drop in the activatin energy above 400K is a kinetic rather than an experimental error effect.

The quality of the Arrhenius plots obtained in this work varied considerably but Figure 6.10 shows an example of a fairly typical result. The error in this can be seen to be $\pm$ 16% and generally, unless otherwise stated, this is the level of accuracy assumed for quoted activation energies.

e) REPRODUCIBILITY

The errors so far quoted are for single experiments, the other major factor is the reproducibility of such experiments on repetition with a fresh sample of catalyst. Figure 6.11 shows the results of repeated experiments for ethene hydrogenation over fresh 0.1%NiNaA samples reduced at 250C. It can be calculated from this that the rate constants are reproducible to $\pm$50% and the activation energy to $\pm$2%.

It can be seen from the above that the error margins in the experimental and analysis techniques are less than the variation due to result irreproducibility. Therefore, only the reproducibility factors were generally considered.

FIGURE 6.11

Arrhenius Plot for Ethene hydrogenation over 0.1%NiNaA reduced at 250C

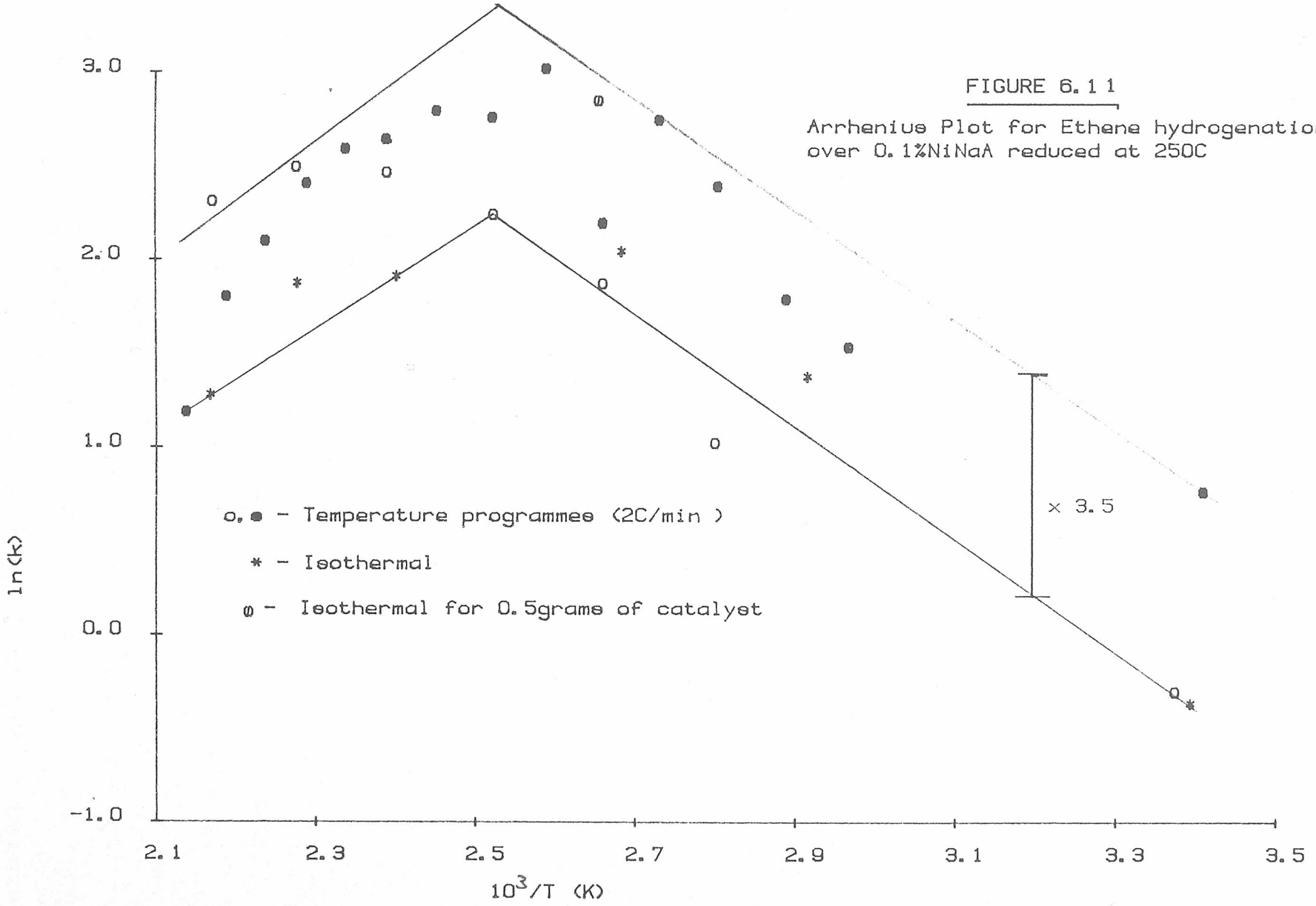

Chapter Seven

CATALYTIC ACTIVITY OF NICKEL LOADED ZEOLITES

7.1 Introduction

Most of the work in this thesis involved the measurement of the hydrogenation rate of ethene, propene and isobutene over the unexchanged, the 0.1% and the 1.0% exchanged NiNaA zeolites. The 10% and 58% samples were not used since they exhibited too great an activity to be easily measured with the equipment available.

7.2 Validity of the Temperature Programming Technique

The initial kinetic measurements were of the catalytic effect of 0.1% exchanged NiNaA on ethene hydrogenation. The temperature programming technique described in Chapter 6.8 was used to obtain complete Arrhenius plots from a single run. A typical example of this is shown in Figure 7.1. As can be seen the initial increase in temperature results in a drop in the apparent rate. Analysis of the raw results revealed that this was due to desorption of ethene causing an increase in the ethene/ethane gas phase ratio and thus invalidating the percentage alkene values used to calculate the rate constant.

To discover the temperature range over which this effect was of great enough magnitude to cause major errors in the apparent rate values, a series of temperature programmed desorption experiments were performed. A zeolite sample was exposed in turn to ethane, ethene, and a mixture of ethene and hydrogen. In each case the system was allowed to equilibrate and then the temperature was linearly increased at a rate of $2^{\circ}C$/min. For comparison purposes a 'blank' run containing ethene+hydrogen but no zeolite was also performed. In these systems no reactions were detected and changes in peak height measurements were assumed to be due to either normal temperature effects or

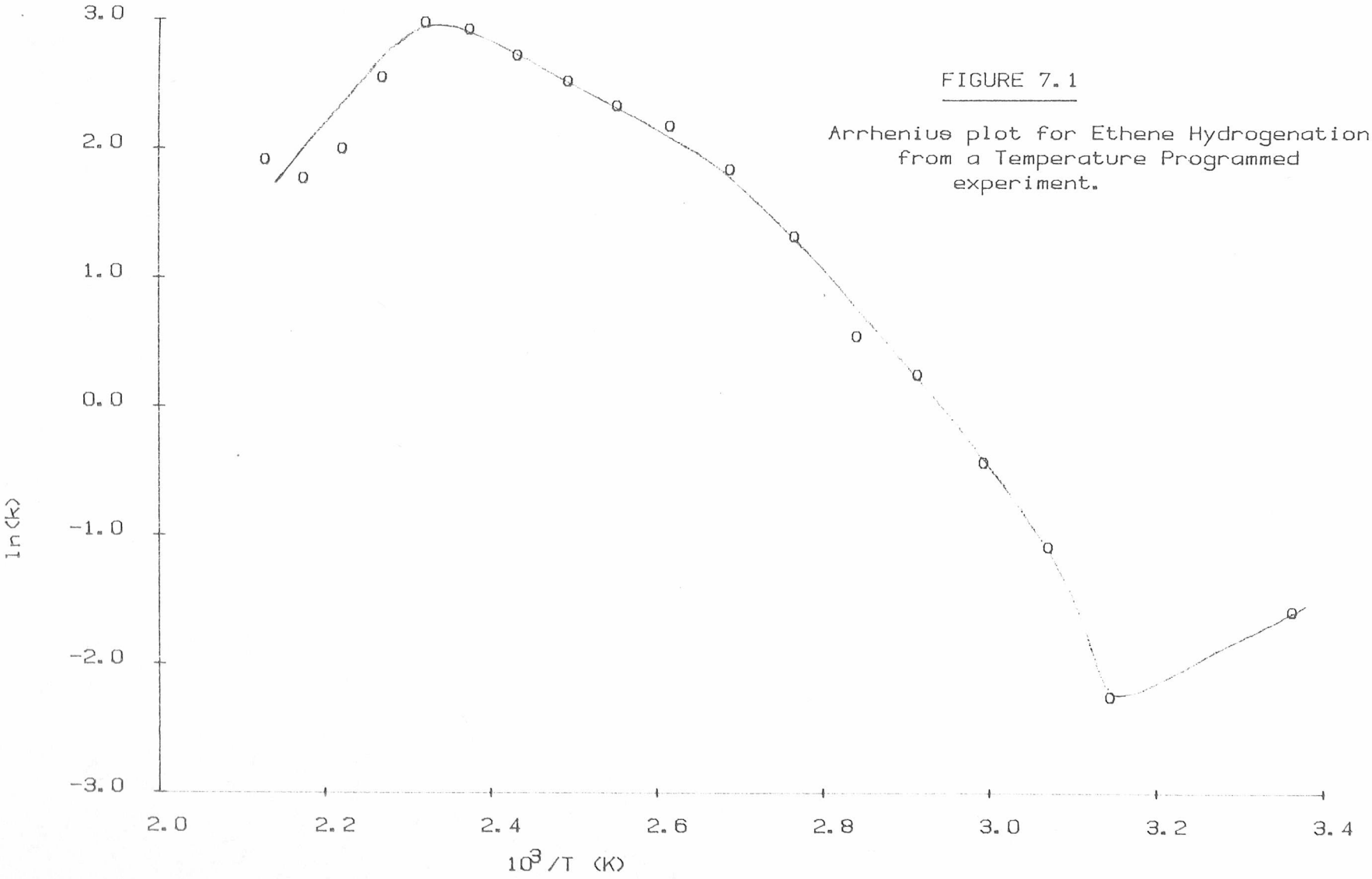

FIGURE 7.1

Arrhenius plot for Ethene Hydrogenation from a Temperature Programmed experiment.

desorption. The pressure-temperature curve for the gas concentration (assuming no adsorption) was then calculated using the Ideal gas equation, and the experimental results normalised to this assuming negligible adsorption at 470-480K. This comparison is valid even though the initial concentration is not accurately known because any error in the Ideal slope $(nR/V)_{\wedge}$ (due to error in the value of $\wedge$) will affect the normalised slopes in a similar manner. It can be seen from the results, shown in Figure 7.2, that the most extreme desorption occurred with ethene, as was expected since zeolites have a high affinity for polar or polarisable adsorbates. Above 380K desorption appears to be almost complete and therefore temperature programme rate results should be valid above this point. Further support for this conclusion can be seen from Figure 6.11 which clearly shows that the differences between isothermal and temperature programmed results are no greater than the variations due to experiment reproducibility. Therefore, the results for ethene hydrogenation over 0.1% NiNaA obtained from temperature programme measurements are valid above 380K.

When work with propene was initiated the zeolite appeared inactive with respect to propene hydrogenation at low temperatures. With the 0.1% NiNaA no reaction occurred until approximately 370K under a programme rate of 2C/min. whilst the 1.0% NiNaA showed no activity even when programmed up to 498K. It was found that the latter became active if a reaction programmed from 298K to above 400K was left to stand for a period of time. To investigate this, a number of isothermal rate measurements were performed on this catalyst above 400K. These showed that after a significant induction period, during which time no detectable reaction occurred, the catalyst became active. This induction period increased with decrease in reaction temperature, therefore further low temperature reactions were performed to discover whether

FIGURE 7.2

Hydrocarbon Pressure vs. Temperature.

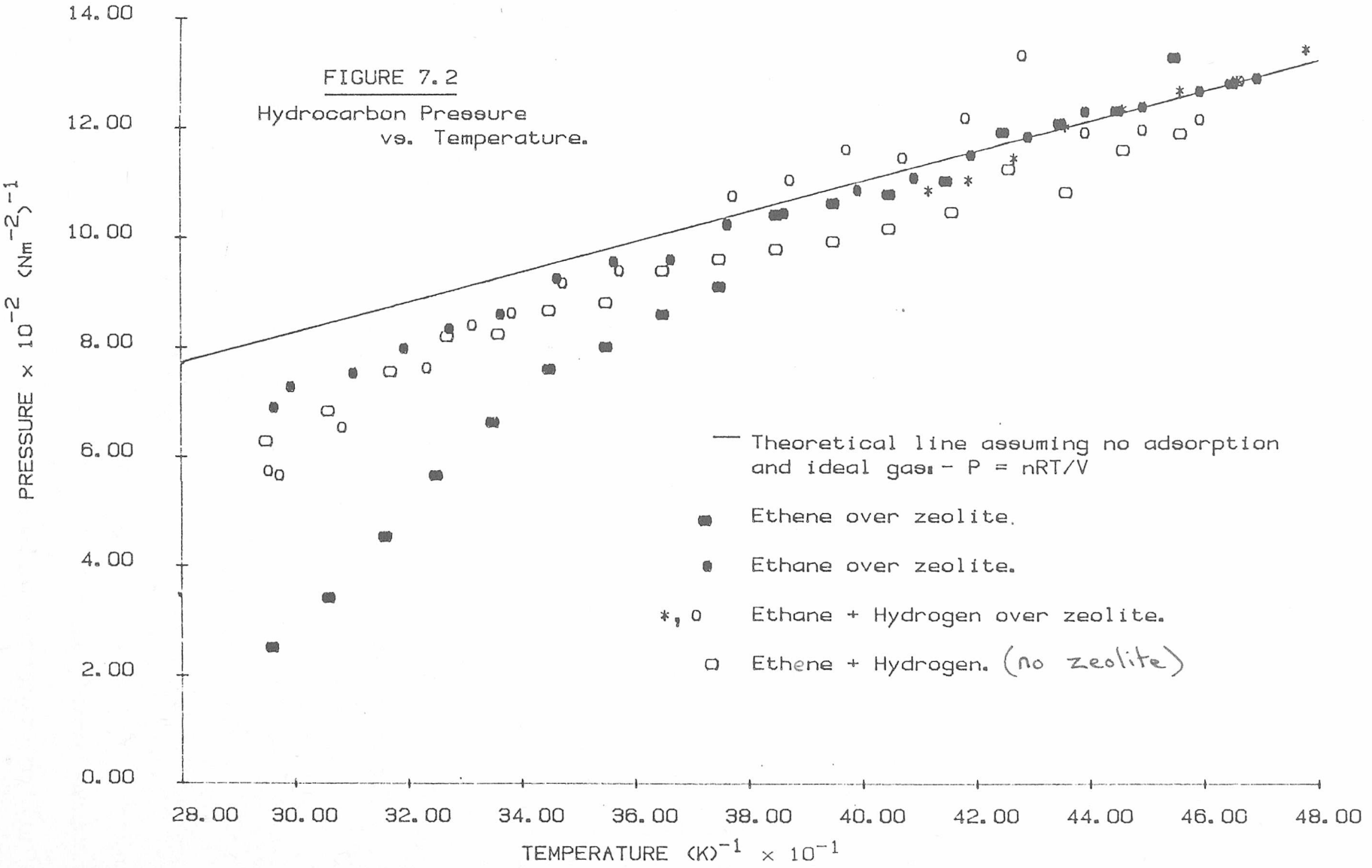

the apparent inactivity was due to extensive induction. With the 1.0% NiNaA this was found to be the case, with induction periods of over 30 hours duration being recorded.

It was decided to measure the extent of adsorption of propene at low temperatures to see if it was great enough to affect temperature programme results in a similar way to the ethene desorption. This was done using the method described in Chapter 6.11. The results are shown in Figure 7.3. along with some comparative results for ethene. As can be seen propene is more extensively adsorbed than ethene. This is not in agreement with the data given in Table 2.1 of Chapter 2.8 for alkene adsorption over 4A zeolite at room temperature and under a pressure of 700 mmHg. It is possible that this disagreement is due to the lower pressure of alkene (6 mmHg) used in this work since it is not unusual for the adsorption isotherms of different adsorbents to cross over one another as the pressure increases. However, another possibility is that some of the adsorption is occurring on sites other than the 4A zeolite. Such sites must be present on the parent zeolite since there appears to be no significant change in extent of adsorption with increase in nickel content.

Because of this extensive adsorption, and also because of the induction effects, it could be seen that the temperature programme results on the 1.0%NiNaA were meaningless. Also, since the extent of adsorption was as great on the 0.1%NiNaA some doubt was cast on the validity of the temperature programme results over this catalyst. Therefore two methods of checking these results were applied. These were isothermal rate measurements and a slower temperature programme. The results are shown in Figures 7.4 and 7.5 along with the 2°C/min. programmes. Figure 7.4 shows that the isothermal and temperature programme results were comparable in magnitude although there is a significant difference

FIGURE 7.3

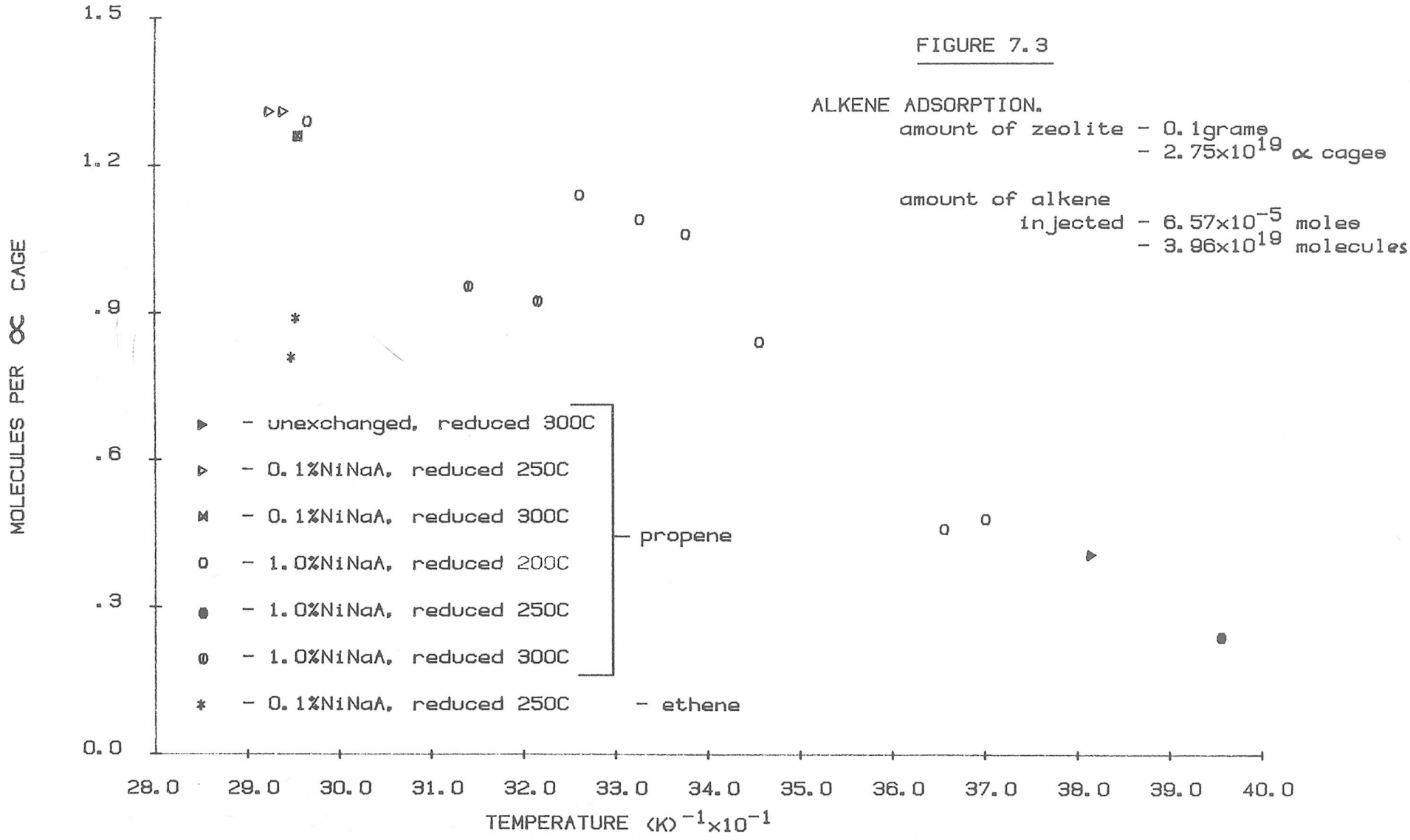
ALKENE ADSORPTION.
amount of zeolite - 0.1grams
- 2.75x10^19 ∝ cages
amount of alkene
injected - 6.57x10^-5 moles
- 3.96x10^19 molecules
MOLECULES PER ∝ CAGE
1.5
1.2
.9
.6
.3
0.0
28.0
29.0
30.0
31.0
32.0
33.0
34.0
35.0
36.0
37.0
38.0
39.0
40.0
TEMPERATURE (K)^-1x10^-1
- unexchanged, reduced 300C
- 0.1%NiNaA, reduced 250C
- 0.1%NiNaA, reduced 300C
- 1.0%NiNaA, reduced 200C
- 1.0%NiNaA, reduced 250C
- 1.0%NiNaA, reduced 300C
- propene
- 0.1%NiNaA, reduced 250C
- ethene

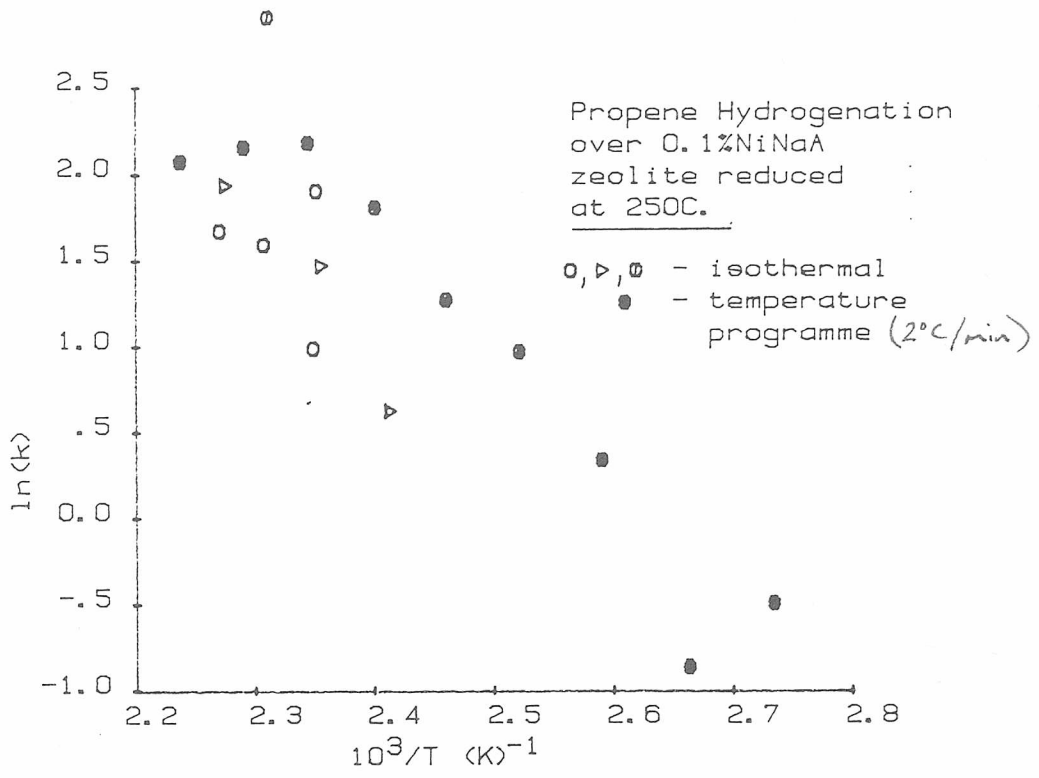

FIGURE 7.4

Comparison of Isothermal and Temperature programme Arrhenius Plots.

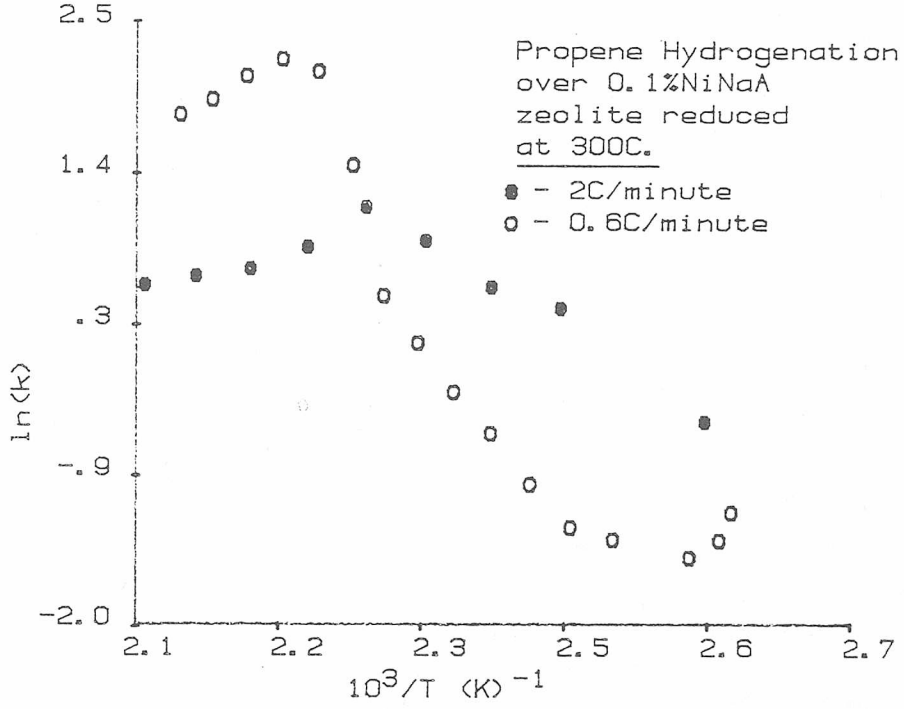

FIGURE 7.5

Comparison of Arrhenius Plots obtained using different Temperature Programming rates.

in the activation energies. However, this may be due to deactivation of the catalyst during repeated use when obtaining isothermal data (this will be discussed fully in section 7.4). Figure 7.5 shows that decreasing the programming rate increased the apparent activation energy. The induction effect found on the 1.0% NiNaA was also found on the lower exchanged zeolite. But, whilst the 1.0% sample showed a little or no reaction during induction, the 0.1% was quite active. An example of this is shown in Figure 7.6. As can be seen the activity during induction was of the same order of magnitude as the later activity. This explains the results for the 0.1% NiNaA discussed earlier. The 2°C/min. temperature programme measured the rate during induction and since this was of the same order of magnitude as the later rate, the Arrhenius plot was correct within the reproducibility limits of the experiment. However, the slower programme rate allowed the induction period to be passed, causing a sudden increase in rate to occur and resulting in an increased, and false, activation energy being obtained.

When the work with ethene was extended to the unexchanged and the 1.0% NiNaA it was found that they also exhibited an induction effect and that the non-occurrence of induction for ethene over the 0.1% NiNaA was the anomaly over these catalysts.

Due to the problems caused by the use of temperature programming all experiments with the butenes were performed isothermally.

7.3 Induction Periods

The induction periods found in this work were a significant reaction effect with the induction length (I) often being longer than the total post induction reaction time. Therefore, this effect was carefully investigated.

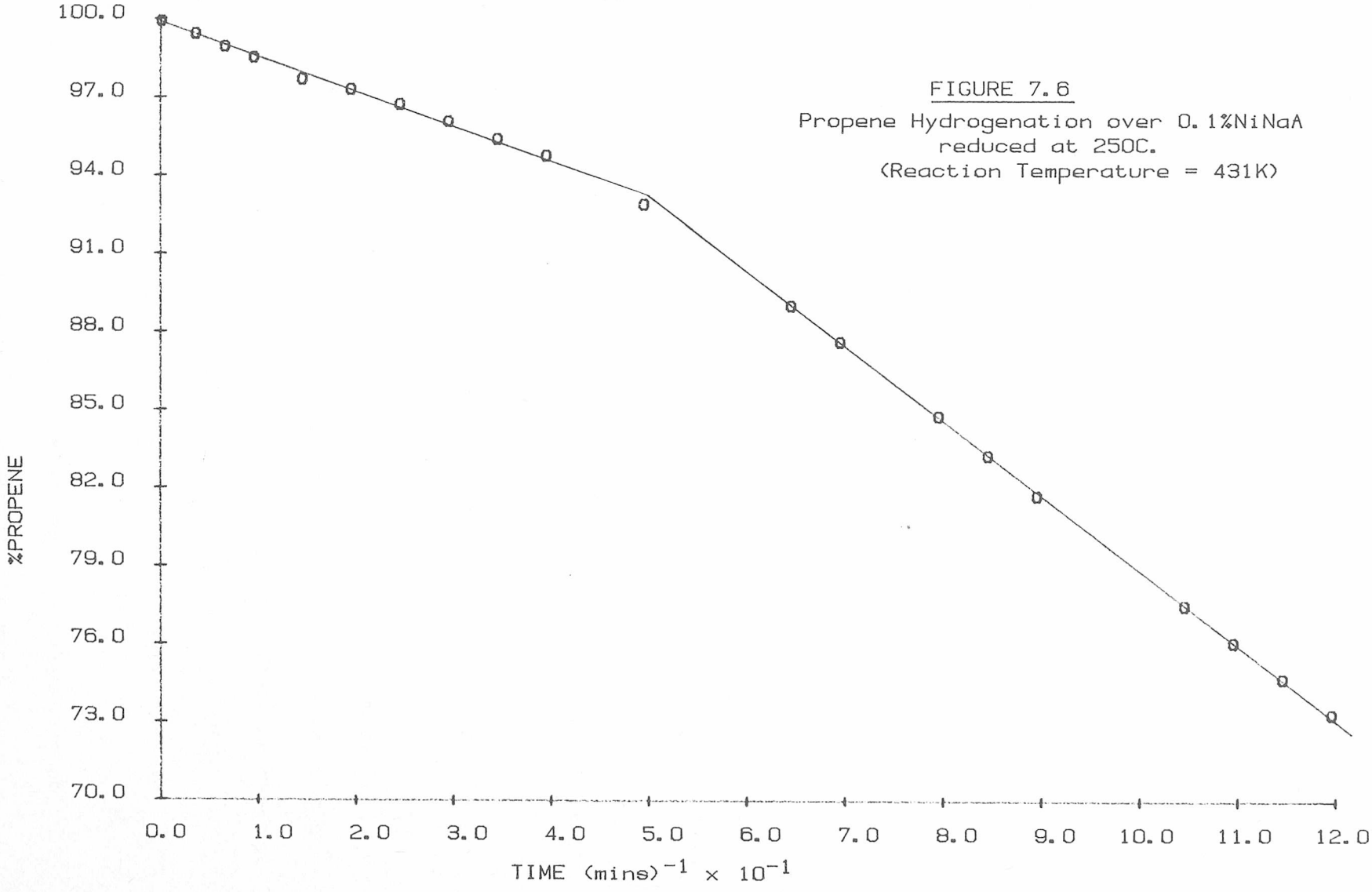

FIGURE 7.6

Propene Hydrogenation over 0.1%NiNaA reduced at 250C. (Reaction Temperature = 431K)

The induction period was found to be directly dependent on the reaction temperature. This implied that it could be an activated process for formation of a reaction intermediate. If this was the case it would be expected to obey the Arrhenius equation. The rate would be proportional to the inverse of the length of induction such that:-

$$\text{RATE} = \frac{1}{I} = A \exp\left(\frac{-E_I}{RT}\right)$$

Therefore, plots of $\ln(\frac{1}{I})$ vs. $\frac{1}{T}$ were made. Figure 7.7 shows some of the results for propene and isobutene. The results gave values of activation energies of between 55 and 70kJ/mole for propene and 70 and 100kJ/mole for isobutene. No trends relating to the catalyst used were noted.

To ascertain the effect of the temperature of reduction and the percentage exchange of the catalyst, on the value of I, a series of tests were performed using isobutene. Isobutene was chosen for the tests because it shows a more distinct induction than ethene and it is not as extensively adsorbed as propene. From the results shown in Figure 7.8, it can be seen that I is minimised by reduction at 250C and is longest on the 0.1% NiNaA.

A comparison was then made of the length of induction at 380K for ethene, propene, and isobutene over the different catalysts. The results recorded in Table 7.1 reveal no significant difference between the alkenes on any particular catalyst except for the 0.1% NiNaA which shows the isobutene to have a much greater induction period than propene.

The irreproducibility of the catalyst was the greatest problem with the analysis of these results. Therefore, the variation of induction period with alkene was qualitatively investigated by using single catalyst samples to hydrogenate the alkenes consecutively.

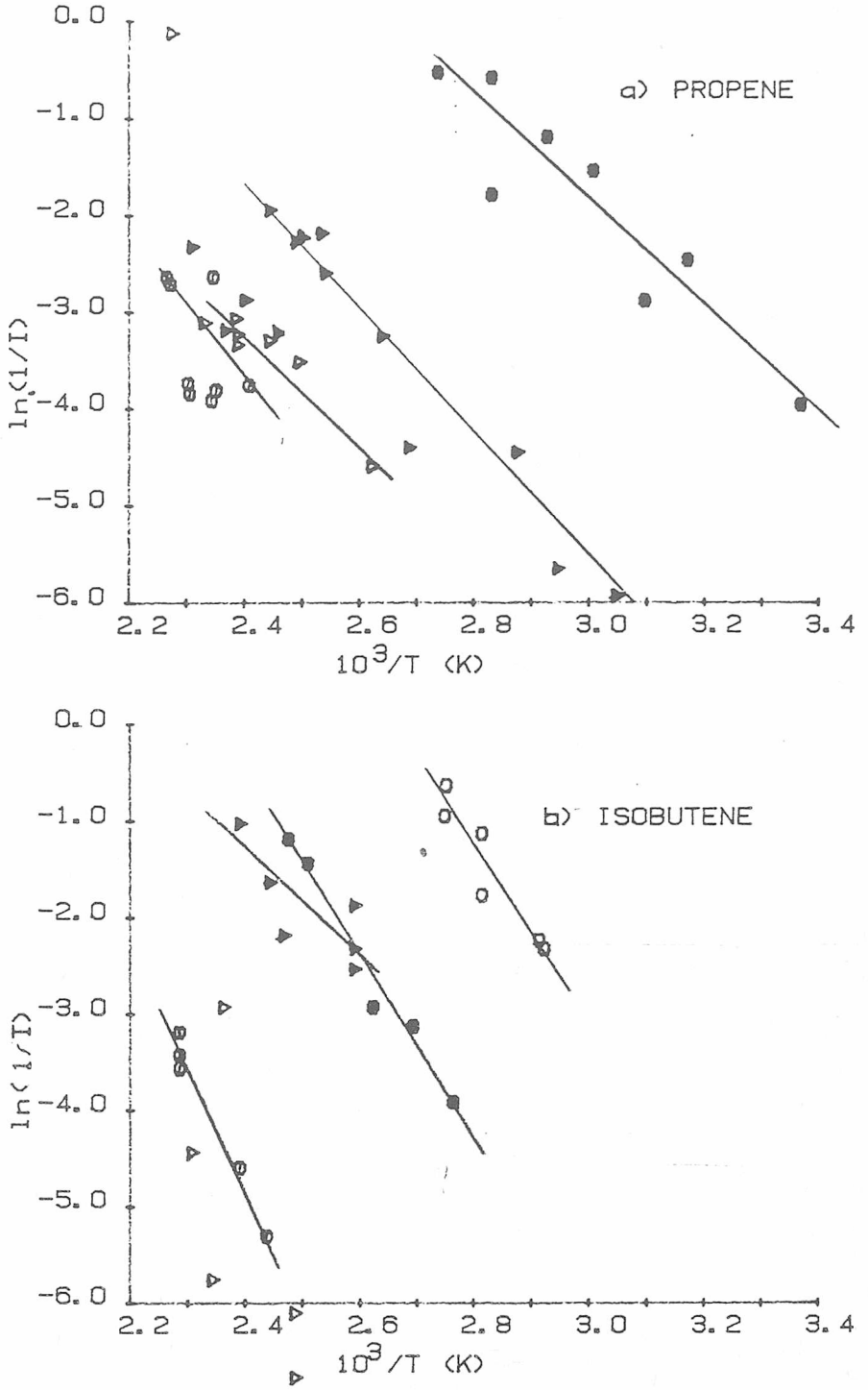

FIGURE 7.7

Pseudo Kinetic Treatment of Induction Periods.
1.0%NiNaA reduced at, ● 300C, ○ 250C, ◗ 200C. 0.1%NiNaA reduced at, ◗ 300C, ◐ 250C.

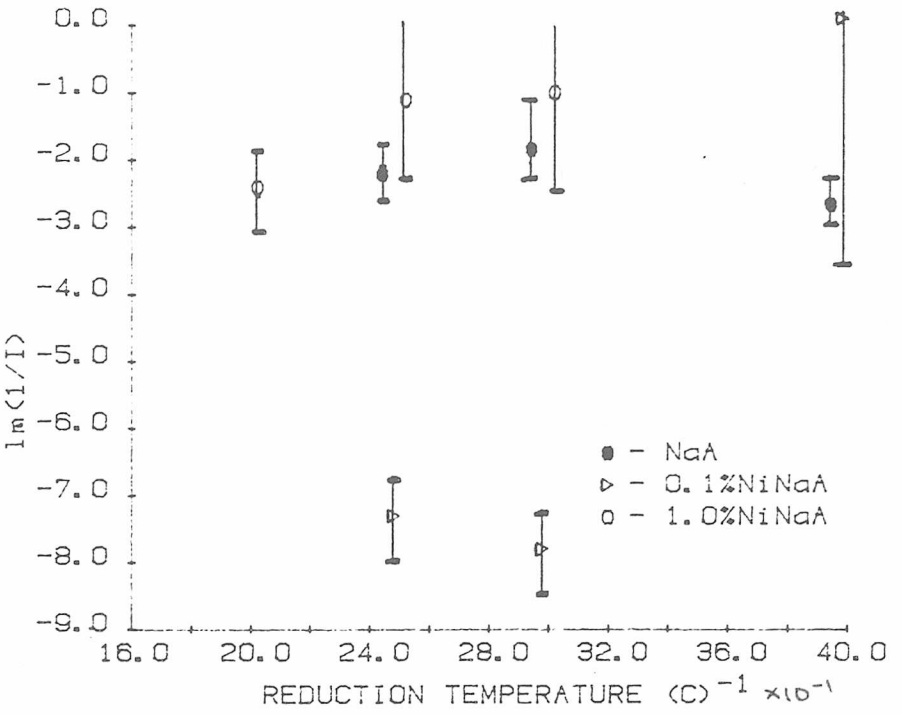

FIGURE 7.8

Effect of Reduction Temperature and %exchange on the length of the Induction Period Isobutene Hydrogenation at 383K.

TABLE 7.1

%EXCHANGE	REDUCTION (C) TEMPERATURE	INDUCTION LENGTH (mins). (at 383K.) ETHENE	PROPENE	ISOBUTENE
unexchanged	200	non apparent	--	--
unexchanged	250	9 ±5	--	9 ±5
unexchanged	300	13 ±7	9 ±5	12 ±6
unexchanged	400	3±1.5	--	20±10
0.1%	200	non apparent	--	--
0.1%	250	non apparent	240 ±122	2060 ±1050
0.1%	300	non apparent	105 ±54	3360 ±1710
0.1%	400	5 ± 3	--	non(*)
1.0%	200	30±15	30 +16	13 ±7
1.0%	250	10 ±5	--	10±5
1.0%	300	12±6	10±5	15 ±8

(*) induction occurred on repeated use.

The problem with this technique is that, as will be discussed in section 7.4, reuse of the catalyst causes deactivation and lengthening of the induction periods. Thus, care had to be taken in interpretation of the results obtained. Figure 7.9 shows a typical example. Generally the results supported the earlier conclusion for the 0.1% catalyst and extended to the 1.0% NiNaA to give the dependence of I on alkene as:

$$I(\text{ETHENE}) < I(\text{PROPENE}) < I(\text{ISOBUTENE})$$

The results for the unexchanged zeolite were inconclusive since its large deactivation with reuse resulted in a continual increase in I irrespective of which alkene was introduced.

Although the length of induction period and the rate of reaction varied inversely on any given catalyst, there was no apparent general correlation between induction and catalyst activity.

7.4 Reuse of the Catalyst

Repeated use of a catalyst resulted in a decrease in its overall activity. Therefore, a series of experiments were performed with ethene to investigate the magnitude of this deactivation and its dependence on reduction temperature, reaction temperature, and percentage exchange. The results of these tests are shown in Figure 7.10 and 7.11 as parameter vs. percentage drop in activity, which is defined as:-

$$\%\text{DROP} = 100 \left(1 - \frac{(\text{activity of catalyst on second use})}{(\text{activity of catalyst on first use})} \right)$$

It can be seen that although the amount of deactivation was directly dependent on the reaction temperature and inversely dependent upon percentage exchange the errors are too large to allow any definite conclusions to be drawn as regards reduction temperature. The errors

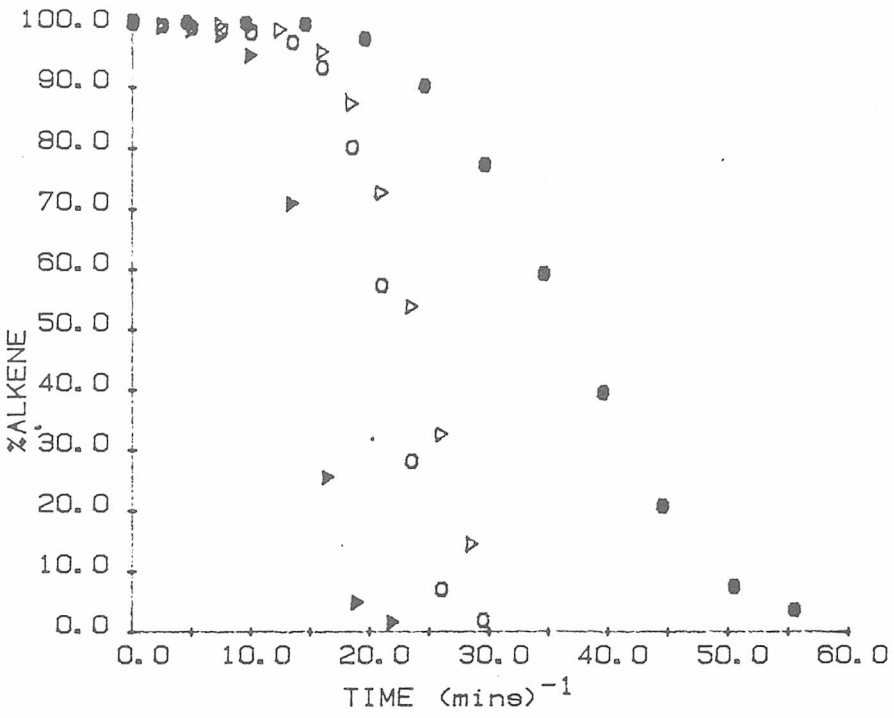

FIGURE 7.9

Variation of Induction Period length with alkene over a single sample of 1.0%NiNaA reduced at 300C.
1) ▶ Ethene. 2) O Ethene. 3) ▷ Propene.
3) ● Isobutene.

Reaction at 383K.

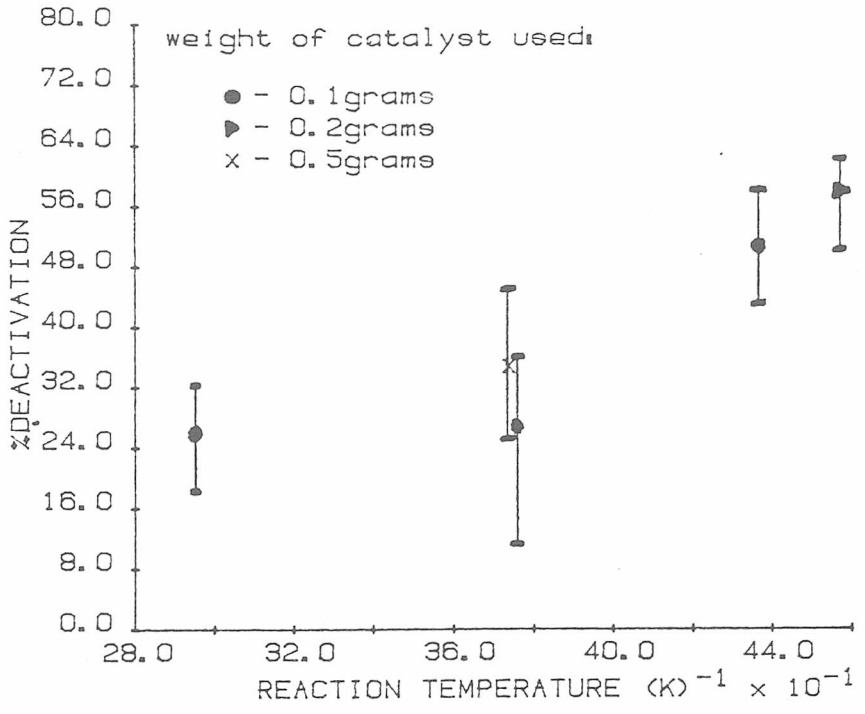

FIGURE 7.10

Variation of %Deactivation with Temperature of Reaction.
Ethene Hydrogenation over 0.1%NiNaA reduced at 250C.

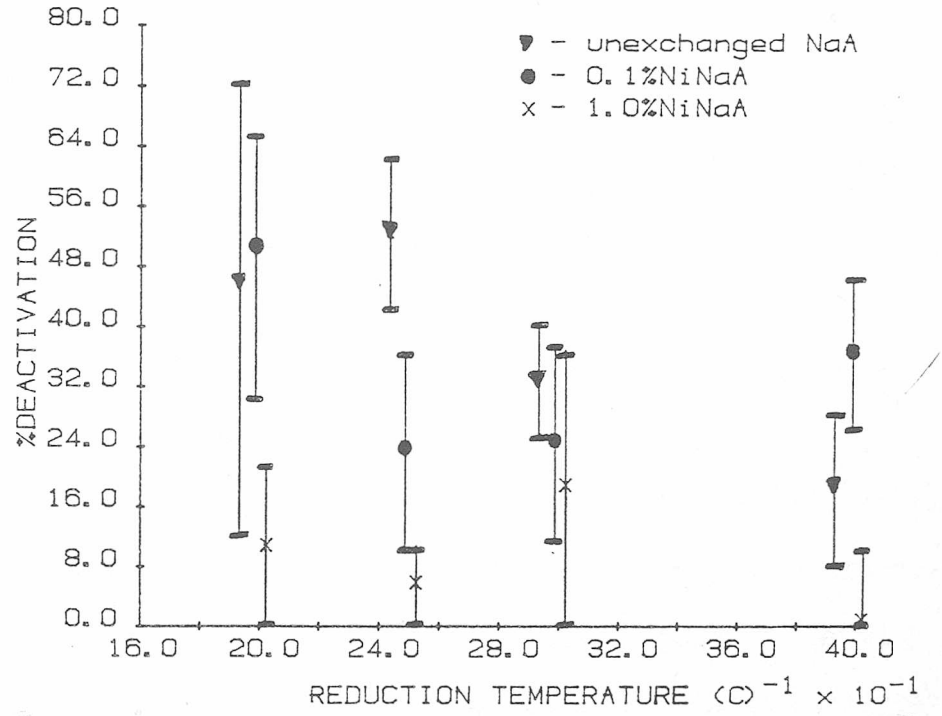

FIGURE 7.11

Variation of %Deactivation with Nickel content and Temperature of Reduction.
Ethene Hydrogenation at 383K.

in the 0.1% and the unexchanged samples were large because the deactivation was so great in these samples that a significant decline in the rate during the initial reaction occurred causing the %alkene vs. time plot to curve. This sometimes resulted in catalysts showing apparent first order behaviour at temperatures which had previously given zero order kinetics. For example, the ethene hydrogenation rate at 380K for the unexchanged zeolite reduced at 200C dropped by 53% during the first reaction.

Catalyst deactivation can be caused by impurities in the reactant mixture. However, such impurities would only be present in very low concentrations and could only poison a specific number of catalytic sites. Thus they would cause a greater percentage deactivation the smaller the catalyst sample. Therefore, to ensure that impurities were not the cause of deactivation in this case, a 0.2gram and a 0.5gram sample of 0.1% NiNaA were reacted under identical conditions to a previous 0.1gram sample experiment. The results in Figure 7.10 show that the deactivation is independent of catalyst weight. However, to reduce the risk of external poisons the mercury manometer which had originally been used to measure reactant mixtures, was replaced by a pressure transducer to ensure that there was no mercury vapour in the system (see Chapter 5.3).

Further tests were then performed to see if the deactivation would eventually destroy all the catalytic activity of a sample. Figure 7.12 shows that the activity declines exponentially with reuse and eventually reaches a steady state wherein it still retains a degree of activity. Figure 7.13 compares the Arrhenius plots of a normal catalyst to one which was stabilised by prolonged exposure to reactants. As can be seen the activity of the stabilised catalyst is approximately one quarter of the full activity. It was also found

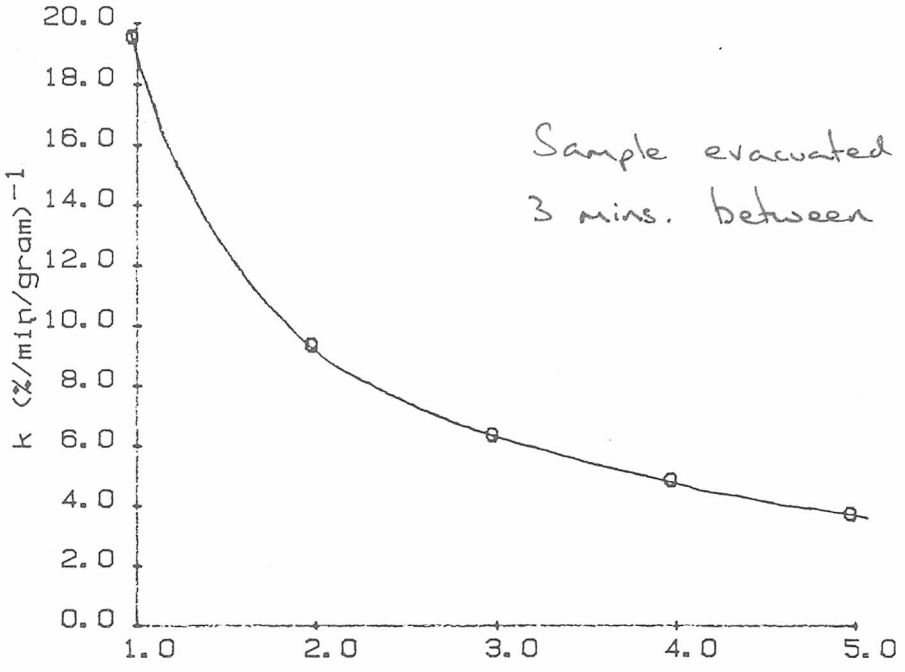

FIGURE 7.12

Decrease in Rate with Catalyst Reuse. (Ethene Hydrogenation at 438K over 0.1%NiNaA reduced at 250C.)

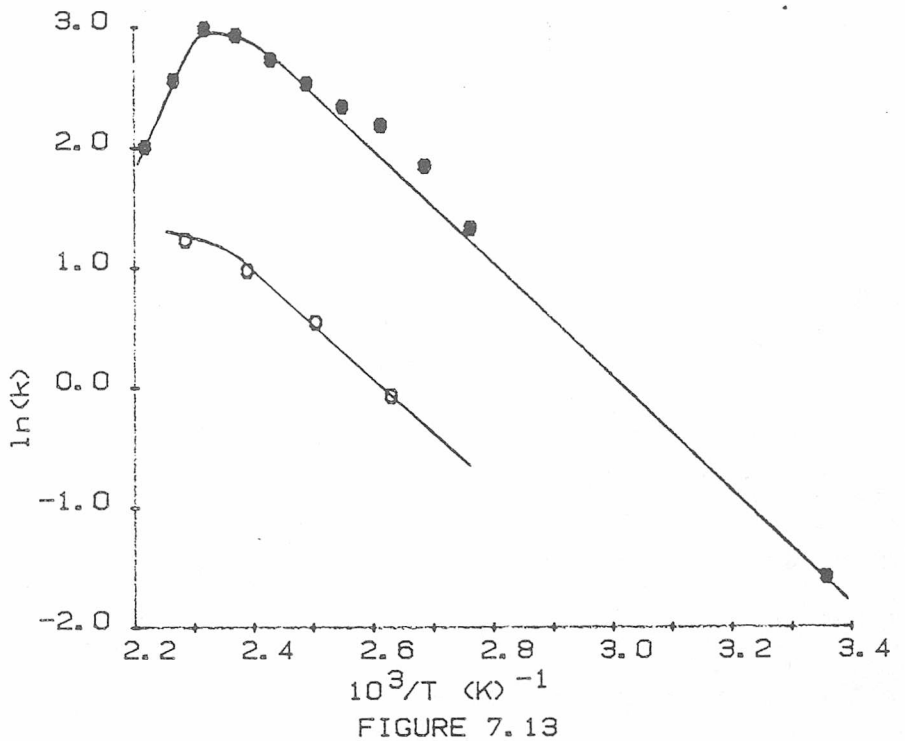

FIGURE 7.13

Arrhenius Plots for Ethene Hydrogenation over, • fresh, and o deactivated 0.1%NiNaA reduced at 300C.

at temperatures below 100°C,
that overnight evacuation, or exposure to hydrogen, resulted in substantial, though not total, reactivation of the nickel exchanged catalysts. This was not found for the unexchanged zeolite.

A number of tests were then conducted with propene and isobutene to discover how the deactivation varied with the alkene used. As with ethene the reaction rate decrease with repeated use on the 1.0% NiNaA was found to be less than 20%, and therefore, within the limits of experimental error, insignificant. On 0.1% samples reduced at 250C the overall propene deactivation at 432K was between 4% and 13%, whilst that for isobutene at 435K was less than 10%. Thus, it initially appeared that the degree of deactivation decreased with increased carbon number. However, it was noticed that on the 0.1% catalyst the isobutene vs. time plots showed a distinct curve during the induction period. An example of this is shown in Figure 7.14. In this case the activity dropped by nearly 92% between region 'A' and region 'B'. On reuse the activity during induction was found to be similar to the activity in region 'B'. This indicates that the sites active during induction were severely deactivated by isobutene. To see if this effect occurred with propene, to a lesser extent since it was not readily visible, the percentage drop in activity during induction for repeated use of the catalyst which had shown the 4% to 13% overall drop in activity was calculated. This was found to be between 36% and 56%. Therefore, it would appear that deactivation of the 0.1% catalyst occurs on the sites which do not exhibit induction, and the degree of deactivation is greater for isobutene than for propene. This would explain why the 1.0% catalyst, which is not active during the induction period, is not susceptible to deactivation.

The anomaly in this interpretation is that the ethene on the

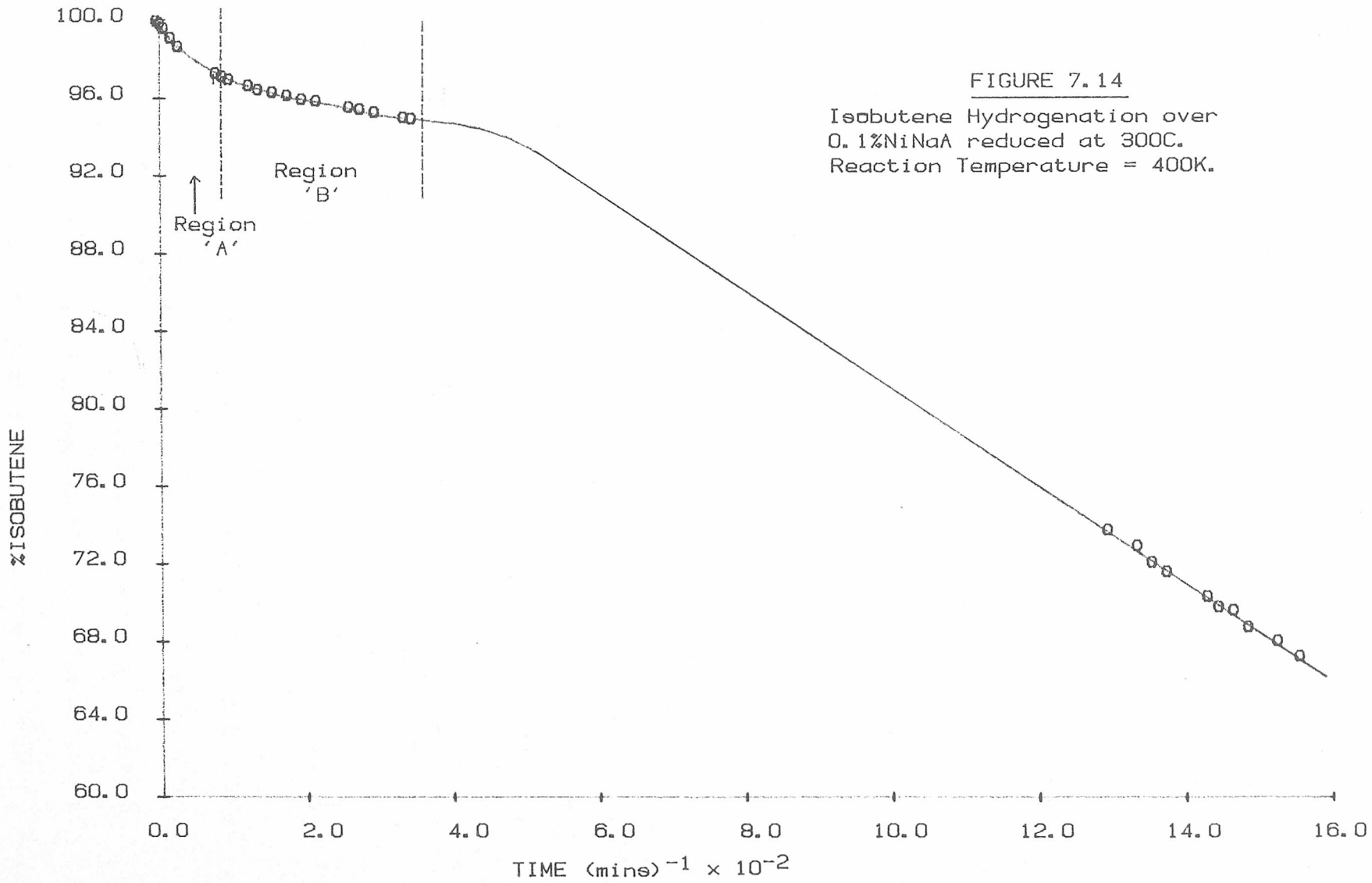

FIGURE 7.14

Isobutene Hydrogenation over 0.1%NiNaA reduced at 300C. Reaction Temperature = 400K.

0.1% NiNaA does not exhibit an induction period, but is prone to deactivate. It is possible that the non-appearance of an induction period in this case could be due to the activity during induction being so great that it masks its own existence. If this were the case then deactivation of the sites of initial activity should produce induction. It was shown above that these sites are most prone to deactivation by isobutene. Therefore, an 0.1% NiNaA sample was reduced at 300C and reacted with isobutene at 425K before exposure to ethene. This reduced the overall activity of the catalyst with respect to ethene hydrogenation and a distinct induction appeared. Even in this deactivated state the activity during induction was over 50% of the overall rate. Thus it would appear that under normal conditions the activity for ethene on the 0.1% NiNaA is almost entirely due to reaction on sites which do not exhibit induction.

Reuse of a sample also resulted in an increase in the length of induction. No proportional correlation between degree of deactivation and increase in induction period was found for the results obtained, but for a given catalyst the greater the deactivation the greater the increase in I, whilst a partially reactived catalyst had an induction period length in between that of the fully active catalyst and the deactivated one.

7.5 Anomalous Results

During this work some anomalous results were discarded. However, two sets of results which do not fit with the others must be noted.

The first was that three consecutive isobutene hydrogenation experiments performed on different samples of 0.1% NiNaA reduced at 300C showed little or no induction effect when reacted at 420K ($<$ 20mins with overall reaction time of over 1200mins). And when one

of these catalysts was then treated with ethene no induction period appeared (see previous section), the level of activity of the catalyst being as for other results after induction.

The second anomalous result also occurred with isobutene over 0.1% NiNaA reduced at 300C. On this occasion no induction was seen and the initial activity was much higher than normal. After about 25% reaction the activity then fell dramatically and levelled off at a lower value than normal. This is shown in Figure 7.15.

7.6 Pressure Dependence

The dependence of both reaction rate and induction length on the partial pressures of the reactants was investigated by exposure of single catalyst samples to various reactant pressures. Repeated reaction over single samples, rather than a series of experiments on fresh samples, was used so as to avoid reproducibility variations. This meant that, as before, care had to be taken to allow for variations due to catalyst deactivation. It was noted in Chapter 6.5 that the rate constants generally quoted in this work were not true rate constants, but were related to the true values by the equation:-

$$k(\text{true}) = k(\text{calculated}) \, (\text{alkene concentration})/\text{hydrogen concentration})$$

Generally this did not matter since the initial reactant concentrations used were the same. However, in this section where the pressure dependence was being measured the true rate constants had to be used.

Results obtained for propene hydrogenation at 407K over 1.0% NiNaA reduced at 200C are shown in Table 7.2, whilst those for isobutene over 1.0% NiNaA reduced at 200C and 250C are given in Tables 7.3 and 7.4.

No systematic variations in either rate constant or induction period length with hydrogen pressure can be seen from these results. This

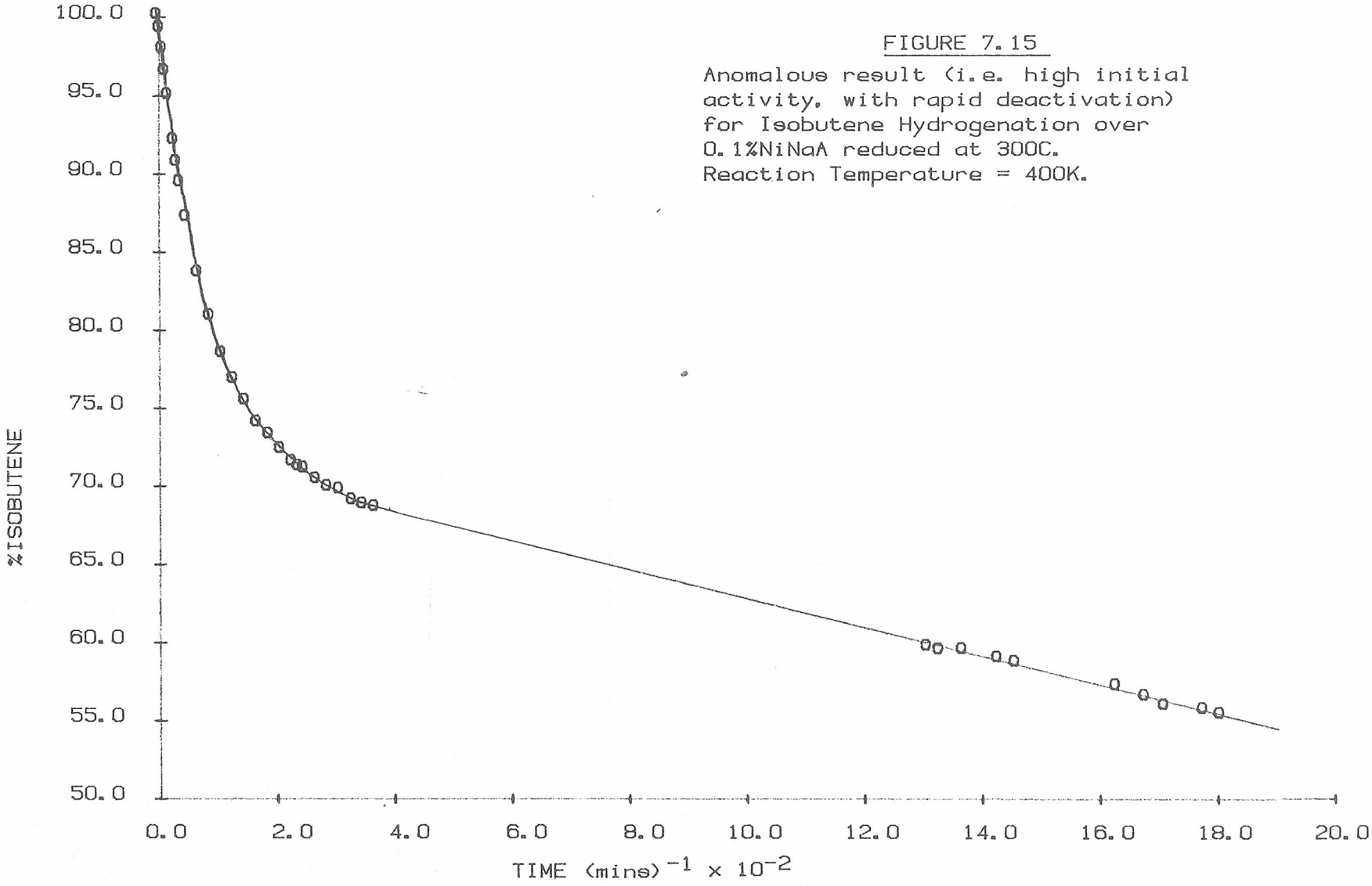

FIGURE 7.15

Anomalous result (i.e. high initial activity, with rapid deactivation) for Isobutene Hydrogenation over 0.1%NiNaA reduced at 300C. Reaction Temperature = 400K.

TABLE 7.2

Effect of Reactant Pressure on Rate and Induction Length

(propene reacted at 407K over 1.0% NiNaA reduced 200C)

Experiment No.	No.Moles PROPENE (10^5)	No.Moles HYDROGEN (10^4)	k(%/min/gram) (measured)	k (true) (mol/min/mol/gram)	Induction (mins.)
1	6.33	12.41	58	0.0296	7.5
2	6.33	12.19	70	0.0363	5.8
3	31.65	12.41	26.5	0.0676	12.6
4	3.165	12.51	89	0.0225	4.3
5	18.99	12.51	41	0.0622	10.2
6	6.33	12.51	76	0.0385	4.5
7	6.33	6.574	45.2	0.0435	5.5
8	6.33	9.013	56.9	0.0400	5.5
9	6.33	2.651	16.5	0.0394	4.5
10	6.33	10.50	60.1	0.0362	5.0

TABLE 7.3

Effect of Isobutene Pressure on Rate and Induction Length

(reaction at 384K over 1.0% NiNaA reduced at 200C)

Experiment No.	No. Moles ISOBUTENE (10^5)	No. Moles HYDROGEN (10^4)	k(%/min/gram) (measured)	k(/min/gram) (true) (10^3)	Induction (mins)
8	6.33	12.3	12.79	6.582	10.5
9	6.96	12.2	12.40	9.927	7.0
10	3.165	12.4	21.63	5.521	5.0
11	18.99	12.4	7.773	11.90	17.0

sample had already been used a number of times before these particular tests were performed. Sample was left overnight between experiments 8 & 9.

TABLE 7.4

Effect of Isobutene Pressure on Rate and Induction Length

(reaction at 392K over 1.0% NiNaA reduced at 200C)

Experiment No.	No. Moles ISOBUTENE (10^5)	No. Moles HYDROGEN (10^4)	k(%/min/gram) (measured)	k(/min/gram (true) (10^2)	Induction (mins)
1	6.33	12.24	53.67	2.776	25.5
6	3.165	12.11	72.4	1.892	14.0
7	18.99	12.36	31.17	4.789	26.5
8	6.33	12.30	59.0	3.036	15.0
9	6.33	2.52	13.6	3.416	19.0

sample had already been used a number of times before these particular tests were performed.

indicates that the reaction is, as had been assumed, first, or close to first order with respect to hydrogen, and the induction period is independent of hydrogen pressure.

However, increasing the alkene pressure causes an increase in both the rate constant and the length of induction. The increase in rate is caused by the fact that it was measured assuming zero order dependence of reaction on alkene when the true order was expected to be fractional. Therefore the rate constant obtained is actually a rate value which allows for hydrogen pressure.

$$\text{RATE} = \text{constant } (\text{alkene})^{x}$$

$$\text{thus} \qquad \ln(\text{RATE}) = x\ln(\text{alkene}) + \text{constant}$$

Therefore a plot of ln(RATE) vs. ln(alkene) should have slope x.

This treatment was applied to the above data and the results obtained are shown in Figures 7.16, 7.17, and 7.18. As can be seen the order obtained in each case was approximately 0.5.

Since the induction period was also found to vary with alkene concentration a similar treatment was performed on the induction data:-

$$\text{assuming} \quad I \propto (\text{alkene})^{x} \quad \text{where (alkene) = alkene concentration}$$

$$\text{then} \quad I = y(\text{alkene})^{x}$$

Thus a plot of ln(I) vs. ln(alkene) should give a slope x. The results shown in Figures 7.19, 7.20, and 7.21 gave values of x of approximately 0.5.

Therefore it appears that the length of the induction period has the same dependence on alkene pressure as the rate but is independent of the hydrogen pressure.

7.7 Pre-exposure to Reactants and Products

To investigate the effect of pre-exposure of the catalysts to reactants a number of tests were performed using isobutene over

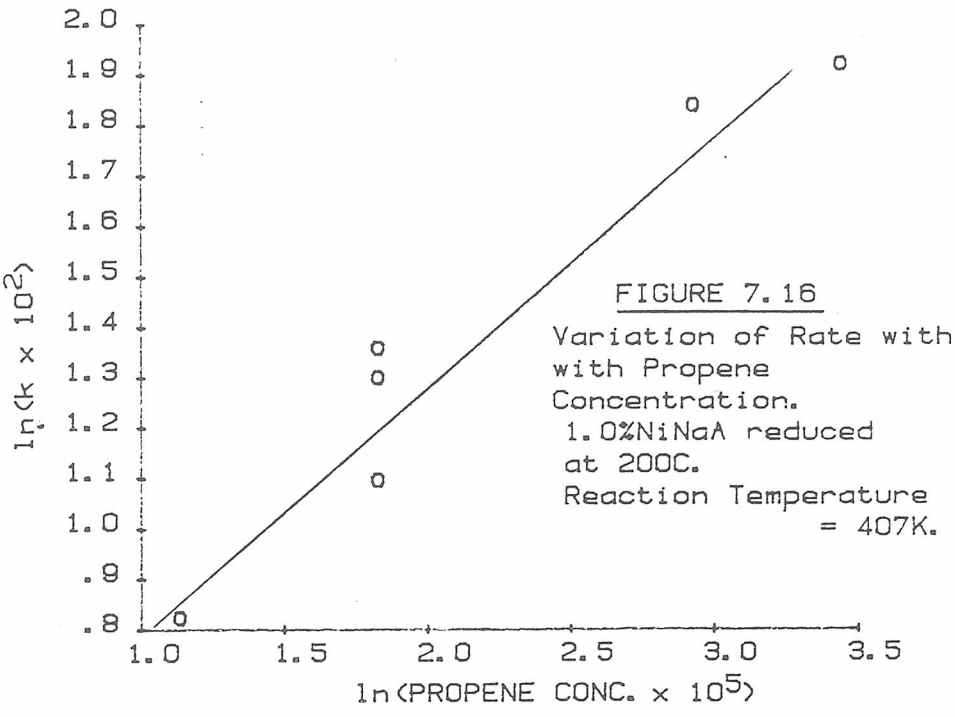

FIGURE 7.16

Variation of Rate with with Propene Concentration.
1.0%NiNaA reduced at 200C.
Reaction Temperature = 407K.

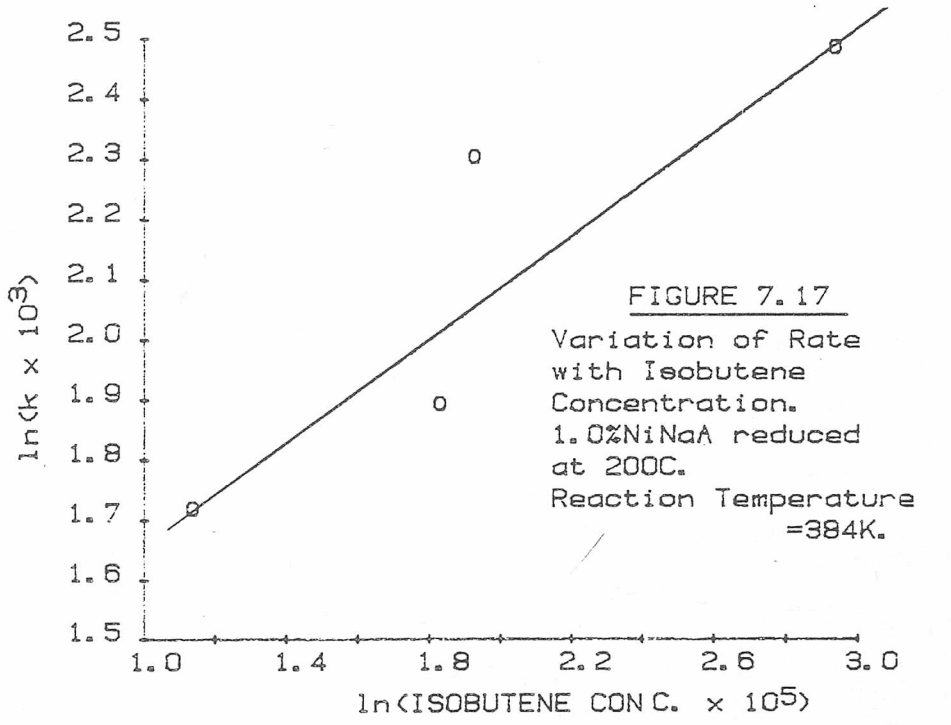

FIGURE 7.17

Variation of Rate with Isobutene Concentration.
1.0%NiNaA reduced at 200C.
Reaction Temperature =384K.

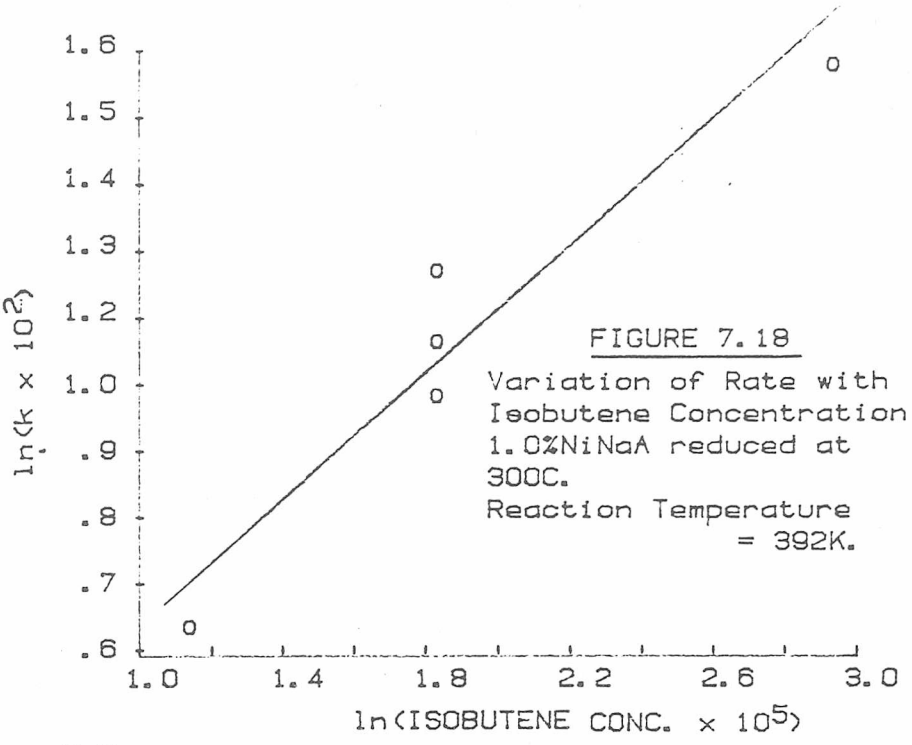

FIGURE 7.18

Variation of Rate with Isobutene Concentration 1.0%NiNaA reduced at 300C.
Reaction Temperature = 392K.

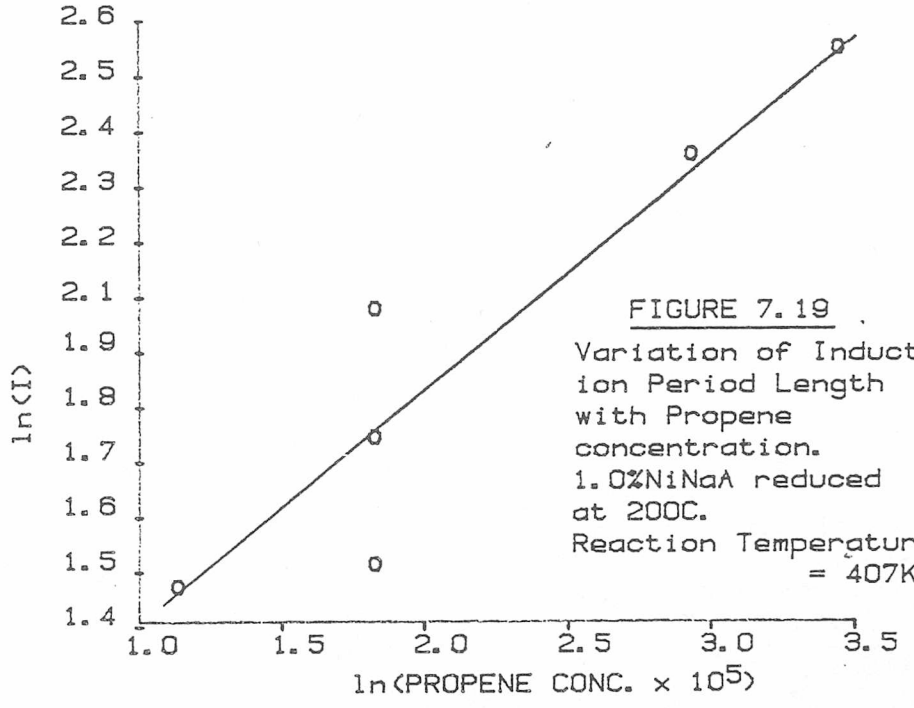

FIGURE 7.19

Variation of Induction Period Length with Propene concentration.
1.0%NiNaA reduced at 200C.
Reaction Temperature = 407K.

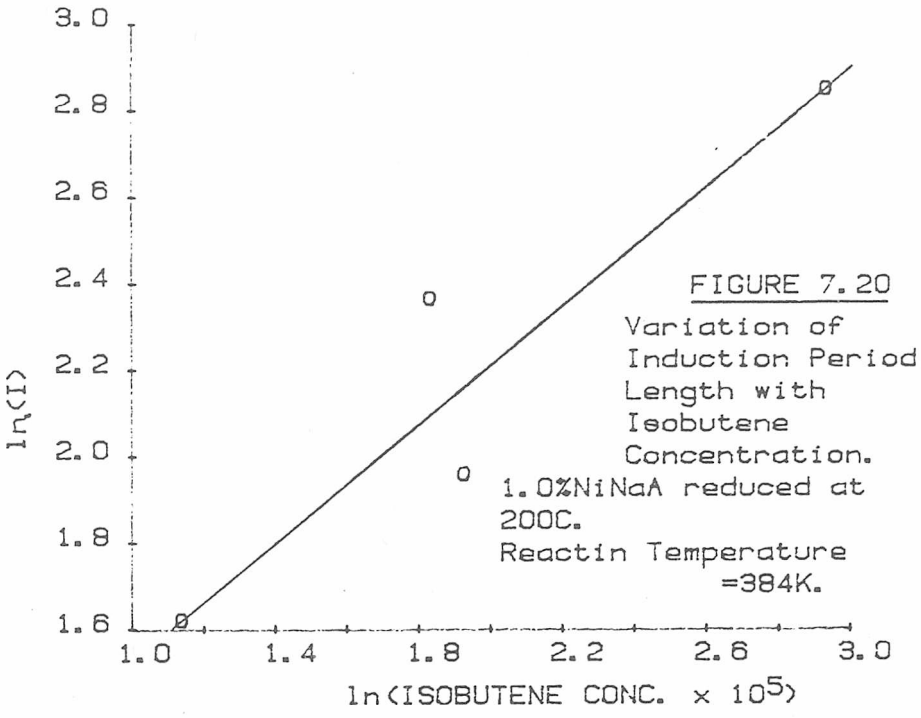

FIGURE 7.20

Variation of Induction Period Length with Isobutene Concentration.
1.0%NiNaA reduced at 200C.
Reactin Temperature =384K.

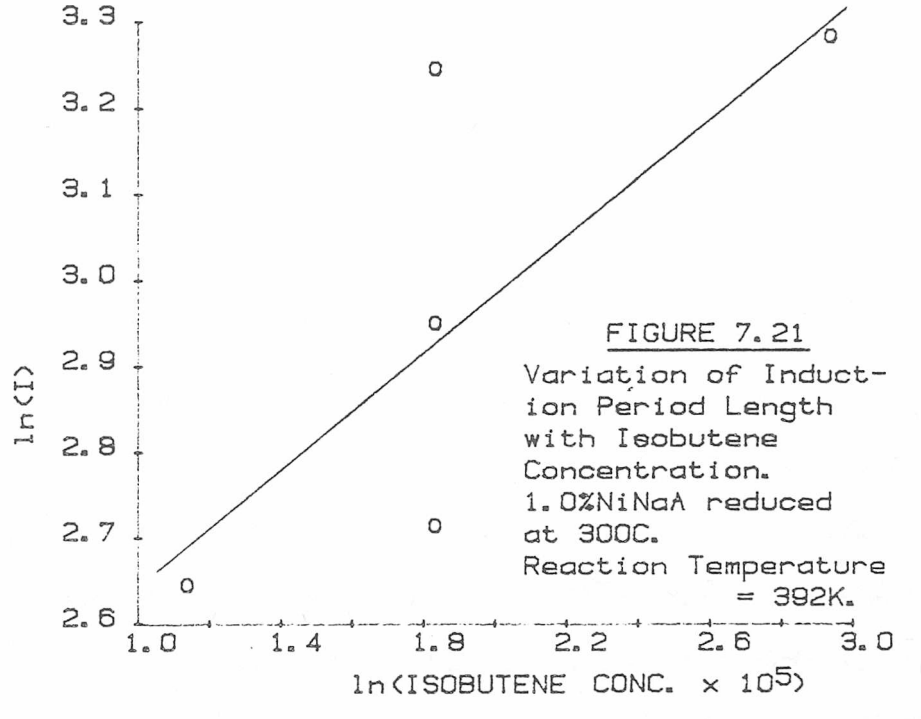

FIGURE 7.21

Variation of Induction Period Length with Isobutene Concentration.
1.0%NiNaA reduced at 300C.
Reaction Temperature = 392K.

1.0% NiNaA reduced at 250C. This system was chosen since the 1.0% sample is not as prone to deactivation as the lower exchanged samples and the isobutene has a convenient induction length and reaction rate.

It was found that exposure of the catalyst to alkene alone tended to deactivate the catalyst to a greater extent than normal and which, as would be expected from the results of section 7.4, caused an increase in induction period length. Therefore, careful analysis was required to see if a change in induction length due to pre-exposure, as well as deactivation, occurred. Since the induction length generally increased as the reaction rate decreased a plot of ln(1/I) vs. ln(k) was made for repeated use of samples including pre-exposure treatments. From this it was hoped that any genuine pre-exposure effects would produce a deviation from the overall curve obtained. The result is shown in Figure 7.22. It can be seen from this that pre-exposure to reactant produced no apparent alteration in the induction period length outside of the increase caused by the catalyst deactivation. Although a deviation was found for isobutane pre-exposure this was almost certainly due to error in the quantity of hydrocarbon injected into the reaction vessel. This occurred because of the difficulty in accurately mixing small amounts of isobutane and isobutene. From the size of the G.C. peaks obtained it was calculated that the concentration of hydrocarbon in this case was about 40% greater than normal. The actual length of the induction was identical to the previous test on that sample which is what would be expected if no pre-exposure effect occurred, since alkanes do not tend to deactivate catalysts.

Therefore, as far as could be ascertained from these results the induction period found on these catalysts was not altered by pre-exposure to reactants or products.

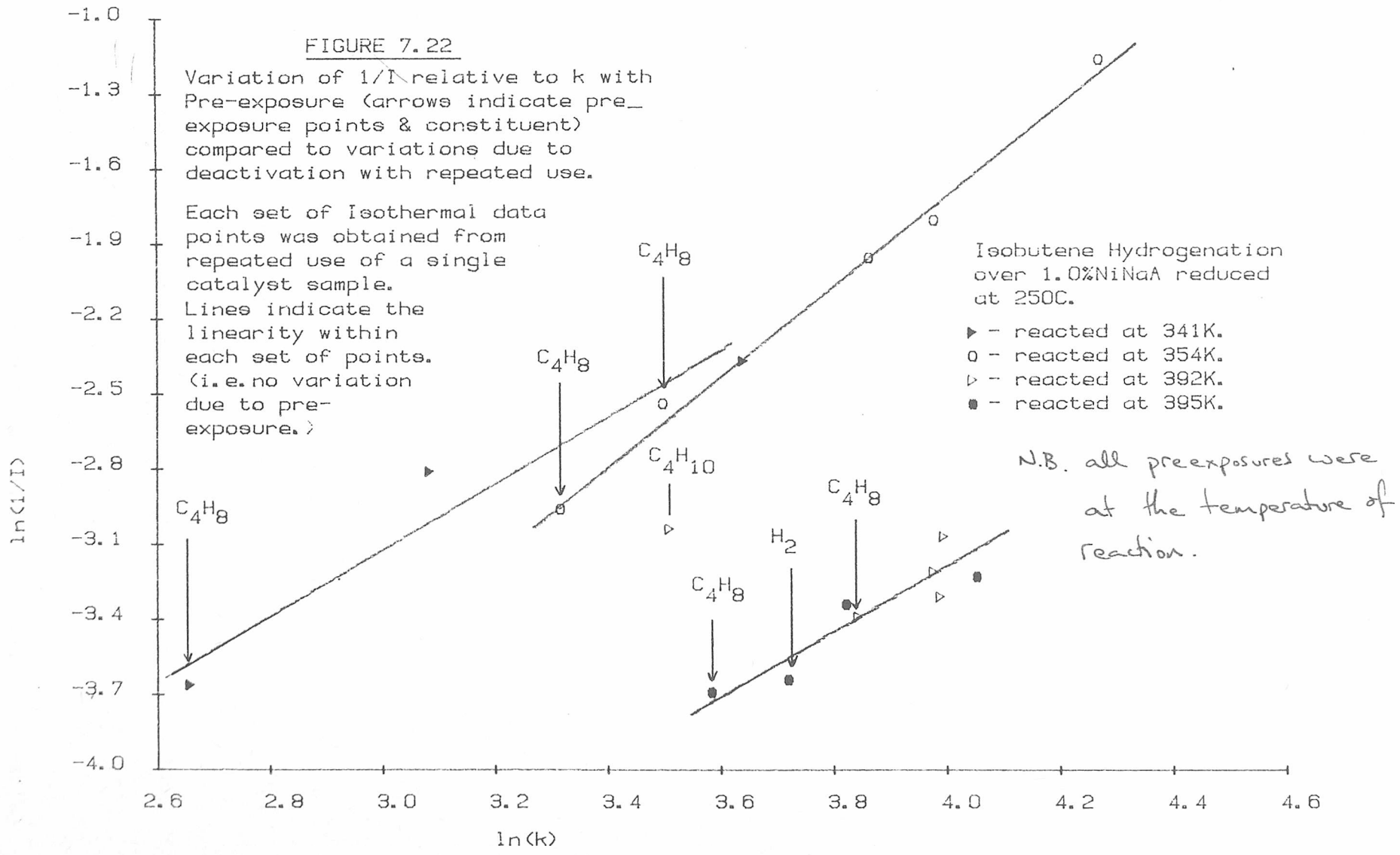

FIGURE 7.22

Variation of 1/I relative to k with Pre-exposure (arrows indicate pre-exposure points & constituent) compared to variations due to deactivation with repeated use.

Each set of Isothermal data points was obtained from repeated use of a single catalyst sample. Lines indicate the linearity within each set of points. (i.e. no variation due to pre-exposure.)

Isobutene Hydrogenation over 1.0%NiNaA reduced at 250C.

▶ - reacted at 341K.
o - reacted at 354K.
▷ - reacted at 392K.
● - reacted at 395K.

N.B. all preexposures were at the temperature of reaction.

7.8 n-Butene Isomerization

A number of experiments were performed with n-butene to study the effect of induction on isomerization. Since the initial stages of isomerization, exchange and hydrogenation are expected to be the same whilst the later stages differ (see Chapter 3.6) the appearance, or non-appearance of induction during isomerization would indicate the stage of the reaction at which the cause of the induction occurred. It would have been interesting to have obtained results for exchange, to extend this comparison, but the G.C. used in the later stages of this work was unsuitable for isotope analysis.

It was found that isomerization exhibited an induction period identical to that for the hydrogenation reaction. Although during pre-exposure of the catalyst to n-butene, isomerization occurred, at a lower level than that obtained after the addition of hydrogen. This is shown in Figure 7.23.

It is also worth noting here, that no significant isobutene formation occurred during the butene reactions.

7.9 Effect of Opening Mixing Volume

A possible cause of the induction effect was that the catalyst was reacting preferentially with some impurity injected into the system along with the reactants. This seemed unlikely because the induction period length was reproducible over a given catalyst, and therefore any contaminants must have been present in the original reactant containers. Also the length of induction depended on the alkene used which implied that the impurity must be different for each alkene.

However, an attempt was made to test for impurity by releasing more reactants into the reaction vessel during a reaction without evacuating the original mixture. If an impurity was causing the

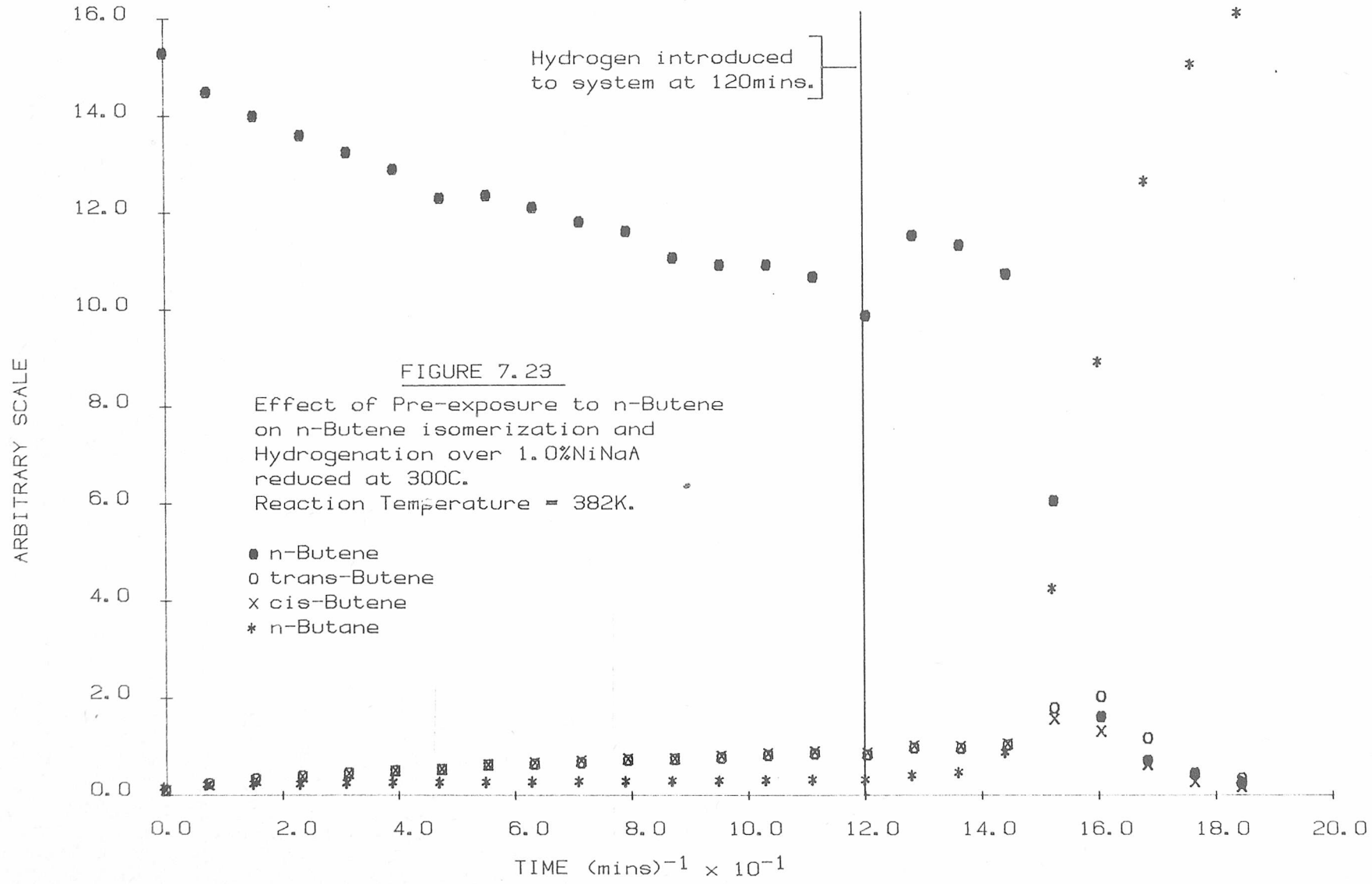

FIGURE 7.23

Effect of Pre-exposure to n-Butene on n-Butene isomerization and Hydrogenation over 1.0%NiNaA reduced at 300C.
Reaction Temperature = 382K.

induction, the introduction of the second batch of reactants might produce a second induction, whilst if a mechanistic effect such as surface complex was the cause the reaction would proceed unhindered. It was not possible to inject further reactants into the reaction vessel without major changes to the system. Therefore, more reactant was introduced to the catalyst simply by reopening the tap to the mixing vessel from which the original reactants had been released. It was expected that this would upset the rate values obtained, since the reaction volume was larger, the mixing vessel was at room temperature, and there was a constriction at the tap between the mixing and reaction vessels. However, the appearance or non-appearance of a second induction period should have been noticeable. The results obtained were rather unusual as can be seen from the two raw peak graphs for isobutene hydrogenation shown in Figure 7.24. Whenever the tap to the mixing vessel was opened the reaction appeared to stop and on closing the tap the reaction immediately started up again. It is unlikely that the reaction actually stopped during the period of the tap being open since the catalyst was maintained at a constant temperature throughout the experiment and this was the area where reaction occurred. It is more probable that the rate of diffusion of alkene from the reaction vessel to the mixing vessel was slow and the rate of production of alkane was similar to the rate of disappearance into the mixing vessel. Thus the results were not as clear as had been hoped. However, because of the fact that, no matter how long the tap to the mixing vessel was left open, the reaction started as soon as it closed it seems unlikely that any impurities were transferred into the reactor.

7.10 Activity

It was found in this work that the Arrhenius plots which were

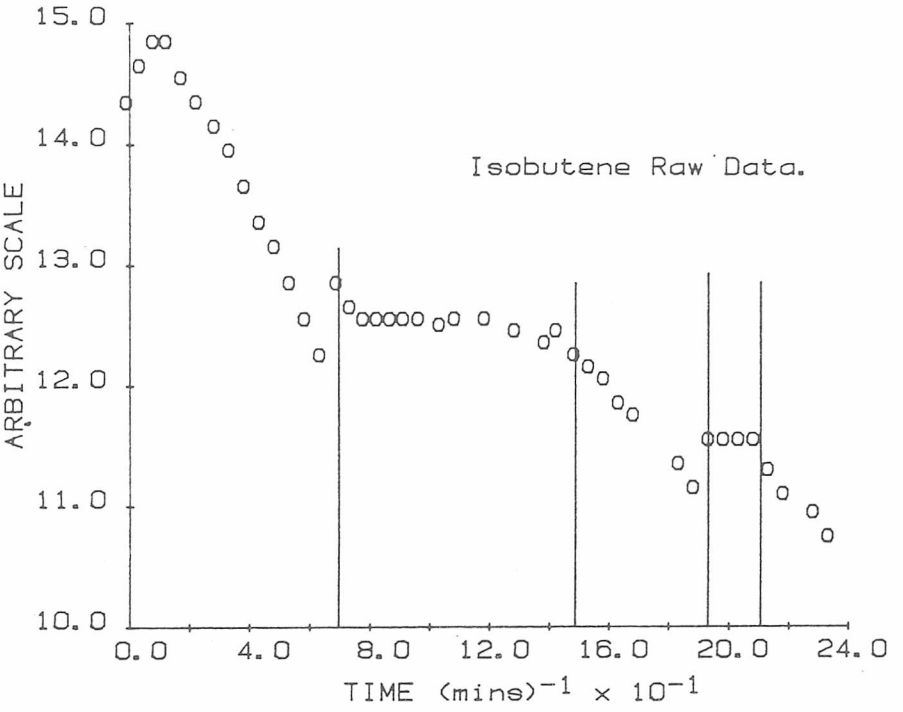

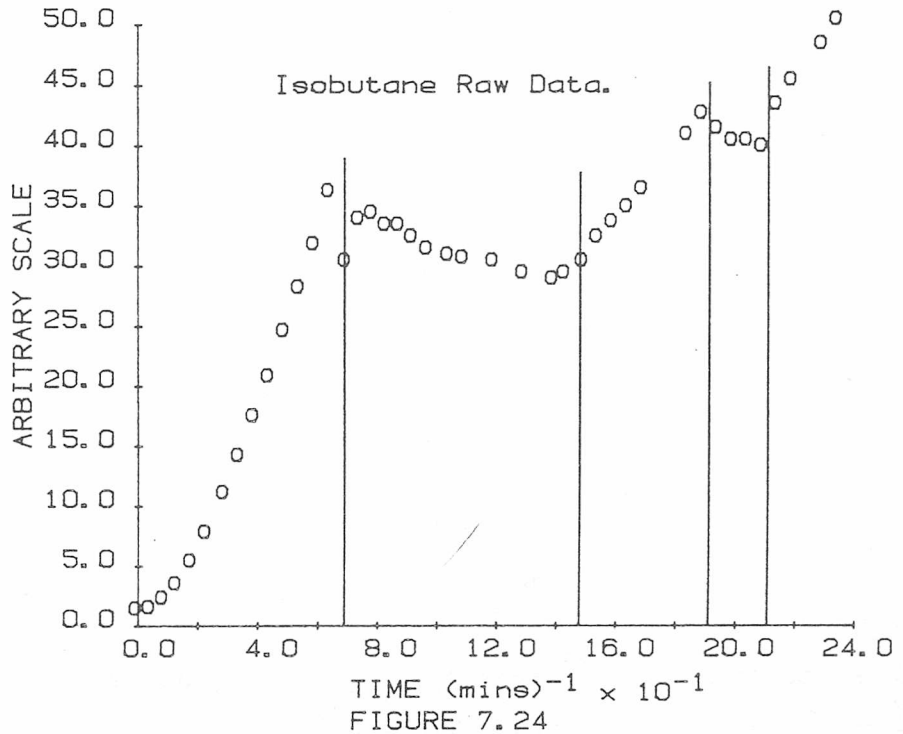

FIGURE 7.24

Effect of opening tap to mixing vessel (Y) on Isobutene Hydrogenation over 1.0%NiNaA reduced at 400C.
Reaction Temperature = 335K.
(tap opened at 70mins. and 195mins. closed at 149mins. and 211mins.)

obtained were not linear. This was assumed to be due to an effect similar to that, discussed in Chapter 3.6, found on other nickel catalysts. Therefore, the activation energies were always related to a temperature range, and rate values at specified temperatures were used rather than pre-exponential factors, the values of which varied depending on the temperature range investigated. The Arrhenius plots for ethene, propene and isobutene over the nickel zeolites are shown in Figures 7.25, 7.26 and 7.27. Whilst the rates of hydrogenation at 100C over all the catalysts are shown in Table 7.5. To evaluate the effect of changing the nickel content of the zeolite, the reaction rate was also calculated as the number of alkene molecules reacted per second per nickel atom present. This was done by multiplying the obtained rate constants by the number of alkene molecules present and dividing them by the number of nickel atoms in a gram of catalyst.

RATE (alkene molecule/second/nickel atom)

= Nickel turnover rate (NTR)

$$= \text{RATE (\%/min/gram)} \times \frac{\text{(no. alkene molecules)}}{100 \times 60} \times \frac{1}{\text{(No. nickel atoms/gram)}}$$

$$= k \times \frac{C_o \times 6.02\times10^{23}}{100\times60} \times \frac{M \times 10^6}{n(6.02\times10^{23})}$$

where m = relative molar mass of nickel

n = amount of nickel in the sample as parts per million.

& 6.02×10^{23} = Avogadros No. (No. of molecules in a mole)

7.11 Competitive Reactions

Up to this point the selectivity of the catalysts with respect to different alkenes had only been considered by measurement of the individual rates. No account being taken of the effect of mixing the alkenes. Mixtures were, therefore, introduced to catalysts to

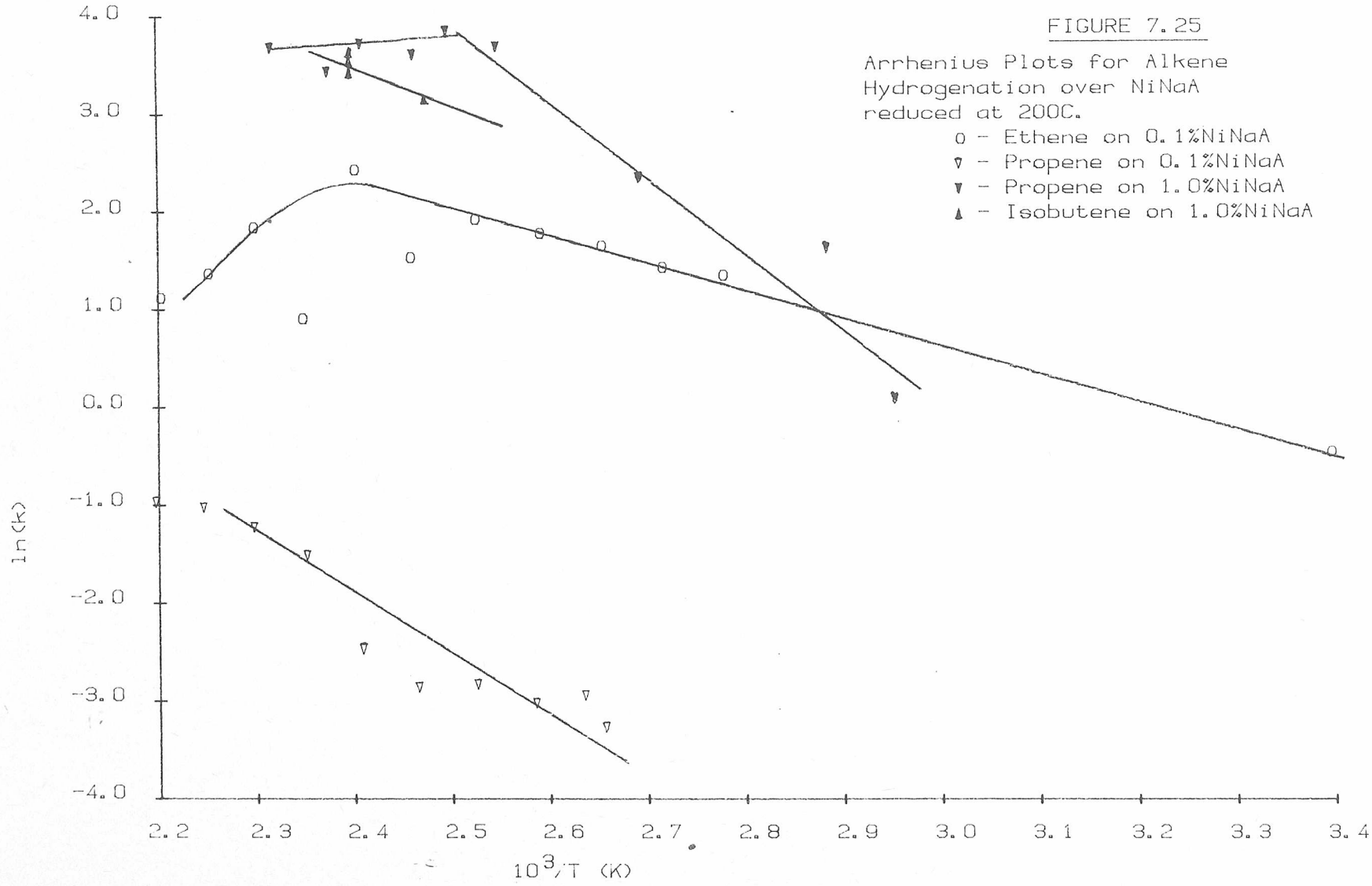

FIGURE 7.25

Arrhenius Plots for Alkene Hydrogenation over NiNaA reduced at 200C.

o - Ethene on 0.1%NiNaA

▽ - Propene on 0.1%NiNaA

▼ - Propene on 1.0%NiNaA

▲ - Isobutene on 1.0%NiNaA

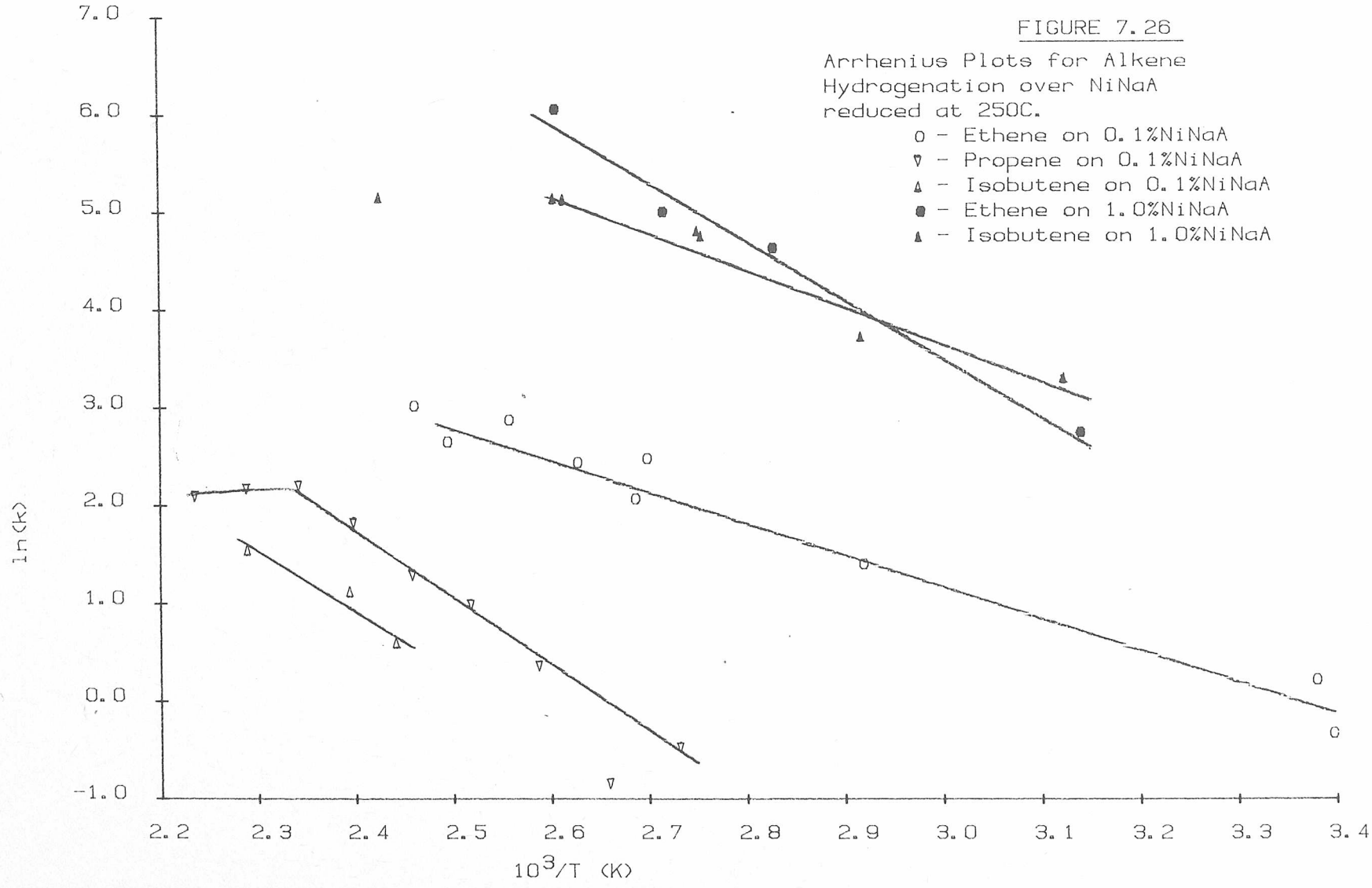

FIGURE 7.26

Arrhenius Plots for Alkene Hydrogenation over NiNaA reduced at 250C.

o - Ethene on 0.1%NiNaA
▽ - Propene on 0.1%NiNaA
△ - Isobutene on 0.1%NiNaA
● - Ethene on 1.0%NiNaA
▲ - Isobutene on 1.0%NiNaA

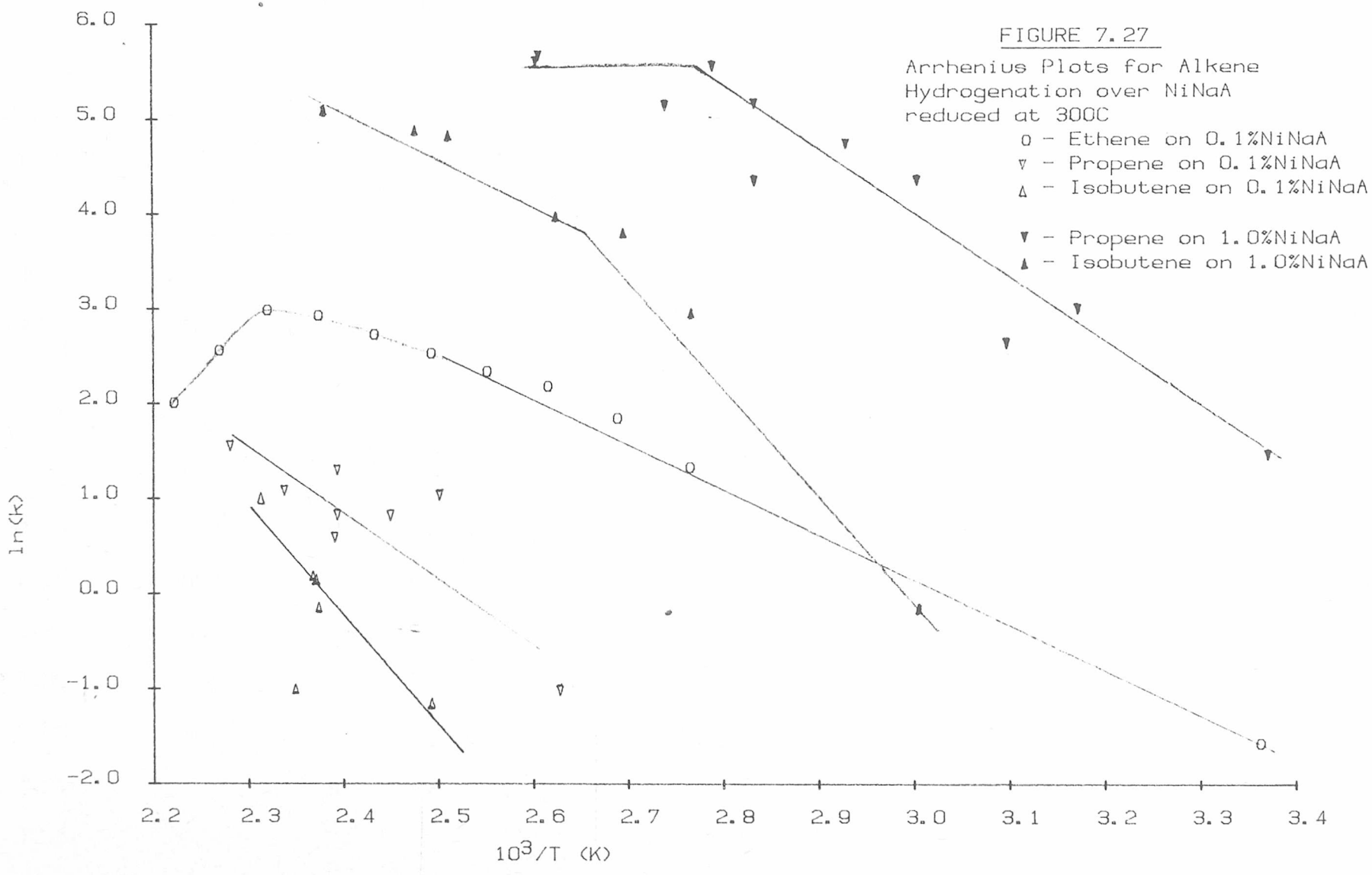

FIGURE 7.27

Arrhenius Plots for Alkene Hydrogenation over NiNaA reduced at 300C

o – Ethene on 0.1%NiNaA

▽ – Propene on 0.1%NiNaA

△ – Isobutene on 0.1%NiNaA

▼ – Propene on 1.0%NiNaA

▲ – Isobutene on 1.0%NiNaA

TABLE 7.5

Activity of Zeolites as Hydrogenation Catalysts at 100 °C

(Values for C_o and n were taken from Chapter Five)

CATALYST	REDUCTION TEMPERATURE	RATE (%/min/gram) ethene	propene	i-butene	RATE (molecules/sec/atom) ethene	propene	i-butene
UNEXCH-	200C	1.7	--	--	0.105	--	--
ANGED	250C	6.9	--	1.1	0.427	--	0.068
"	300C	20	7	3	1.239	0.433	0.186
"	400C	26	--	3.7	1.610	--	0.229
0.1%	200C	5	0.036	--	0.021	1.48×10^{-4}	--
0.1%	250C	10	0.94	0.57	0.041	3.88×10^{-3}	2.35×10^{-3}
0.1%	300C	6.9	0.25	0.055	0.028	1.03×10^{-3}	2.27×10^{-4}
0.1%	400C	9.1	--	1.0	0.037	--	4.13×10^{-3}
1.0%	200C	30	18	12	9.29×10^{-3}	5.57×10^{-3}	3.72×10^{-3}
1.0%	250C	314	--	132	0.097	--	0.041
1.0%	300C	300	270	74	0.093	0.084	0.023
1.0%	400C	550	--	170	0.170	--	0.053

investigate the effect of competition on activity and selectivity. The mixtures were made up of equal quantities of two alkenes, the individual amounts being the same as for the non-competitive work. Therefore, the total amount of alkene was doubled. The amount of hydrogen added was the same as before.

Because of catalyst irreproducibility most competitive reactions were carried out on used catalysts for which the activity with respect to one of the alkenes had already been measured. Generally it was found that the higher alkene in any mixture had the same activity in the mixture as it had alone, along with an induction period of similar length. Whilst the activity of the lower alkene was reduced, and its induction period length was increased. Also in the case of ethene over 0.1% NiNaA, where no induction period was apparent during individual reaction, one was often induced during competitive reaction either with propene or isobutene. Thus the selectivity during competitive reaction was even less than was predicted from individual reactions. However, because of induction effects the higher alkene often did not show full activity until most of the lower alkene had been reacted. An example of this, for ethene/isobutene on 0.1% NiNaA, is shown in Figure 7.28. Therefore, analysis of the competitive reaction using a static reaction system was limited.

7.12 Hydrogenation Activity of Nickel on Alumina

To ensure that the kinetic effects found in this work were not artifacts of the reaction vessel, a small number of experiments were performed on nickel supported on alumina 0.1g samples of 0.4% (by weight) nickel on alumina were pretreated in a similar manner to the zeolite by dehydration at 350C for 16 hrs. followed by reduction in

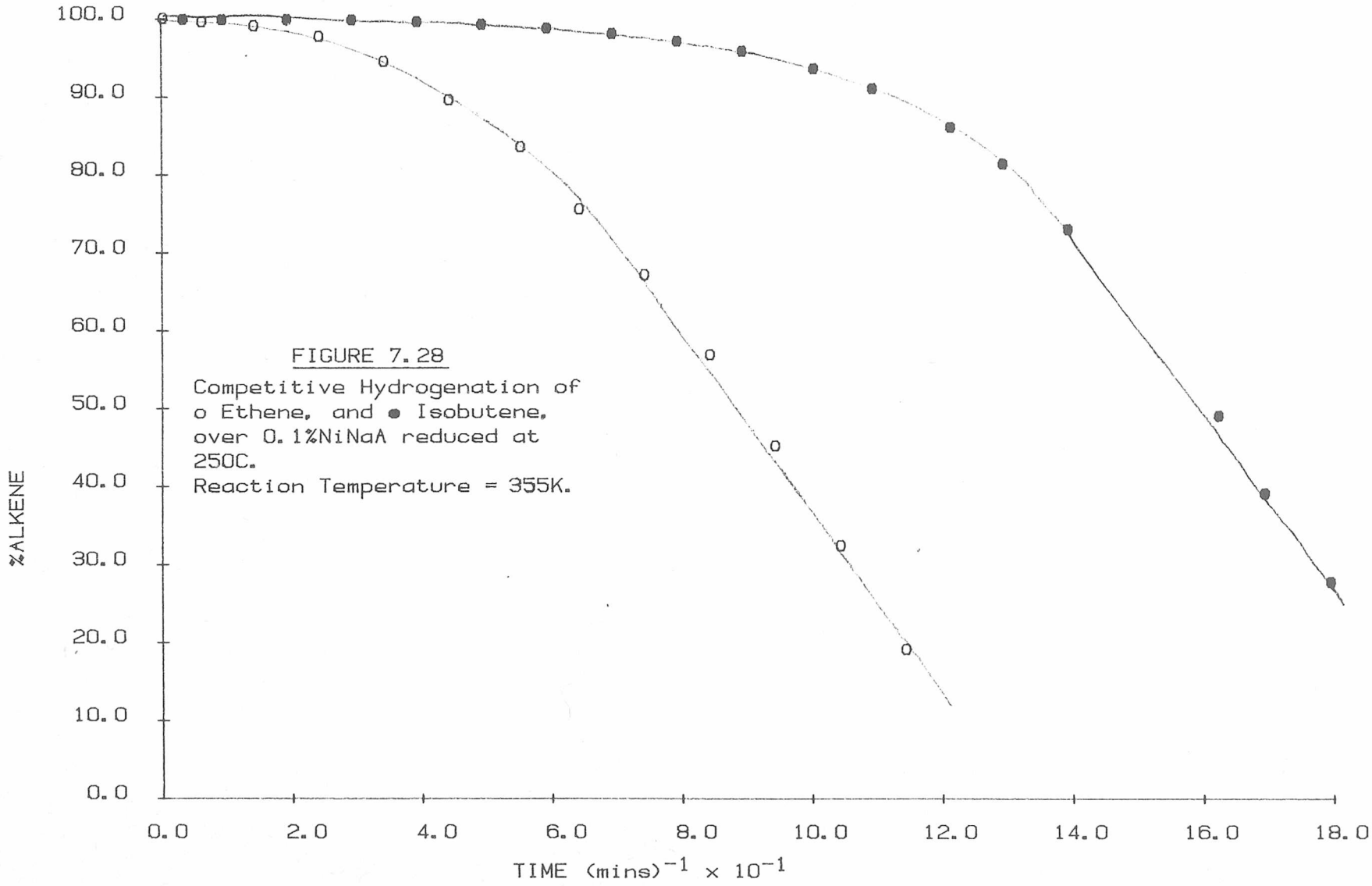

FIGURE 7.28

Competitive Hydrogenation of o Ethene, and ● Isobutene, over 0.1%NiNaA reduced at 250C.
Reaction Temperature = 355K.

hydrogen at 250C. Their hydrogenation activity with respect to ethene and isobutene was then measured.

Neither ethene nor isobutene showed the distinct induction period found over the zeolites, although the isobutene rate of plots were slightly curved. This can be seen from Figure 7.29. This curvature, however, was not due to the same effect as the induction because it did not have a distinct temperature dependence. Like the zeolites the catalytic activity fell on reuse but in this case the activity could not easily be restored. Also during ethene hydrogenation significant amounts of normal butenes and butane were found. The general kinetic characteristics including turnover number and percentage deactivation as shown in Table 7.6, along with the turnover numbers calculated from the data of Koh and Hughes(1). In this case the turnover number, (NTR) or the number of alkene molecules reacted per nickel atom per second is calculated as:-

NTR = (k(%/min/gram) x Co)/60 x wt% nickel/100 (molecules/atom/second)

REFERENCES

1) H. KOH, R. HUGHES, J. Cat., 33,7, (1974)

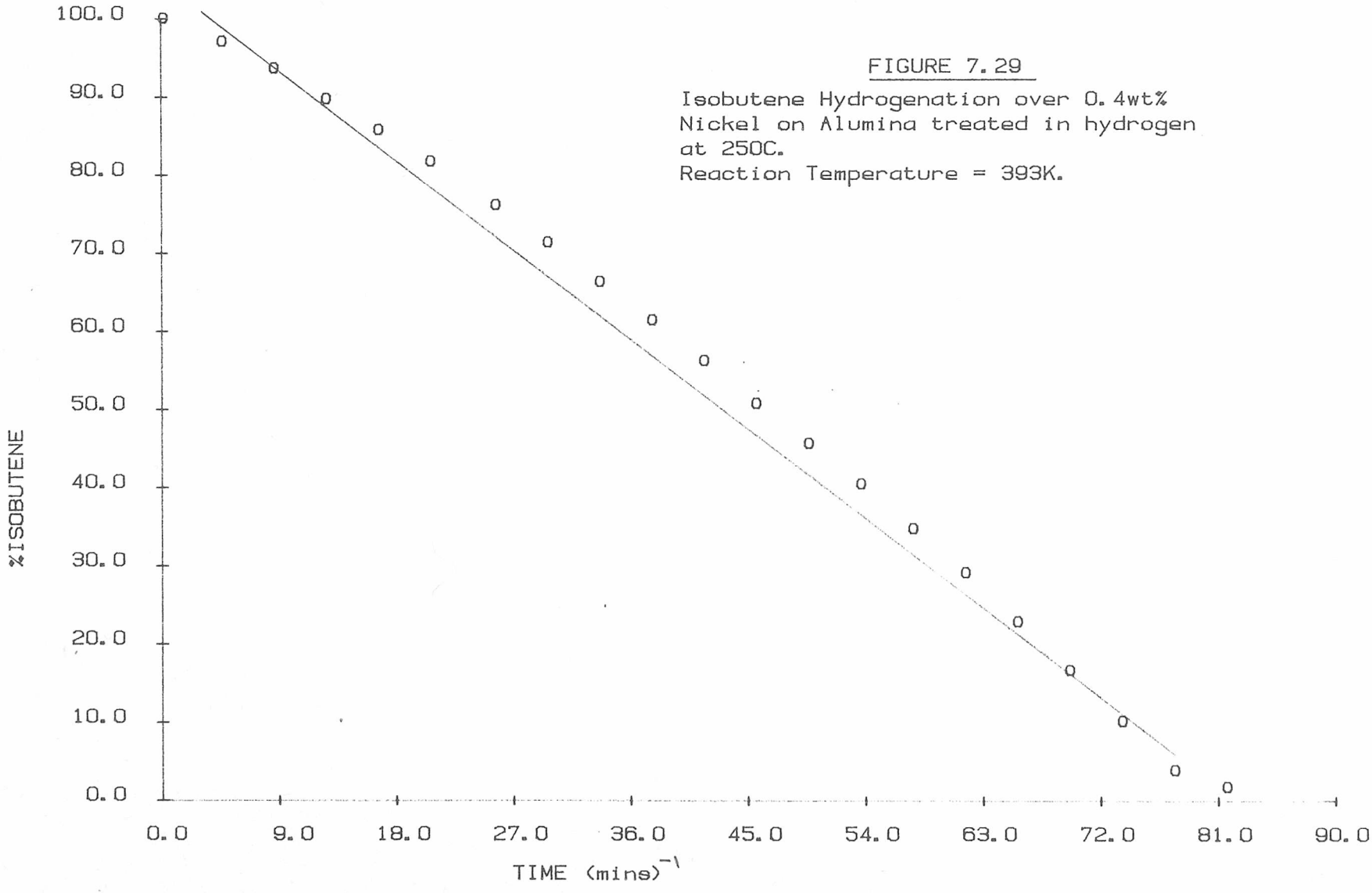

FIGURE 7.29

Isobutene Hydrogenation over 0.4wt% Nickel on Alumina treated in hydrogen at 250C.
Reaction Temperature = 393K.

TABLE 7.6

Hydrogenation Activity of 0.4%Ni on Alumina

ALKENE	REACTION TEMPERATUPE	k (%/min/gram)	NTR (mol/atom/s)	DEACTIVATION (%)
ETHENE	383K	98	1.6e-2	39
"	350K	16 ( )	2.5e-3	--
ISOBUTENE	393K	11.8	1.8e-3	54
"	383K	18.6	2.9e-3	--
"	359K	0.51 ( )	7.9e-5	--
	338K	3.57 ( )	5.5e-4	--
ETHENE (1)*	383K	--	4.7e-2	--

* Nickel on silica-alumina.

Chapter Eight

DISCUSSION

8.1 Introduction

The original objective of this work was to produce a nickel catalyst using Linde 4A zeolite as a chemically inert support. It was hoped that this would create a shape selective catalyst due to the molecular sieve action of the zeolite. However, the alkene hydrogenation reaction chosen to determine the catalyst selectivity has shown some interesting characteristics not normally found over nickel. Therefore, the work has concentrated more on the reaction kinetics rather than the physical characterization of the catalyst and the effect of varying pretreatment conditions. Interpretation of the results thus obtained has proven difficult because all the kinetic effects appear to be interdependent.

8.2 Physical Characteristics

The results of the physical characterization of the nickel 4A zeolites used in this work are given in Chapter Four. These showed that the bulk of the support was Linde 4A zeolite. However, there were a number of trace metal impurities in them, the most significant of these being iron. Also the parent zeolite appeared to have a quantity of iodine on, or in, it which was removed by the nickel exchange process. Perhaps most significantly, electron microscopy revealed the presence of a quantity of small particles which were not 4A zeolite. Therefore, even though these impurities are present in equal quantities in all the samples, the possibility of their catalytic effect must be born in mind throughout the following discussion.

8.3 Induction Period

One of the most interesting aspects of the alkene hydrogenation

reaction over these catalysts was a significant induction period at the start of the reaction. In some instances this induction period lasted for a longer period of time than was required for completion of the post-induction reaction. The most significant features of this effect were:-

i) During the induction period the unexchanged and the 0.1% exchanged catalysts showed a definite activity which could be readily seen as distinct from the post induction activity. This was not found on the 1.0% catalyst which showed no significant activity during induction.

ii) The induction period was shortest on the unexchanged catalyst and longest on the 0.1% samples. Therefore, it did not show any obvious trend with respect to degree of exchange. However, for a given degree of exchange it was found that the induction period was generally longer the lower the overall activity.

iii) The length of the induction period was inversely dependent on temperature.

iv) The onset of post induction reaction was quite sudden; not gradual as might be expected if the catalyst was being activated by exposure to reactants. i.e. a gradual build up of active catalyst sites might be expected.

Possible causes of this induction period will be discussed in section 8.9.

8.4 Activity

Pure 4A zeolite is normally used as a drying agent and not as a catalyst. Forster and Seelemann found it to be catalytically inactive for n-butene isomerization (1), and had previously found no infra red spectral evidence of carboniogenic activity even though the molecule was capable of penetrating the zeolite structure (2). Ushakova et. al.

(3) found that nickel containing 4A zeolite was not active as an alkene hydrogenating catalyst unless the nickel had been reduced at high temperatures. Therefore, it was surprising to find that the unexchanged zeolite catalysed alkene hydrogenation at temperatures below 100C in this work.

A possible source of catalytic activity in zeolites is Bronsted acidity. Forster and Seelemann (2) found no detectable Bronsted acid hydroxyl groups in NaA. Although Szymanski et. al. (4) detected surface hydroxyls which they proposed as being due to cation deficiencies in the system. However, acid hydroxyl groups are generally found to be good isomerization and cracking catalysts (5, 6, 7), and no such side reactions were noted in this work.

The only other obvious sites for catalytic reaction in zeolites are those where significant electrostatic fields exist. These are generated between the negative charges on the structural aluminium and the positive charges on the interstitial sodium cations. However, large monovalent cations such as sodium do not generate strong electrostatic fields (8), although A zeolite has stronger fields than X or Y zeolite (9). Also, since such fields would be present in all 4A zeolite samples, carboneogenic catalysis would have been expected in the other work discussed above.

Thus it would appear that the hydrogenation reactions on the parent zeolite is due to impurities in the material. Such impurities must be either trace elements, or the non 4A zeolite material that was revealed by the electron micrographs discussed in Chapter 4.4.

The only substance found on the unexchanged sample and not on the others was iodine. It is unlikely that this would catalyse the reaction, although the reduced 0.1% NiNaA was slightly less active than the unexchanged sample and the iodine was the only observed impurity loss.

As mentioned above, and as shown in Table 7.5, the overall alkene hydrogenation activity of the reduced 0.1% NiNaA was slightly less than that of the unexchanged sample. This indicates that some of the original active centres have been either removed from the zeolite, or rendered inactive in some way. However, as will be discussed more fully in section 8.7, the type of activity exhibited by the 0.1% sample is very different from that exhibited by the unexchanged sample: particularly with respect to the induction period. Therefore, it seems likely that the centres of activity have been changed. Most probably some, if not all, of the activity will be due to the exchanged nickel. However, the catalytic sites are activated by reduction at 250C with no significant increase in activity on reduction at 400C. This is surprising since most workers (9, 10, 11) report that significant reduction of the nickel in 4A zeolite does not occur below a temperature between 250C and 300C. A minimum reduction temperature of 350C has also been quoted (3), and in all cases both the degree of reduction and the nickel surface area increased rapidly up to 450-500C. This difference may be due to the fact that all these workers used zeolites containing much higher levels of nickel than 0.1% sodium exchange which contains only 0.006 nickel atoms per unit cell of the zeolite.

The 1.0% NiNaA is considerably more active than the other two samples. This must be due to the increased nickel content. However, as reported in Chapter 7.2, the 0.1% NiNaA was active during its induction period whilst there was no observable activity on the 1.0% catalyst over this period. Therefore, the sites which cause the induction period reaction must be completely removed, blocked or altered on the 1.0% NiNaA. Also unlike the 0.1% sample the activity of the catalyst does increase on changing the reduction temperature

from 250C to 400C, although the increase is not as great as found by other workers.

8.5 Activation Energies and Reaction Order

Although the reaction on the unexchanged zeolite must be due to some active centres other than nickel, the reaction over the 0.1% NiNaA and the 1.0% NiNaA was kinetically similar to that found over pure nickel. For ease of analysis the reaction was generally treated as zero order with respect to alkene in this work. However, as was shown in Chapter 7.6 the order was actually 0.5 at 100C. And, although it was not actually measured it seems likely, from the fact that the % alkene vs. time plots became increasingly curved with increase in temperature, that the order increased with temperature. Also the apparent activation energy decreased with increase in temperature, and generally became negative at temperatures above about 170C.

Both these facts are consistent with the results found for other nickel catalysts. These effects were discussed in depth in Chapter 3.5 and 3.6 but are basically due to a decrease in coverage of the nickel surface with increase in temperature (12). They are consistent with a rate equation such that:-

$$\text{Rate} = k \frac{b_a P_a P_h}{1 + b_a P_a}$$

Therefore, a comparison was made of the activation energies for alkene hydrogenation found over the nickel zeolites used in this work with those reported for other nickel catalysts. The results recorded in Table 8.1 also show the temperature range over which they were measured since the apparent activation energy is temperature dependent. It is very difficult to draw any definite conclusions from these results due to the large errors involved. However, the work on the

TABLE 8.1

Activation Energies for Alkene Hydrogenation over various Nickel Catalysts

CATALYST	ALKENE	TEMPERATURE RANGE $(K)^{-1}$	ACTIVATION ENERGY $(kJ/mole)^{-1}$
0.1%NiNaA (red.200C)	ETHENE	295-420	20 ± 5
"	PROPENE	375-435	50 ± 12
0.1%NiNaA (red.250C)	ETHENE	295-400	25 ± 6
"	PROPENE	365-425	60 ± 15
"	ISOBUTENE	410-435	50 ± 12
0.1%NiNaA (red.300C)	ETHENE	295-420	40 ± 10
"	PROPENE	380-435	77 ± 20
"	ISOBUTENE	400-430	80 ± 20
1.0%NiNaA (red.200C)	PROPENE	325-390	60 ± 15
"	ISOBUTENE	385-415	37 ± 9
1.0%NiNaA (red.250C)	ETHENE	315-385	50 ± 12
"	ISOBUTENE	320-385	30 ± 8
1.0%NiNaA (red.300C)	PROPENE	295-360	60 ± 15
"	ISOBUTENE	330-385	65 ± 20
Ni on Silica-Alumina (13)	ETHENE	370-410	50
	ETHENE	410-455	25
Ni on Silica (14)	ETHENE	195-273	35
Ni on Alumina (15)	ETHENE	303-353	49
Ni Wire (16)	ETHENE	294-357	15
Ni Wire (16)	PROPENE	294-357	11
Ni Wire (17)	ETHENE	333-383	34
Ni Wire (17)	PROPENE	333-383	25
Ni Wire (17)	ISOBUTENE	333-383	14

nickel wire showed a decrease in activation energy from ethene, through propene, to isobutene, whilst no such trend is apparent on the zeolite catalysts. Also the ethene shows a slight tendency to display an increase in activation energy with reduction temperature and nickel content. This may be indicative of the change in active sites discussed in the last section.

A pseudo kinetic treatment of the pressure and temperature dependence of the length of the induction period was also attempted in Chapter 7.6 and 7.3 respectively. This showed that the inverse of the induction period was dependent on pressure such that:-

$$\frac{1}{I} = \text{constant } (\text{Alkene})^{x} \quad \text{where I = length of induction period}$$

At 100C x was found to be approximately 0.5 which is the same as the reaction order with respect to alkene at this temperature. Although the induction period was independent of hydrogen pressure whilst the reaction had a first order dependence on hydrogen.

Also the temperature dependence of the induction period was such that:-

$$\frac{1}{I} = A \exp\left(\frac{-E_I}{RT}\right)$$

where E_I was between 55 and 70 kJ/mole for propene and 70 and 100 kJ/mole for isobutene.

This may indicate that the induction period mechanism is linked in some way to the rate controlling factor in the overall reaction mechanism.

8.6 Catalyst Deactivation

It was shown in Chapter 7.4 that some of the catalysts used in the work were prone to deactivation with use. Both the unexchanged and the 0.1%NiNaA showed significant loss of activity with reuse, whilst the 1.0%NiNaA seemed virtually immune. Close examination of the 0.1% samples revealed that the deactivation was greatest on the sites which exhibited no induction period. This fact gives an explanation for the 1.0% sample's immunity; it is inactive during this period. However, the unexchanged zeolite, which was the one most prone to deactivate, appeared to be much less site specific.

It was also found that upto 35% of the lost activity of a reused sample of 0.1%NiNaA could be recovered if it was allowed to stand overnight at 100C, in either hydrogen or a vacuum. However, such treatment did not reactivate used samples of the unexchanged zeolite.

One cause of catalyst deactivation is the presence of impurities in the reactant gases. However, in this work, where specific amounts of reactants were released into the reaction vessel the level of impurity would be the same in all experiments. Thus the impurity would deactivate a specific number of catalyst sites no matter what quantity of catalyst was present. Therefore, the greater the amount of catalyst the less effect the deactivation would have on the overall rate, whilst it was shown, in Chapter 7.4, that the percentage deactivation was the same no matter what weight of catalyst was used.

Another possible cause of the loss of activity could be agglomeration, or migration to inaccessible positions, of the active centres. However, there is no reason to believe that this would occur

during the hydrogenation reaction if it had not occurred during the reduction in hydrogen which was carried out at much higher temperatures. Also it seems unlikely that such a process would be reversed by leaving the catalyst overnight.

A common cause of catalyst deactivation on nickel catalysts is the formation of coke on the metal surface (16, 18). This is formed from the dissociative adsorption of alkene as acetylenic residues which are then further dehydrogenated to form a layer of carbon on the catalytic sites. Coke deposition is also found on zeolites (19), although more commonly polymeric species that are not so severely dehydrogenated are produced and only at temperatures much higher than those used in this work do they form coke. Such polymerization occurs both on nickel zeolites (20), and on acid zeolites (21, 22). However, both polymerization and coking are inhibited to some extent by the presence of hydrogen (10, 18). Also removal of coke requires treatment in hydrogen at temperatures above about 180C (18), and removal of of polymeric species from NiX was found to require heating in vacuum at 370C (20). Therefore, since the nickel zeolites used in this work could be partially regenerated by leaving overnight at 100C, either in hydrogen or in vacuum, it could not be the sole cause of the deactivation on the 0.1%NiNaA. However, it could be partly responsible, and may have been the main cause on the unexchanged zeolite which was not so easy to regenerate. Coke or polymer formation can also cause a significant decrease in the gas phase hydrocarbon concentration as the surface complex is formed (23). In this work no such loss was detected above temperatures of about 390C. Below this some loss was found for ethene and propene. However, this loss was the same over all the zeolites, whether or not deactivation occurred, and was therefore

assumed to be due to adsorption. This could be taken as evidence that coke formation was not the cause of the catalyst deactivation. However, the argument is not very strong since it would not require very much coke, or polymer, to deactivate a significant number of the small number of active sites present on these catalysts.

A deactivation effect similar to the coke/polymerization effect is zeolite pore blockage by alkene or alkene oligomer. Although caused by a similar effect as polymerization such deactivation is more readily removed if the blocking species can slowly diffuse out of the zeolite. Such pore blockage does not necessarily require oligomerization since the reactants themselves can sometimes block the zeolite structure. For example, Chutoransky and Kranich (19) showed that, without oligomerization, n-butene inhibited its own hydrogenation reaction on nickel A zeolite at temperatures below about 385K.

A very small amount of oligomer (mainly butene during ethene reactions) was occasionally noted in the gas phase. Also, as was mentioned earlier, the greatest deactivation occurred on sites active during the induction period. It will be shown in the next section that these sites are the most shape selective in alkene hydrogenation and thus appear to be contained in the zeolite structure. Therefore, pore blockage by alkene, or alkene oligomer, appears to be the most likely cause of the deactivation of the 0.1%NiNaA. This would explain why the catalyst reactivates when it is left to stand, since the blockage would be cleared as the species diffused into the gas phase or were hydrogenated or cracked by the zeolite. This conclusion is supported by the results, which will be discussed in Section 8.8, for competitive reactions where selective reactions are

blocked by the presence of a second alkene. It is also supported by the fact shown in Chapter 7.4, that pre-exposure to isobutene created an induction period in the hydrogenation of ethene over 0.1%NiNaA.

The general conclusion must therefore be that the active centres on the nickel zeolite which exhibit an induction period are not prone to deactivation. Whilst the centres active during induction are prone to deactivate.mainly by pore blockage, although some coking may also occur. The deactivation on the unexchanged zeolite is however, due to a stronger coking effect since it occurs on both induction and post induction reaction sites, and is not readily removed.

8.7 Relative Rates

Weisz et. al.(24) showed that selective hydrogenation of propene can be performed in the presence of isobutene on platinum loaded 5A zeolite at 343C. In such a competitive reaction no detectable conversion of isobutene was noted whilst upto 70% of available propene was hydrogenated. In reaction of the individual alkenes at 25C the propene hydrogenation rate was over 26 times faster than that of isobutene. The rate ratio was probably much greater than this since the propene rate was measured after that of the isobutene but on the same catalyst, and significant catalyst aging (deactivation) occurred with use; for example at 343C the propene reaction rate dropped by over 60% in 200 minutes. It was concluded from this that the catalytically active sites were mainly located within the zeolite pores and the selectivity was due to the molecular sieve effect of the 0.42 nm pore openings in the crystal structure. Ushakova et. al. (3) showed that, if care was taken in the exchange of nickel into NaA, reduction

in hydrogen produced a catalyst which was much more active for the hydrogenation of but-1,3-diene than for isobutene. For example 25% sodium exchanged NiNaA completely hydrogenated the linear molecule at 80-90C without affecting the isobutene. This selectivity was found to increase with degree of exchange upto 50% exchange, after which it fell off rapidly. The loss of selectivity at high exchange levels was attributed to deposition of nickel hydroxide on the zeolite surface when concentrated exchange solutions were used. The selectivity was also found to fall slightly with increase in temperature. This was probably due to activated diffusion of the isobutene into the zeolite with the intensification of rotational and vibrational motions leading to changes of short duration in the configuration of both the molecules and the zeolite structure. However, this effect was not great enough to remove reactant selectivity below temperatures of about 200C. For example complete conversion of but-1,3-diene was achieved at 170C with only 20% conversion of isobutene. Steinbach and Minchev (11) experienced great difficulty in retaining the nickel loading within CaA zeolite and found that, no matter how mild the reduction conditions were, some migration of the nickel to the exterior of the zeolite occurred. They found however, that if the external sites were deactivated, by treatment with 2,3 dimethylbutene, or removed by carbon monoxide which formed $Ni(CO)_4$ when contacted with the nickel, upto 60% of the catalyst activity for n-hexene hydrogenation remained. Therefore, a significant amount of nickel was retained within the zeolite.

If the active centres of the A type zeolite used in this work are located mainly within its structure the relative hydrogenation rates of the ethene, propene, and isobutene should reflect the ease of access of reactants to the reaction sites. A comparison was therefore made of

the ratios of the individual rates used in this work and those found by other workers for various catalysts. The results are shown in Table 8.2. As can be seen, the general preference of the nickel zeolites for the smaller alkene is slightly greater than for the unsupported nickel, Co_3O_4 and NiO, but not as great as found by Weisz et. al. for the Platinum A zeolite. It is concluded from this that a substantial fraction of the total catalytic activity is due to active sites located on the external surface of the zeolite or on impurities present in the samples.

The exception to this is the 0.1%NiNaA which does show a significant preference for the ethene hydrogenation reaction. However, this catalyst did not generally exhibit an induction period for the ethene reaction, whilst long ones were recorded for propene and isobutene. It was shown in Chapter 7.4 that this was due to the catalyst being extremely active during the induction period. The sites active during this time were most susceptible to deactivation by the higher alkenes and an induction period for the ethene reaction was revealed if the catalyst was first treated with isobutene. This was taken as an indication that the measured reaction rate for ethene on this catalyst was due almost entirely to catalyst sites active during the induction. If it is assumed that this is true then the overall rate for ethene on the 0.1%NiNaA should be compared with the activity during induction for the other two alkenes. Table 8.3 shows the relative rates when measured in this way. As can be seen the catalysts preference for ethene is even greater than was shown in Table 8.2. This indicates that the catalytic sites that are active during the induction period on the 0.1%NiNaA may be held within the zeolite structure.

This supposition is supported by the fact that the 1.0%NiNaA,

TABLE 8.2

Ratios of Catalyst Activity for Alkene Hydrogenation

(reacted at 373K, except * 298K)

CATALYST	ethene/propene	ethene/isobutene	propene/isobutene
NaA (red. 250°C)	-	6.3	-
NaA (red. 300°C)	2.9	6.7	2.3
NaA (red. 400°C)	-	7.0	-
0.1%NiNaA (red. 200°C)	140	-	-
0.1%NiNaA (red. 250°C)	10	17	1.6
0.1%NiNaA (red. 300°C)	27	120	4.5
0.1%NiNaA (red. 400°C)	-	9.0	-
1.0%NiNaA (red. 200°C)	1.7	2.5	1.5
1.0%NiNaA (red. 250°C)	-	2.4	-
1.0%NiNaA (red. 300°C)	1.1	4.0	3.7
1.0%NiNaA (red. 400°C)	-	3.2	-
Nickel wire (17)	1.7	5.9	3.5
Nickel wire (16)	3.0	-	-
PtCaA (24)	-	-	26
Co_3O_4 (25)*	0.98	-	-
Ni O (26)*	1.11	2.1	1.9

TABLE 8.3.

Ratios of 0.1%NiNaA Activity for Alkene Hydrogenation During Induction: - assuming overall rate for ethene is rate during induction (reacted at 373K)

CATALYST	ethene/propene	ethene/isobutene	propene/isobutene
0.1%NiNaA (red. 250°C)	110	350	3.2
0.1%NiNaA (red. 300°C)	88	230	2.6

which shows no significant preference for the ethene hydrogenation, shows no significant hydrogenation activity during its induction period.

Since the preference for the ethene hydrogenation reaction is greater on the 0.1%NiNaA than on the parent zeolite it seems probable that the selective reaction occurs on nickel in the zeolite interior. However, in the case of the 1.0%NiNaA where there is no reactant preference there is no indication that nickel has entered the zeolite micropores. This would imply that the nickel has simply adsorbed onto the zeolite exterior or precipitated out alone. Ione et.al. (27) have shown that unless special precautions are taken some nickel hydroxide adsorbs onto the zeolite surface during exchange. Whilst Tungler et.al. (28) showed that $Ni(NO_3)_2$ adsorbs onto the surface during exchange and cannot be removed by washing. Why the exchange process was less successful on the 1.0% NiNaA than on the 0.1% NiNaA is unknown. The most probable cause of poor exchange would be a high pH exchange solution. But the pH measurements of the exchange solutions used, which are shown in Table 4.1 of Chapter 4, indicate that the pH was very similar for both the 0.1% and the 1.0% exchanges. Another alternative would be that the nickel in the interior of the 1.0%NiNaA was inaccessible to any of the alkenes. Nickel nitrate, or nickel hydroxide on the zeolite surface, would be decomposed during calcination to form nickel oxide, and it has been shown (27) that the formation of NiO on the zeolite surface inhibits access to its interior. However, it seems unlikely that complete blockage of the pores could occur with the low exchange levels used in this work.

The rate of reaction during the induction period on fresh samples of unexchanged zeolite could not be measured because the

induction period was so short. However, on catalyst reuse longer induction periods were obtained. Since the rates then obtained were on deactivated catalysts, precise measurement was meaningless. But a rough estimate of the relative rates for ethene, propene, and isobutene was obtained by carrying out the individual hydrogenation reactions consecutively on a single catalyst sample. During induction the rate ratios were between two and six for ethene/propene, and upto twenty-five for ethene/isobutene. Although twenty-five seems a significant ethene preference it is an upper limit as regards experimental error, and is also much poorer than was found on the 0.1% catalyst. Therefore, it is concluded that the selectivity during induction on the unexchanged catalyst is poor. Thus the majority of active sites both during and after induction are on the catalyst exterior.

8.8 Selectivity

The relative rates of hydrogenation for the alkenes discussed in the previous section were for the individual reactions. It was shown in Chapter 7.11 that the competitive reaction of a mixture of alkenes affected both the post induction rates and the length of the induction periods. The post induction selectivity appeared to be less during competitive reaction than that indicated by the relative rates of the individual reactions. During competitive reaction the lower alkene hydrogenation rate was lower than that for individual reaction, whilst the higher alkene rate remained approximately the same. This general result was however, complicated by the presence of induction periods of differing time intervals for the two reactants. The higher alkene had the longer induction period, and in many cases, by the end of this induction period the lower alkene had virtually all reacted. Therefore, meaningful analysis of these results was difficult and in many cases it was not possible to observe both post induction rates simultaneously.

Initially an attempt was made to use the analysis technique developed by Wauquier and Jungers (29) for competitive hydrogenation reactions, which was recently used to study the competitive hydrogenation of alkenes over nickel oxide (26). The kinetic equations, which have been discussed in Chapter 3.6, and were shown to be applicable to the nickel zeolites in Section 8.6, can be modified for the case of competitive reaction as follows:-

$$RATE_1 = \frac{dP_1}{dt} = k_1 \frac{K_1 P_1 P_H}{K_1 P_1 + K_2 P_2}$$

and $$RATE_2 = \frac{dP_2}{dt} = k_2 \frac{K_2 P_2 P_H}{K_1 P_1 + K_2 P_2}$$

where the subscripts 1 and 2 denote the lower and higher alkene respectively. These equations can be combined to give:

$$\frac{dP_2}{dP_1} = \frac{k_2 K_2 P_2}{k_1 K_1 P_1}$$

$$\ln\left(\frac{P_2}{P_{2i}}\right) = \frac{k_2 K_2}{k_1 K_1} \ln\left(\frac{P_1}{P_{1i}}\right)$$

where P_{xi} is the initial pressure of x.

Thus a plot of $\ln \frac{P_2}{P_{2i}}$ vs. $\ln \frac{P_1}{P_{1i}}$ should give a straight line of slope $\frac{k_2 K_2}{k_1 K_1}$

Such a plot did produce a straight line, an example of which is given in Figure 8.1. However, it was found that the higher alkene was reacted by less than 5% before linearity was lost due to tailing off of the lower alkene reaction. Therefore, it was felt that the analysis could not be considered as particularly meaningful.

A different approach to estimate reaction behaviour was therefore tried. The differential rates for the two reactions were measured by

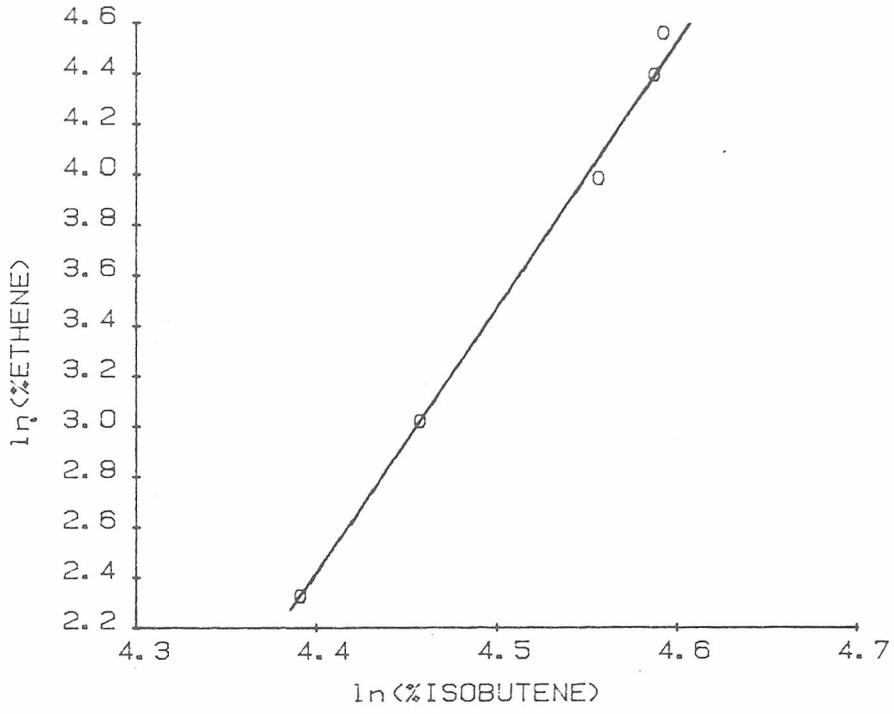

FIGURE 8.1

Competitive Reaction of Ethene and Isobutene over 1.0%NiNaA reduced at 250C.
Reaction Temperature = 382K.

$$\text{Slope} = \frac{k_2 K_2}{k_1 K_1} = 10$$

taking the tangents of the percentage alkene vs. time plots at various time intervals. These were then plotted as $\frac{k_1}{k_2}$ vs. time. A typical example of the technique and the result are shown in Figure 8.2. As can be seen, the selectivity gradually increases as the lower alkene begins to react, reaches a maximum, and then quickly falls away as the higher alkene begins to react and the lower alkene is depleted. The apparent changes in selectivity are thus due to differing lengths of induction periods and reaction times. In cases such as this it is impossible to compare steady state relative rates using a static reaction system. If more meaningful results are to be acquired a flow system, where the reactant concentrations can remain approximately constant, would be required.

It was shown in the last section that the cause of the activity on the 0.1%NiNaA appears to be catalyst sites on the interior of the zeolite, and only when these are deactivated are external sites, which exhibit an induction period, of significance. It would seem likely therefore, that the appearance of an induction period for ethene on this catalyst during competitive reaction is due to blockage of the zeolite pores by the higher alkenes. This is supported by the work of Chutoransky and Kranich (19) who showed that at low temperatures (below 100°C) n-butene inhibited its own hydrogenation reaction by blockage of the pores of NiA, NiX, and Ni mordenite zeolites. These conclusions conflict with the results of Ushakova et. al. (3) who achieved the selective hydrogenation of but-1,3,-diene in the presence of isobutene over NiNaA zeolite at temperatures as low as 80°C. However, it is possible that the relative adsorption strengths of the alkenes they used were similar and a more equal amount of each was attracted to the pore openings.

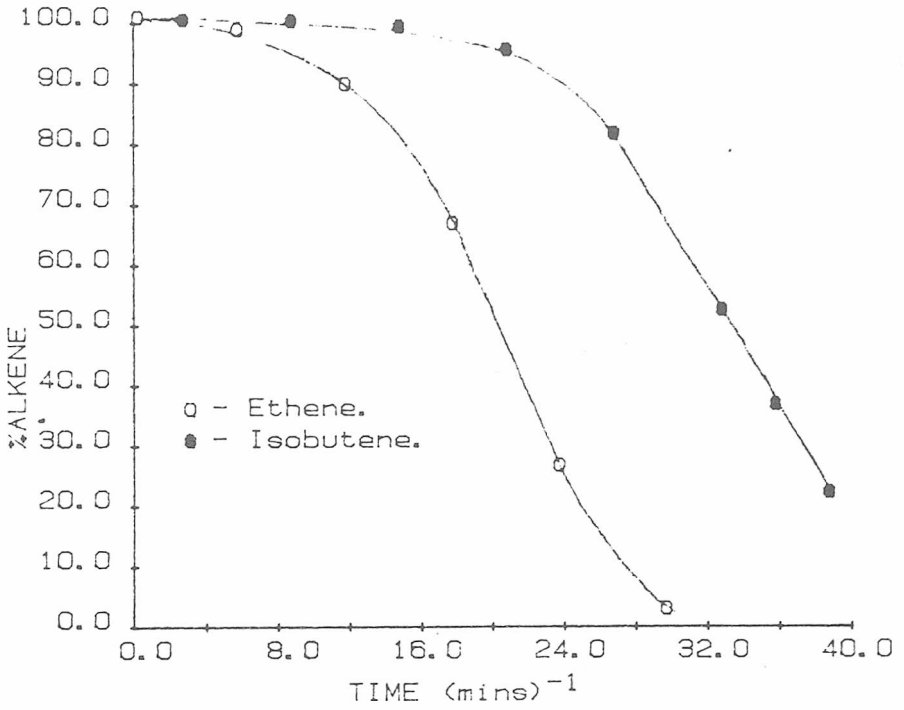

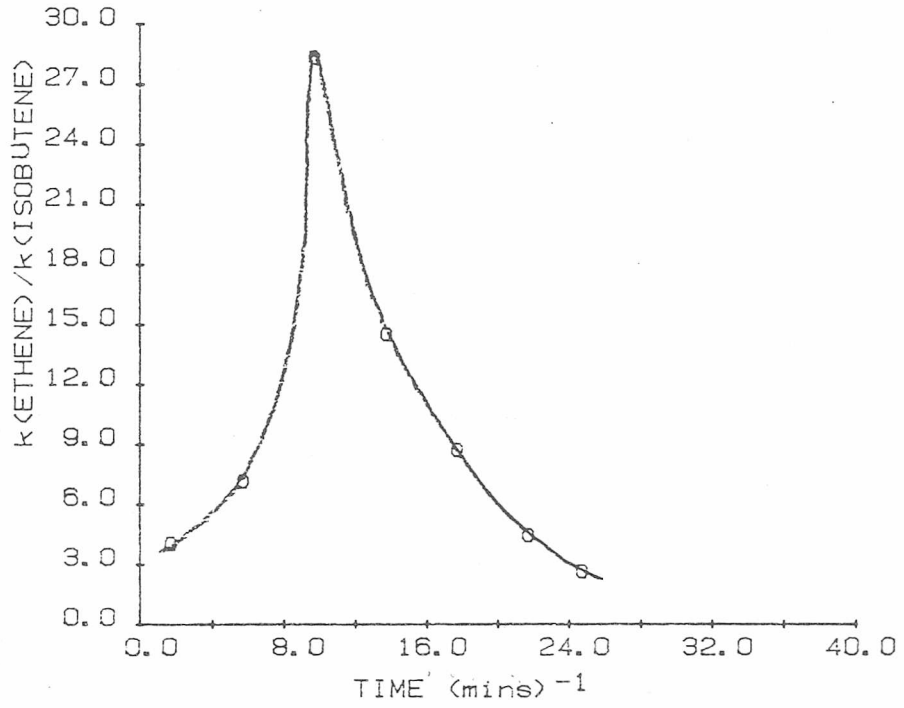

FIGURE 8.2

Competitive Reaction of Ethene and Isobutene over 1.0%NiNaA reduced at 250C.
(same data as for Figure 8.1)

8.9 Mechanism

There are five main points to take into account in consideration of the reaction mechanism on the zeolite catalysts used in this work.

i) The active centres on the unexchanged and the nickel zeolites seem to be different. However, since they behave in a kinetically similar manner it is likely that the mechanisms are similar.

ii) It was shown in Chapter 7.8 that the double bond migration reaction for 1-butene was affected in a similar manner to the hydrogenation reaction. That is, it exhibits an induction period of the same length. Therefore, the controlling step must be at, or before, the formation of the surface intermediate common to both reactions (30).

iii) Pre-exposure of the catalyst to hydrogen or alkene does not affect the induction period. Therefore, whatever mechanism or effect causes the induction period must require the presence of both reactants.

iv) Deactivation, by alkene, of the sites active during induction lengthens the induction period. Therefore, those sites are capable of aiding in the induction mechanism.

Although, since there are no such sites on the 1.0% catalyst, they are not essential.

The primary factor in the mechanism must be the induction period. Induction effects are not uncommon in zeolite catalytic systems. There are several causes all of which are related to sorption or site activation.

Riekert (23) found that an induction period occurred before the polymerization of ethene over NiY zeolites. He attributed this to the initial diffusion into the zeolite interior, during which time no

reaction occurred. This is unlikely to be the cause of the effect in this work because the amount of adsorption for a given alkene is the same on all samples whilst the length of the induction period is dependent on the overall activity. Also the activation energy for diffusion is usually low, whilst it was shown in Chapter 7.3 that the induction periods had activation energies of between 55 and 100 kJ/mole. And such a diffusional effect would be expected to be reduced, or removed, by pre-exposure to one or other of the reactants, and it was shown in Chapter 7.7 that this was not found.

Another potential cause of induction is product desorption limitation. This was shown to be the most probable cause of the induction period found during benzene alkylation over Y zeolite (31). The delay being caused by the desorption of the product from the zeolite pore mouths. Weisz et. al. (24) proposed a type of selectivity in zeolites where two product species could be formed in competition, but one could not escape from the structure.

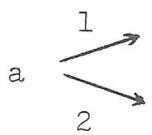

where a = reactant
B = product unable to escape from the zeolite.
b = product which can enter the gas phase.

The two products (B and b) would form initially. However, B would only be formed either, until its concentration was high enough to interfere with the reaction (i.e. by catalyst site blockage), in which case the reaction to form b would be poisoned, or until an internal steady state concentration of B was established. In this latter case, if reaction path 1 was kinetically more favourable than path 2 an induction period might be produced. However, in this work the induction period was often longer than the total post induction

reaction time. Therefore, the rate of reaction to form B would need to be very fast. This would mean that a great deal, if not all, the reactant would be converted into B during the induction which would have resulted in the disappearance of virtually all the gas phase reactant. No such effect was found.

An induction period can also result if the catalyst sites require activation. Dimitrov and Leach (32) found that n-butene isomerization over Copper X zeolite exhibited an induction which was explained by the reduction of Cu^{2+} to Cu^{+}. However, this induction period was irreversibly removed by either pre-exposure to hydrogen or reuse of the catalyst. Ione et.al. (27) postulated that, even after pre-treatment with hydrogen, some of the nickel in NiY zeolite was reduced in the presence of the reactants, and was reoxidised on their removal:

i.e.

$$Ni^{2+}\ \mathbb{Z} + H_2 \rightleftharpoons^{C_6H_{12}} Ni^{o} + \text{-C-C-}\ H_2\ \mathbb{Z}$$

where $\mathbb{Z}$ = zeolite structure.

Thus the process discussed by Dimitrov and Leach could apply in this work if the reduction process were reversible.

However, all of the above arguments would be expected to give a gradual build up of reaction, not a sharp increase as was found in this work. They also require all the catalytic sites to be incorporated into the zeolite structure, whilst the evidence indicates that this was not the case for the catalysts used in this work.

Another reason often given for the appearance of an induction period before the appearance of products, is the formation of a strongly adsorbed species, such as a coke, which then acts either as a reaction intermediate or a catalytic site. Langer (5) found that 1-butene cracking over $NaNH_4Y$ zeolite exhibited an induction

period which he proposed to be due to the formation of a cyclic species:

i.e.

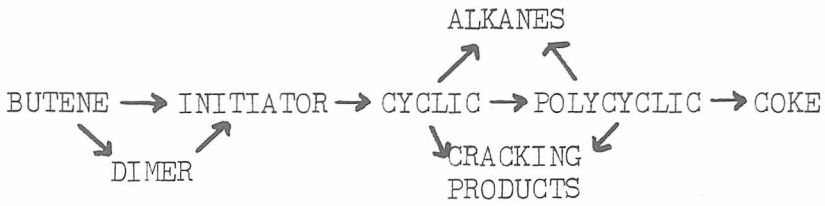

However, he found that the length of the induction period increased with the temperature of reaction, which he explained as being due to more extensive adsorption at lower temperatures; causing a more rapid catalyst deactivation and a more extensive coke build up. Whilst in this work the induction period was found to be inversely dependent on temperature.

The induction period found during Fischer-Tropsch synthesis has similarly been explained as being due to either:-

i) a surface complex which is slowly formed on the iron, and the products are then formed from this (33).

ii) carbiding and synthesis are competitive reactions and the carbiding predominates until a given degree of carbide surface is formed (34).

iii) the active centres for synthesis are present on the carbide surface and not on the iron. Therefore, synthesis does not occur until the carbide layer is formed (35, 36).

The latter approach is similar to the suggestion of other workers that n-butene isomerization over silica alumina (37), and dehydroxylated Y zeolite (38), proceeds via proton donation from a polymeric complex.

However, all such carbiding stages would be expected to cause a reduction in the length of the induction period with catalyst

reuse. Whilst with the nickel zeolites used in this work the reverse was found to be the case.

Habgood (39) showed that competitive adsorption of nitrogen and methane over 4A zeolite proceeded via initial adsorption of nitrogen followed by its displacement by methane. If such a displacement effect occurred with hydrogen and alkene then, if a species which had to be chemisorbed before reaction could occur had to first displace the other reactant, a delay in the start of the reaction might occur. However, such an induction effect would be removed by preadsorption of one of the reactants.

Karge and Ladebeck (21) found that an induction period occurred before ethene conversion to light hydrocarbons and polymers over beryllium mordenite. They suggested that this was due to the slowness of the conversion of π bonded ethene to a carbonium ion over Bronsted acid sites:-

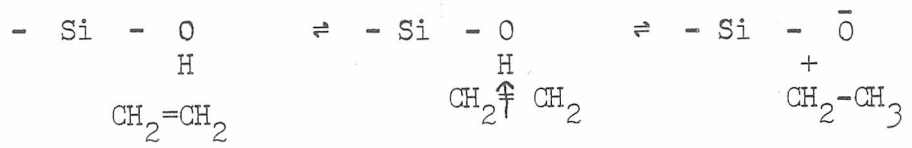

They said that the ethene was partially physically adsorbed, partially bound as a π complex, and partially converted to carbonium ions which then react. Reaction was between carbonium ions and could therefore only proceed after a build up of carbonium ions had occurred. Therefore, since the slow step was π complex transformation an induction period occurred. They showed that this conversion was the slow step by infra red analysis of the adsorbed species, and supported the argument by showing the length of the induction period was shorter on more acidic mordenite catalysts. Their conclusion is supported by the work of Penchev et. al. (10) who showed that the induction period which they found for toluene disproportionation

over NiCa Y zeolite was also directly proportional to acidity, although they attempted no explanation of the cause. However, in a static reaction system an induction period of this type must be short with respect to the overall reaction time since it is controlled by the same step, and thereby the same rate constant, as the overall reaction.

The hydrogen spillover effect suggested by Sinfelt and Lucchesi (40) for ethene hydrogenation over Pt/Al_2O_3 could also cause some kind of induction effect. They suggested that hydrogen was activated on the platinum surface and then proceeded via surface migration towards ethene that was chemisorbed at Al_2O_3 sites. It has been suggested that this is not of major significance on Pt/Al_2O_3 (41,42), but the occurrence of the mechanism itself is not refuted. If this type of spillover effect occurred on the zeolite in this work, and if it were a slow step, then it could cause an induction period. However, for the change from induction period to post induction reaction to be as sharp as it is, an activated hydrogen 'pool' would have to be built up before migration. Otherwise the rate increase would have been gradual.

Tanaka and Okuhara (43) found an induction period before alkene isomerisation over single MoS_2 crystals which was very similar to the one found in this work. That is, the change from induction to full reaction was sudden, there were sites active during the induction period, and the effect was not reduced by pre-exposure to either of the two reactants (butene and hydrogen). The explanation they proposed was tentative but was based on restricted rotation of adsorbed alkyl groups preventing reaction until reconstruction of the adsorption site had occurred. They did not specify how the reconstruction occurred

except to say that it required the presence of both hydrogen and butene and was completely reversed on evacuation. Such a reaction scheme could be applied to this work although the active sites would have to be something more complex than nickel metal or Bronsted hydroxyl groups.

Another mechanism which could explain the induction effect is that the reaction takes place on a single adsorption site:-

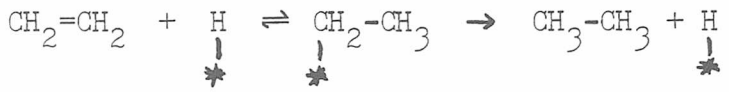

If this were the case then the initially adsorbed hydrogen would need to be supplied by a proton donator. Such a donator has been shown to exist for n-butane isomerization over silica gel (6) by the process:-

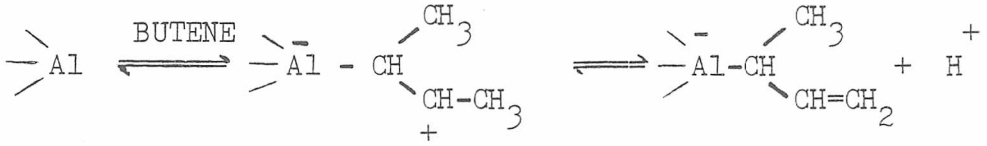

This mechanism could show an induction effect if the above supply of the initial proton was slow, since the hydrogenation of the alkene would regenerate the proton and there would therefore be no need of a continual supply. However, it does not explain why the end of the induction period is sudden rather than gradual unless the protons which are formed initially are 'mopped up' by another process and only when this process reaches equilibrium are the protons available for reaction with alkene.

However, both the above mechanism are extremely speculative and for more definite conclusions to be reached much more work is required. It would be particularly useful if denterium tracer work was used to identify the source of the initial hydrogen supply.

8.10 General Conclusions

The investigation of the selectivity of nickel 4A zeolite for light alkene hydrogenation was thwarted both by impurities in the original catalyst and possible poor exchange technique. In any further work more care must be taken in testing the original zeolite and also in performing the cation exchange process. However, the indications are that even with retention of the active sites within the zeolite structure, good selectivity would not be obtained for long with these reactants. The catalyst is rapidly deactivated by blockage of the structure both by reactant and product molecules.

The catalysts, as prepared, showed extremely interesting kinetic phenomena which however proved very difficult to explain satisfactorily.

REFERENCES

1) H. FORSTER, R. SEELEMANN, J.C.S. Far.I, 75, 2744, (1979)

2) H. FORSTER, R. SEELEMAN, J.C.S. Far.I, 74, 1435, (1978)

3) V.A. USHAKOVA, D.P. DOBYCHIN, M.A. PIONTKOVSKAYA, I.E. NEIMARK, V.N. MAZIN, L.E. FENELONOVA, Zhur.Prikladnoi Khimii, 48,780 (1975)

4) H.A. SZYMANSKI, D.N. STAMIRES, G.R. LYNCH, J. Opt.Soc.Am. 50,1323 (1960)

5) B.E. LANGER, J.Cat., 65,416, (1980)

6) A.J. VAN ROOSMALEN, M.C.G. HARTMANN, J.C. MOL, J.Cat., 66,112, (1980)

7) J.T. RICHARDSON, J.Cat., 21,122, (1971)

8) J.A. RABO, C.L. ANGELL, P.H. KASAI, V. SCHOMAKER, Disc.Far.Soc., 41,328, (1966)

9) D. GARBOWSKI, V.M. MATHIEU, M. PRIMET, Chem.Phys.Letter, 49,247, (1977)

10) V. PENCHEV, N. DAVIDOVA, V.KANAZIREV, H. MINCHEV, Y. NEINSKA, Adv. Chem. Ser., 121,461, (1973)

11) F. STEINBACH, H. MINCHEV, Zeit. fur Phys. Chem., 99,235, (1976)

12) I. MATSUZAKI, A. TADA, J.Cat., 13,215, (1969)

13) H. KOH, R. HUGHES, J.Cat., 33,7, (1974)

14) G.C.A. SCHUIT, L.L. VAN REIJEN, Adv. Cat., 10,242, (1958)

15) L.A. WANNINGER, J.M. SMITH, Chem. Weekblad, 56,273, (1960)

16) O. TOYAMA, Rev.Phys.Chem. of Japan, 14,86, (1940)

17) G.H. TWIGG, Trans. Far.Soc., 35,934, (1940)

18) G.I. JENKINS, E. RIDEAL, J. Chem. Soc., 2490, (1955)

19) P. CHUTORANSKY, W.L. KRANICH, J. Cat., 21,1, (1971)

20) P.B. VENUTO, P.S. LANDIS, Adv. Cat., 18,259, (1968)

21) H.G. KARGE, J. LADEBECK, Acta Physica et Chemica, 24,161, (1978)

22) B.V. LIENGME, W.K. HALL, Trans. Far. Soc., 62,3229, (1966)

23) L. RIEKERT, J. Cat., 19,8, (1970)

24) P.B. WEISZ, V.J. FRILETTE, R.W. MAATMAN, E.B. MOWER, J. Cat., 1,307, (1962)

25) H. NIHIRA, T. FUKUSHIMA, K. TANAKA, A. OZAKI, J.Cat., 23,281, (1971)

26) T. FUKUSHIMA, A. OZAKI, J. Cat., 59,465, (1979)

27) K.G. IONE, V.N. ROMANNIKOV, A.A. DAVYDOVA, L.B. ORLOVA, J. Cat., 57,126, (1979)

28) A. TUNGLER, J. PETRO, T. MATHE, G. BERENGEI, Acta Physica et Chemica, 319,24,(1978)

29) J.P. WAUQUIER, J.C. JUNGERS, Compt. Rend., 243,1766, (1956)

30) G.C. BOND, "CATALYSIS BY METALS", Chap.11, Academic Press, London and New York (1962)

31) J.P. NOLLEY, J.R. KATZER, Adv. Chem. Ser.,121,563, (1973)

32) CHR. DIMITROV, H.F. LEACH, J. Cat., 14,336, (1969)

33) J.W. NIEMANTSVERDRIET, A.M. VAN DER KRAAN, J. Phys. Chem. W.L. VAN DIJK, H.S. VAN DER BAAN, 84,3363, (1980)

34) J.W. NIEMANTSVERDRIET, A.M. VAN DER KRAAN, J. Cat., 72,385, (1981)

35) J.A. AMELSE, J.B. BUTT, L.H. SCHWARTZ, J.Phys. Chem., 82,558, (1978)

36) G.B. RAUPP, W.N. DELGASS, J. Cat., 58,361, (1979)

37) J.N. FINCH, A. CLARK, J. Phys. Chem., 73,2234, (1969)

38) T.J. WEEKS, C.L. ANGELL, I.R. LADD, A.P. BOLTON, J. Cat., 33,256, (1974)

39) H.W. HABGOOD, Can. J. Chem., 36,1384, (1958)

40) J.H. SINFELT, P.J. LUCCHESI, J. Am. Chem. Soc., 85,3365, (1963)

41) J.C. SCHLATTER, M. BOUDART, J. Cat., 24,482, (1972)

42) D. BRIGGS, J. DEWING, C.J. JONES, J. Cat., 29,183 (1973)

43) K. TANAKA, T. OKUHARA, J. Cat., 78,155, (1982)